BHT2 J/ψ R$_{pA}$ Run15 AnaNote

Ziyue Zhang

January 27, 2025

Contents

1 Data QA - Bad Run Rejection

The data taking encounters random and unexpected events from time to time. Some effects on performance may also accumulate over time. These could result in abnormal detector readout and therefore unreliable reconstruction. The data QA - bad run rejection defines a list of runs to be rejected due to significant difference of reconstruction variable distributions compared to the other runs. Only the variables that are related to this analysis are looked at.

1.1 Procedure

The rejection happens in an iterative manner. Each iteration is called a "round". The remaining runs in the previous round will be the complete set that the next round will work on. In each round, profile histograms of 39 variable distributions vs run index are checked independently. For each variable, the runs that satisfy "the criteria" will be marked as "to be rejected", and will be rejected at the end of each round collectively, after all 39 variables are checked. I.e., a run could be marked as "to be rejected" multiple times in a round. The iteration ends when not a single run is marked as "to be rejected" in the latest round. All the runs that have been rejected, as well as runs without any entries, are listed as "bad runs".

The following is a complete list of 39 checked variables:
hRefMult, hnPrimary, hnBEMCMatch, hTPCVz, hTPCVx, hTPCVy, hnHitsFit, hnHitsDedx, hDca, hPt, hEta, hPhi, hDedx, hNSigmaE, hNSigmaPi, hNSigmaK, hNSigmaP, hZDCX, hBemcZDist, hBemcPhiDist, hBemcbTowE, hBemcE0, hBemcAdc0, hBemcEvP, hBBCX, hBemcE, hTrgdBemcAdc0, hTrgdBemcE0, hTrgdBemcE, hTrgdBemcbTowE, hTrgdBemcEvP, hTrgdBemcZDist, hTrgdBemcPhiDist, hTrgdNSigmaE, hTrgdPt, hTrgdEta, hTrgdPhi, hnBemcE, hnTrgdE

1.2 Criteria

The criteria is used when checking each profiles histograms (PH) of variable distribution in order to mark the "to be rejected" runs.

Define: Center Fit the PH of *val* vs *RunIdx* to a straight line with least square method, but with the error bar ignored. This straight line is considered as the **Center**. In each collision system for certain variables, the profile histogram shows obvious discontinuity and a linear fit will yield a slope that does not correspond to development of any trend. In such cases, the slope parameter is fixed at 0. The following is a list of variables with the slope fit parameter fixed to 0.

p+p hTPCVx, hTPCVy, hEta, hPhi

p+Au hnBEMCMatch, hTPCVz, hTPCVx, hTPCVy, hBemcEvP, hTrgdBemcEvP, hTrgdEta, hTrgdPhi

Define: μ, σ Move the axis in the Y axis direction by b, which is the y intersection of **Center**, and then rotate the axis by θ where θ is the slope angle of **Center**. The new Y coordinates are $y' = (y - b)cos\theta - xsin\theta$. μ is the mean of y' and σ is the standard deviation of y'. μ is close to 0 but slightly deviate from 0 due to float accuracy and fit details. Such a deviation is negligible.

Define: 5σ Band Area between the straight lines $y' = \mu \pm 5 \times \sigma$ is defined to be the **5σ Band**. The band is carried over back to the original coordinate system before rotation and transition.

Rejection Let the **segment**: $x = Center, \quad Center - Error \leq y \leq Center + Error$ represent the corresponding run, where "Center" and "Error" are the bin center and bin error respectively. If the **segment** has no overlap with the **5σ Band**, then it is marked as "to be rejected".

1.3 Result

The runs rejected in different rounds are collectively presented in Fig.1 for p+p collisions and in Fig.2 for p+Au collisions.

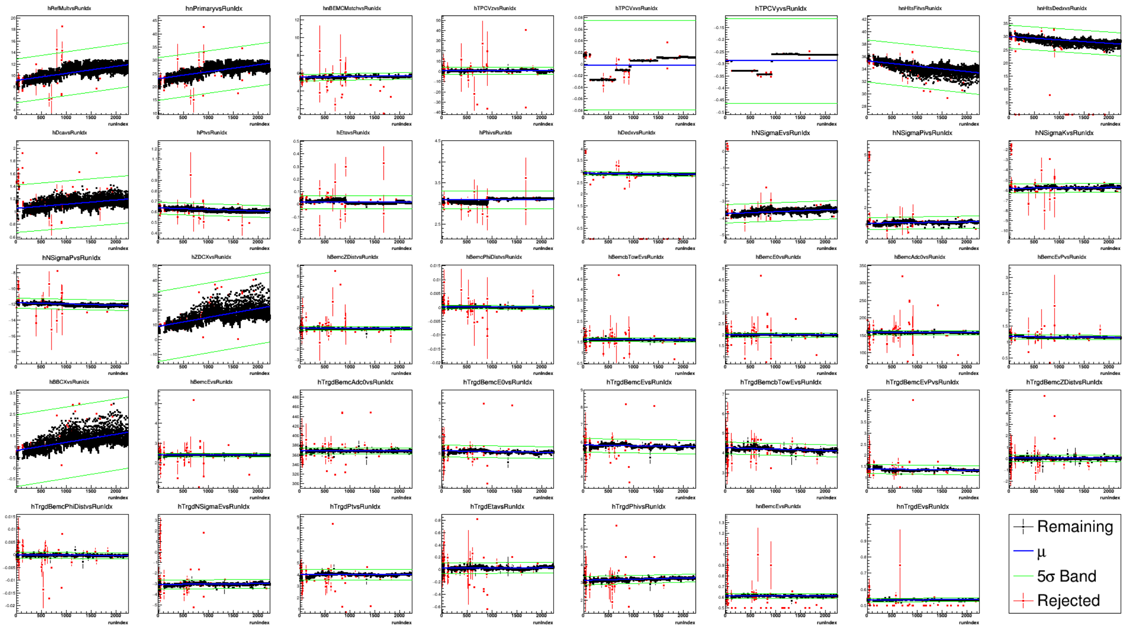

Figure 1: Bad Run Rejection for p+p

The following is a list of rejected runs in p+p collisions (including "empty" runs without any entry): 16044110, 16044111, 16044112, 16044123, 16044124, 16044125, 16044126, 16044127, 16044128, 16044129, 16044132, 16044133, 16044138, 16045001, 16045047, 16045048, 16045049, 16045070, 16045082, 16045083, 16045084, 16045085, 16045086, 16045087, 16045088, 16045089, 16045090, 16045093, 16045095, 16045096, 16045097, 16045098, 16045099, 16045100, 16045102, 16045103, 16045104, 16045105, 16045106, 16045108, 16045109, 16045110, 16045111, 16045112, 16045113, 16045114, 16045115, 16045116, 16045117, 16045118, 16045119, 16045120, 16046003, 16046005, 16046006, 16046007, 16046008, 16046009, 16046010, 16046011, 16046012, 16046013, 16046014, 16046015, 16046016, 16046017, 16046018, 16046019, 16046020, 16046021, 16046032, 16046033, 16046034, 16046035, 16046036, 16046037, 16046038, 16046039, 16046040, 16046041, 16046042, 16046043, 16046044, 16046045, 16046046, 16046048, 16046049, 16046050, 16046057, 16046058, 16046059, 16046061, 16046062, 16046064, 16046065, 16046066, 16046067, 16046073, 16046076, 16046077, 16046078, 16047004, 16047005, 16047008, 16047101, 16047102, 16047103, 16047104, 16047106, 16050048, 16050049, 16052046, 16052048, 16052051, 16052087, 16052088, 16055124, 16055127, 16058070, 16058073, 16060018, 16060036, 16060043, 16060064, 16061035, 16061076, 16062008, 16062009, 16062011, 16062014, 16062048, 16063096, 16063097, 16063099, 16065011, 16066028, 16067045, 16067046, 16067047, 16069045, 16069050, 16069052, 16069060, 16071001, 16071002, 16071003, 16071006, 16071007, 16071076, 16072046, 16072047, 16073004, 16073007, 16073015, 16079045, 16080012, 16080043, 16082014, 16083003, 16084003, 16085005, 16087018, 16088014, 16089021, 16091039, 16091040, 16091042, 16091050, 16095027, 16096030, 16097028, 16100023, 16100024, 16100025, 16101006, 16101032, 16104002, 16104022, 16107004, 16107042, 16108032, 16110006, 16115029, 16115056

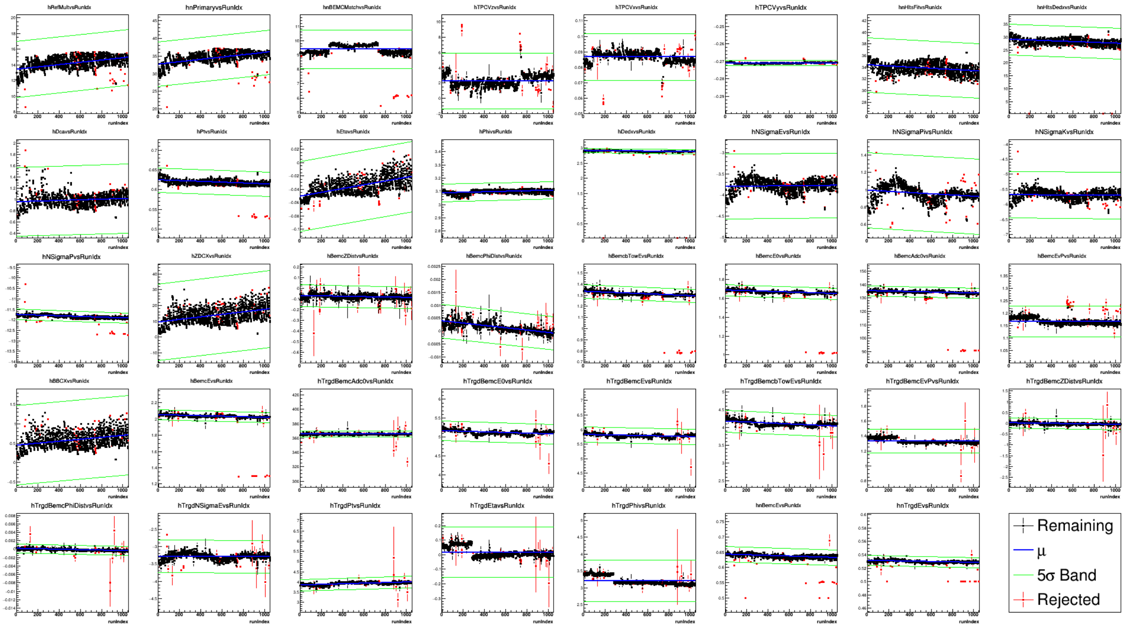

Figure 2: Bad Run Rejection for p+Au

The following is a list of rejected runs in p+Au collisions (including "empty" runs without any entry): 16125038, 16125046, 16125052, 16127005, 16127048, 16127049, 16128006, 16128056, 16129019, 16130012, 16130015, 16130016, 16130032, 16131030, 16131032, 16132021, 16132022, 16134012, 16134042, 16139021, 16142046, 16142061, 16142065, 16142069, 16142073, 16142077, 16143005, 16143009, 16143011, 16143013, 16143015, 16143031, 16143036, 16143039, 16143052, 16144002, 16144013, 16144037, 16144069, 16148016, 16149001, 16149002, 16149003, 16149004, 16149005, 16149008, 16149009, 16149010, 16149011, 16149013, 16149014, 16150001, 16150003, 16150042, 16154010, 16154021, 16155017, 16155031, 16155039, 16156010, 16156028, 16157034, 16157047, 16157048, 16157071, 16158021, 16158039, 16159009, 16159019

2 Embedding QA

Efficiency is studied with J/ψ embedding in real data and an event generator **EvtGen**. Embedding are mainly used in order to study the behavior of single electron's in terms of efficiency. Together with **EvtGen**, we calculate the J/ψ reconstruction efficiency. Such combination of these tools is due to the limitation of decay models of J/ψ in embedding and lacking of description of detector response in **EvtGen**.

The purpose of embedding QA is to confirm that the embedding has good enough representation of the data in most aspects. Additional treatment and arguement is needed where embedding can't describe the real data well. All related single track variable distribution is compared betweent the data and embedding. The distributions of kinematics of J/ψ candidates are also compared. The difference between data and embedding is also covered by systematic uncertainty estimation. The exhausted list of plots can be found in the appendix 7.1.

The conclusion is that the embedding describes the data well enough in most aspects. The momentum resolution is underesitmated, therefore needs additional smearing. The consistency between data and embedding of E/p and dca distubution is not as satisfactory as others, therefore cuts on those are loosened in order to reduce the systematic uncertainties.

3 Event and Track Selection

The event and track selection cuts used in p+p and p+Au are identical in order to reduce the systematic uncertainty. The event trigger is the $BHT2 \times BBC$ trigger.

Only events not rejected by the event level selection will be studied. In the di-electron pairs, both $e^{\pm}$ are required to pass all tracking quality cuts and electron identification cuts. At least 1 of the $e^{\pm}$ needs to pass the electron trigger cuts. After J/ψ reconstruction, the only the RC J/ψ within the interested kinematics range are studied. The J/ψ mass window is not listed here and will be discussed in later sections. The selection cuts are listed below in the tables:

Event Selection	
$\lvert Vz\rvert \leq 80$ [cm]	Ranking < 0

Tracking Quality					
nHitsFit≥20	nHitsDedx≥10	0.52≤nHitsRatio≤1.02	DCA<1.5 [cm]	$p_T \geq 1$	$\lvert\eta\rvert < 1$

Electron Identification		
$0.5< \frac{E}{p} <2.5$ [c]	$-1.5< n\sigma_e <2.5$	e>0.1 GeV/c^2

Electron Trigger Cut		
Dsmadc>18	Adc0≥300	$p_T > 4.3$ (3.5) [GeV/c]

Note: The electron trigger p_T cut used to extract the invariant cross section (invariant yield) in p+p (p+Au) collisions (4.3 GeV/c) is different from the cut used when calculating nuclear modification factor R_extpA (3.5 GeV/c).

Near the start of the electron trigger threshold, the trigger efficiency from embedding is at higher risk of being unreliable. This difference is taken into account in the systematic uncertainty by varying the trigger cut regardless of the trigger p_T. The systematic uncertainty can be reduced by moving the trigger p_T cut towards the trigger efficiency plateau (see plots for the EID efficiencies, TRG type)

In terms of invariant cross section (invariant yield) measurement, a higher trigger p_T cut is used in order to reduce the systematic uncertainty.

When it comes to R_extpA, since the data of the 2 collision systems were taken from the same year and the related detector setup were identical, such a difference between embedding and data should be mostly cancelled out by taking the ratio. One can worry less about the systematic uncertainty when reaching away from the plateau. Therefore, trigger electron p_T cut is lowered to 3.5 GeV/c in order to gain more J/ψ counts raw yield in the first p_T bin.

J/ψ Kinematics Range	
$4<p_T^{J/\psi} <12$ [GeV/c]	$\lvert y^{J/\psi}\rvert <1$

4 TPC Vz, Zdc Rate and Hot Tower Rejection Weighters

On the event level, the TPC Vz and luminosity (Zdc Rate) distribution have small but noticiable difference between data and embedding. A weighting factor as a function of TPC Vz (Zdc rate) is needed in order to reduce the effect from possible efficiency dependence on TPC Vz (Zdc rate). The weighting factor is calculated by taking the ratio of the normalized TPC Vz (Zdc rate) distribution, of the data against embedding. Due to the limit of statistics, TPC Vz and Zdc rate dependencies are assumed to be uncorrelated.

The real data used to do embeding is only a subset of the entire dataset. As a result, the Zdc Rate in some bins have 0 entries in embedding while the data have entries. This makes it impossible to do weighting for these bins. Therefore those Zdc rate bins in data are discarded and defined as “Bad Bins”. Hot Tower Rejection is applied in order to avoid fired BEMC towers which leads to fake candidates. The Hot Tower is defined run by run, i.e., there exists a hot tower list for each run. The probability fraction that a tower is working properly can be calculated by taking the ratio of number of events that a tower is normal against the total number of events. There is noticeable difference in the such a fraction between real data and embedding. To compensate for such difference, a similar weighting factor is calculated for Hot Tower Rejection by taking the ratio of normal fraction in data against that in embedding for each individual tower.

p+p Around 0.09% of events is discarded due to absence of Zdc rate in embedding:

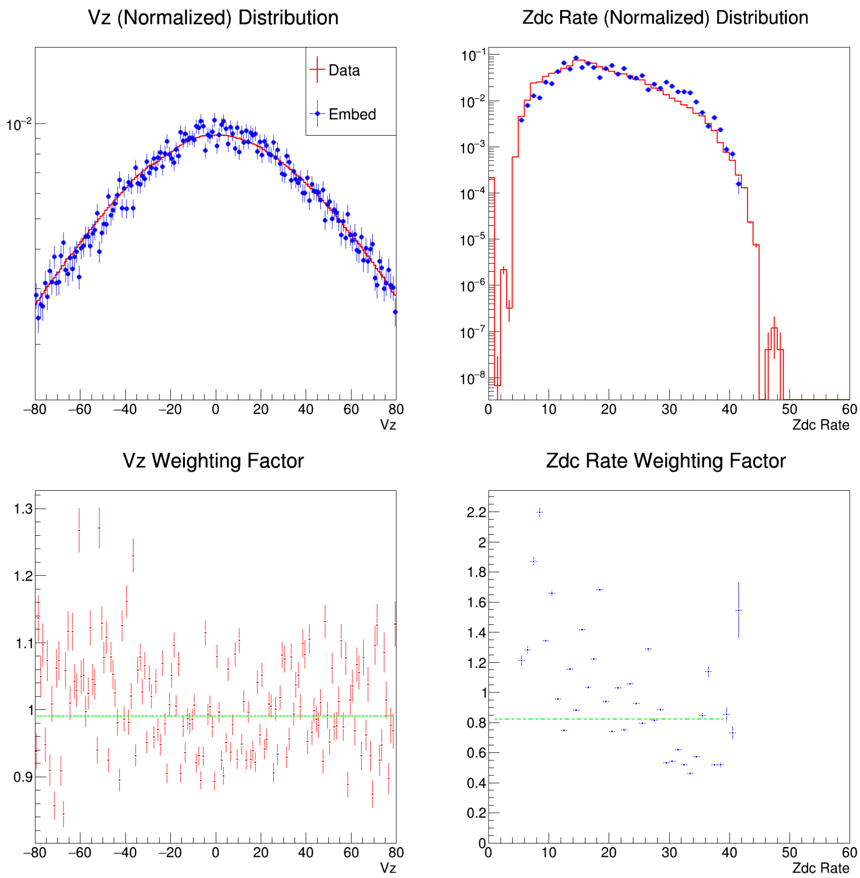

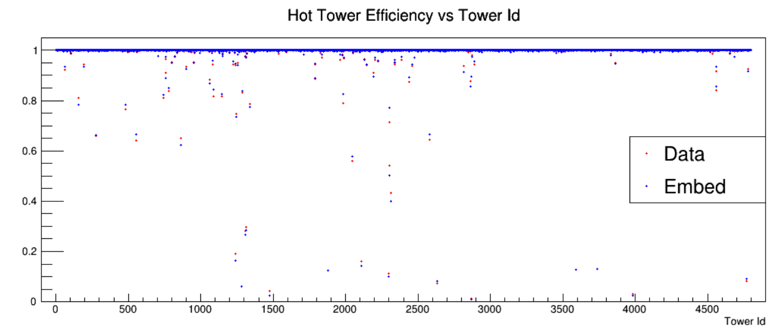

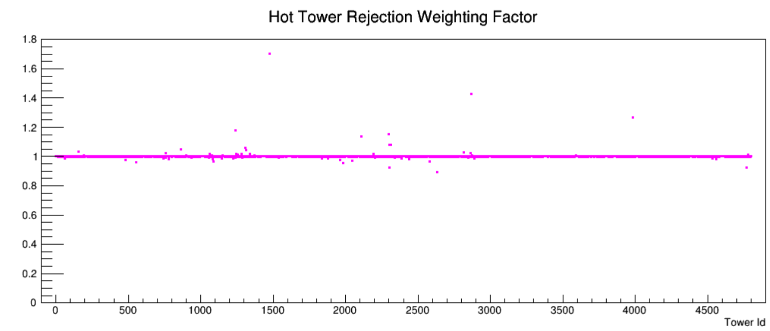

p+Au Around 1.1% of events is discarded due to absence of Zdc rate in embedding:

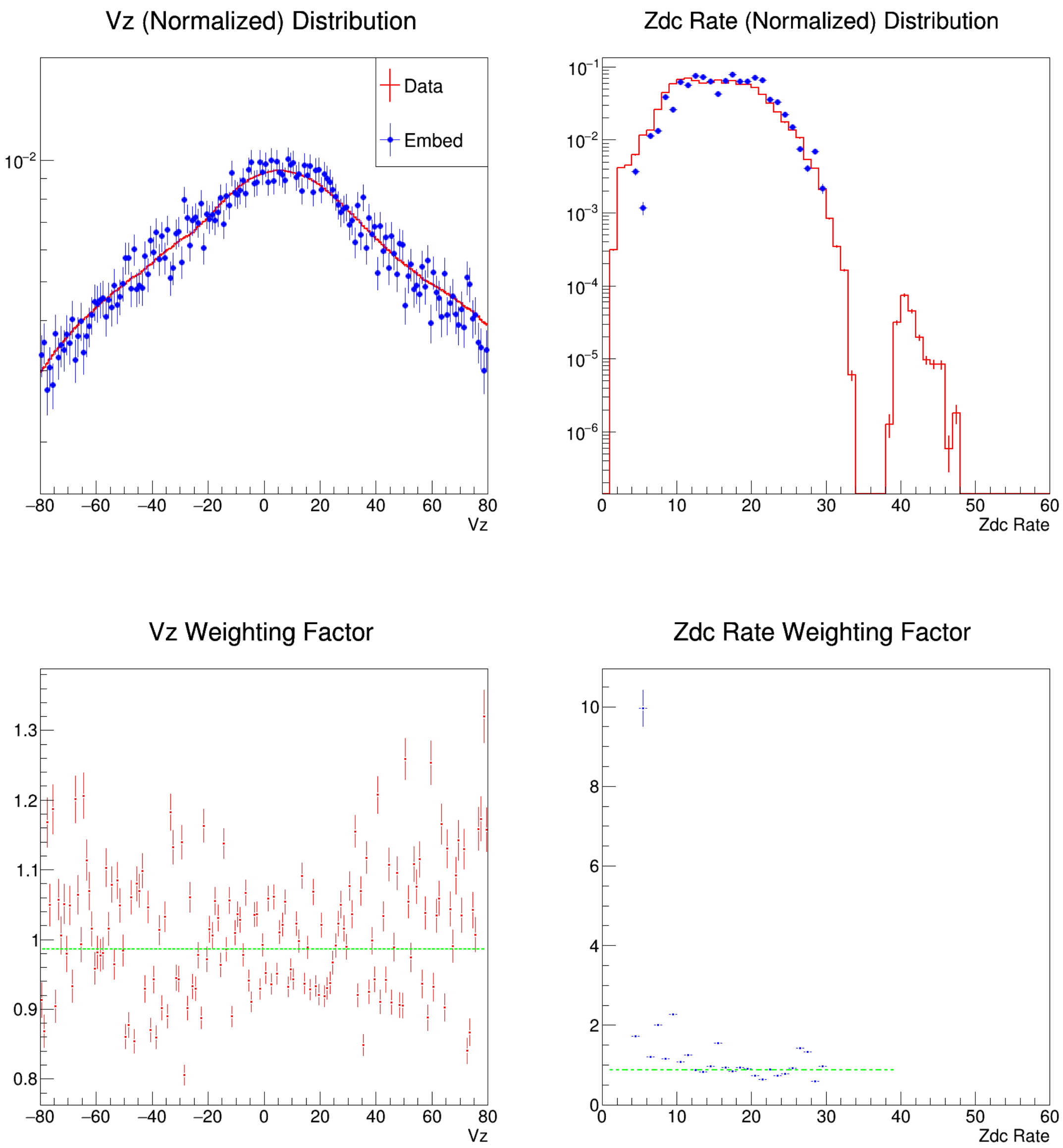

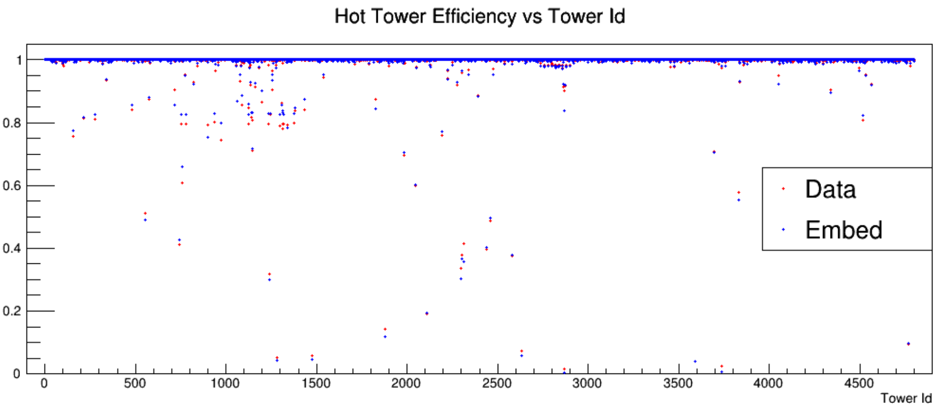

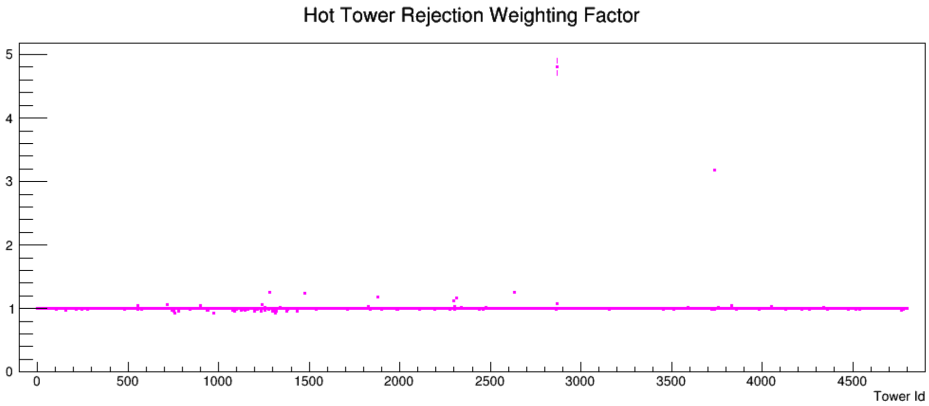

These weighting factors are applied in embedding on event level.

5 The Analysis

5.1 Overview

There are 3 physics results in this analysis: the differential cross section in p+p collisions, the invariant yield in p+Au colisions, and the nuclear modification factor R$_{e}xtpA$.

The cross section in p+p is proportional to the invariant yield with a difference of a scale factor of the non-single diffractive (**NSD**) cross section in p+p.
The R$_{e}xtpA$ is the yield ratio of p+Au against p+p, scaled by the average number of binary nucleon-nucleon collisions $\langle N_{coll} \rangle$.

The p$_T$ differentiated yield per unit rapidity is calculated by the following formula:

$$\frac{d^2N}{dp_T dy} = \frac{1}{\Delta p_T \Delta y} \cdot \frac{1}{N_{MB}^{eqv} \epsilon_{MB}^{gvtx}} \cdot \frac{\epsilon_{MB}^{BBC} \epsilon_{MB}^{gvtx}}{\epsilon_{J/\psi}^{BBC} \epsilon_{J/\psi}^{gvtx}} \cdot \frac{N_{J/\psi}^{raw}}{\epsilon_{J/\psi}^{RC}}$$

where:

$\Delta y = 2$ corresponds to the rapidity acceptance $|y| < 1$

N_{MB}^{eqv} is the equivalent number of MB events, which is calculated based on BBCMB trigger with in-bunch pileup correction.

ϵ_X^{gvtx} is the good vertex efficiency of X (X = MB, J/ψ). This is studied with PYTHIA(p+p)/HIJING(p+Au) + GEANT embeded in zero-bias data.

$\frac{\epsilon_{MB}^{BBC} \epsilon_{MB}^{gvtx}}{\epsilon_{J/\psi}^{BBC} \epsilon_{J/\psi}^{gvtx}}$ is the trigger bias factor, in which ϵ_X^{BBC} is the beam-beam counter efficiency of X (X = MB, J/ψ). This is studied with PYTHIA(p+p)/HIJING(p+Au) + GEANT embeded in zero-bias data.

$N_{J/\psi}^{raw}$ is the raw yield of J/ψ

$\epsilon_{J/\psi}^{RC}$ is the J/ψ reconstruction efficiency

The $\epsilon^{RC}_{J/\psi}$ consists of many aspects and they are studied in different ways.

The $n\sigma_e$ is entirely data driven due to the its discrepancy between data and embedding.

The single electron (track level) efficiencies as well as the momentum resolution (in principle also the resolution of pseudo-rapidity η and azimuthal angle ϕ, but they appears to be negligible) extracted from embedding are translated to EvtGen in order to simulate the J/ψ reconstruction with a more realistic decay model. The resulting reconstructed J/ψ mass distribution from EvtGen serves as the fit template of the signal part for raw yield extraction in real data. At the same time, by comparing the reconstructed (**RC**) J/ψ mass distribution to the Monte Carlo (**MC**) one, one can get the RC efficiency.

In terms of the raw yield extraction, the unlike-sign minus like-sign (**US-LS**) mass distributions is fit to a fit function which consists of the J/ψ signal and residual background:

$$f(M_{e^+e^-} = N_{J/\psi} \times TEMPLATE(M_{e^+e^-}) + N_{ResBG} \times e^{-bM_{e^+e^-}}$$

where $N_{J/\psi}$, N_{ResBG} are the normalization factors of the signal and residual background respectively, and the formula for resudual background is empirical and arbitrary. The raw yield is then extracted by integrating the $N_{J/\psi} \times TEMPLATE(M_{e^+e^-})$. The raw yield is then corrected by the J/ψ RC efficiency.

The embedding samples for STAR experiments usually overestimate the performance in terms of measuring momentum (underestimate the resolution). In order to overcome this issue, a technique of "additional smearing" is performed. The general idea is to assign a new RC p_T to each RC track in embedding and in EvtGen, while η and ϕ stay untouched, where the new RC p_T is determined by the old RC p_T and MC p_T in a pattern. The "pattern" can be varied, and among the variations it is determined by minimizing the difference between the RC mass distribution from EvtGen and from the fit result of real data.

5.2 Number of equivalent MB events based on BBCMB

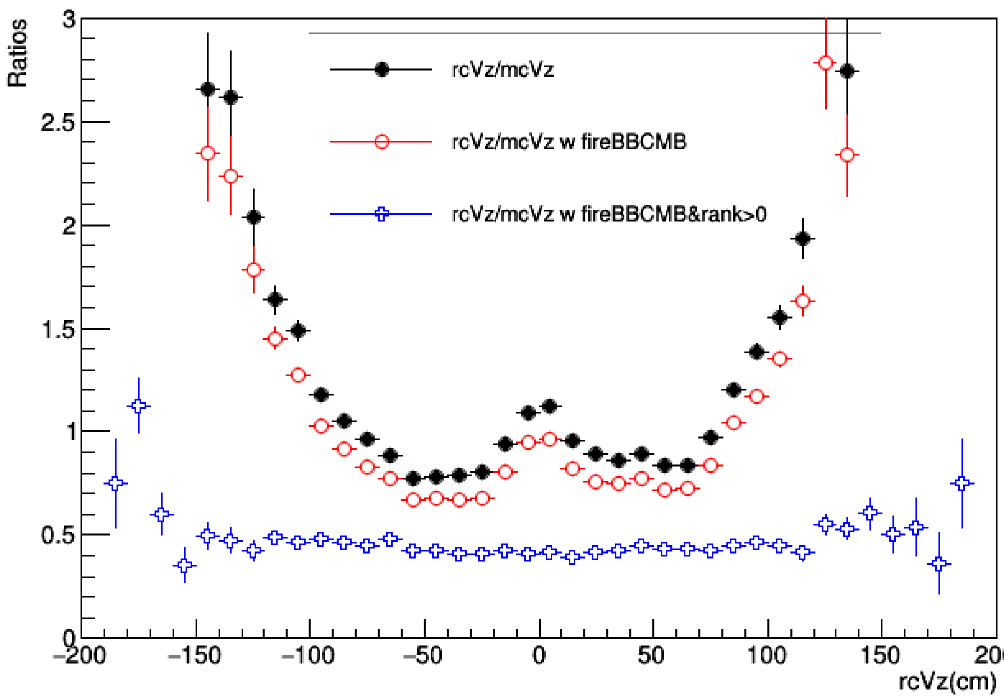

Figure 3: Ratio $\frac{rcVz}{mcVz}$ in the simulation

The figure 3 shows the Ratios of reconstructed Vz over the MC Vz in the simulation, as the blue points shown, after requiring $Ranking > 0$ for the BBC triggered events, the ratio $\frac{rcVz}{mcVz}$ is flat, which suggests that the reconstructed Vz distribution should have the same shape as the true Vz (mcVz is the input true Vz in the simulation). Based on this we could get the fraction of events falling in our analysis cut window $|Vz| < 80$ cm.

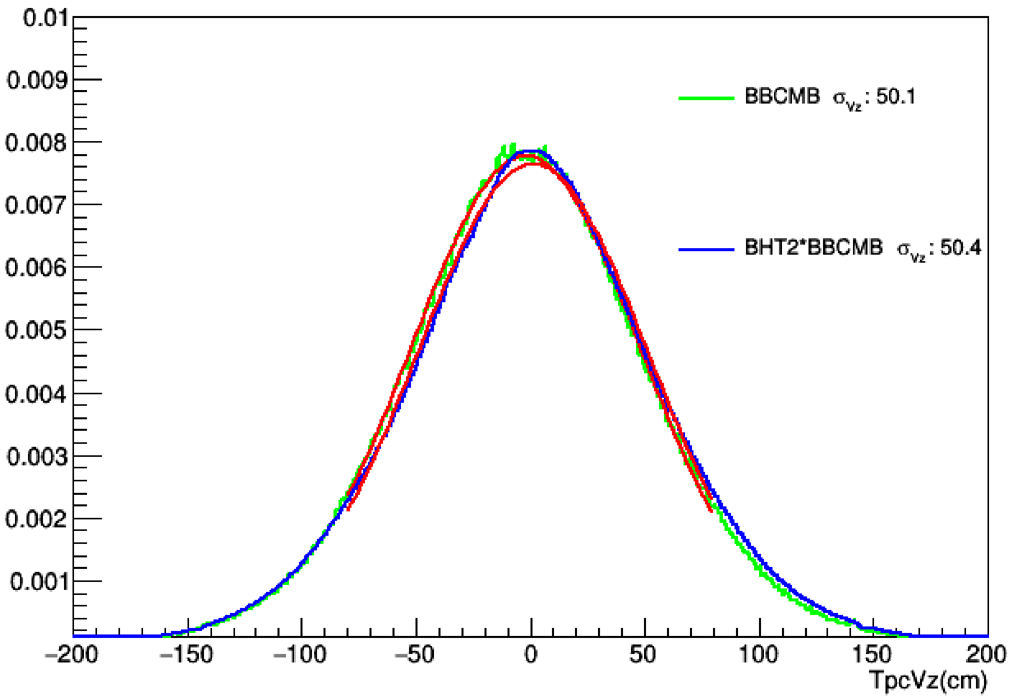

Figure 4: The Tpc Vz with $Ranking > 0$ in the Run15pp real data

figure 4 show the reconstructed Vz by TPC of BBCMB and BHT2*BBCMB triggered events. Based on the real shape of these histograms, we can get the fraction of $\frac{|Vz|<80}{|Vz|<200}$ is 0.8698 for all recorded BBCMB events and 0.8584 for all recorded BHT2*BBCMB events.

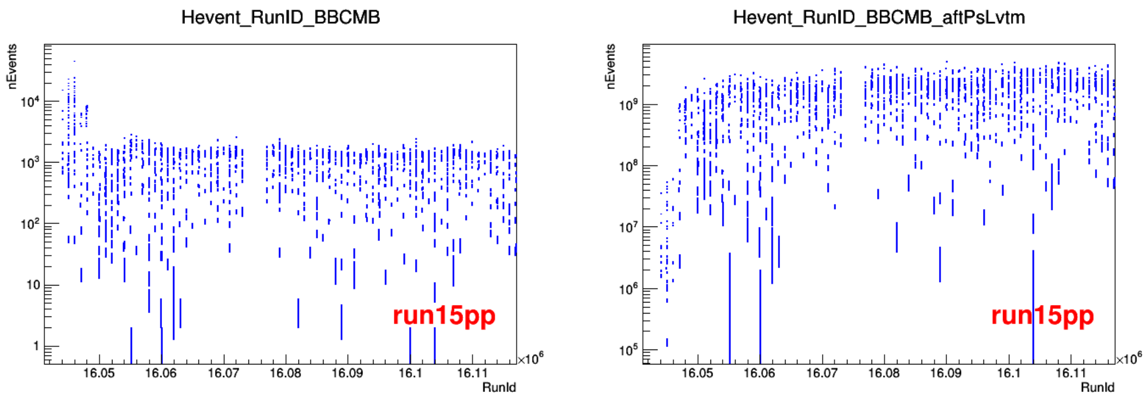

Figure 5: The left panel shows the number of recorded BBCMB events with both BBCMB trigger and BHT2*BBCMB trigger on-line vs Run number, the right panel shows the number of equivalent BBCMB events vs Run number

And after sum of the number of equivalent MB BBC MB events over all runs and multiply the fraction of $\frac{|Vz|<80}{|Vz|<200}$ and multiply the fraction of analyzed BHT2*BBCMB events, the total number of equivalent MB events corresponding to our analyzed BHT2*BBCMB data can be obtained as:

$$N_{MB}^{eqv.}(\text{for all analyzed BHT2 events}) = N_{MB}^{eqv.}(\text{BBCMB and BHT2 on-line}) * \frac{N_{BHT2}(analyzed)}{N_{BHT2}(\text{BBCMB and BHT2 on-line})} =$$

$2.7621 * 10^{12}$

Same thing can be done to p+Au collisions and the plots are shown as following:

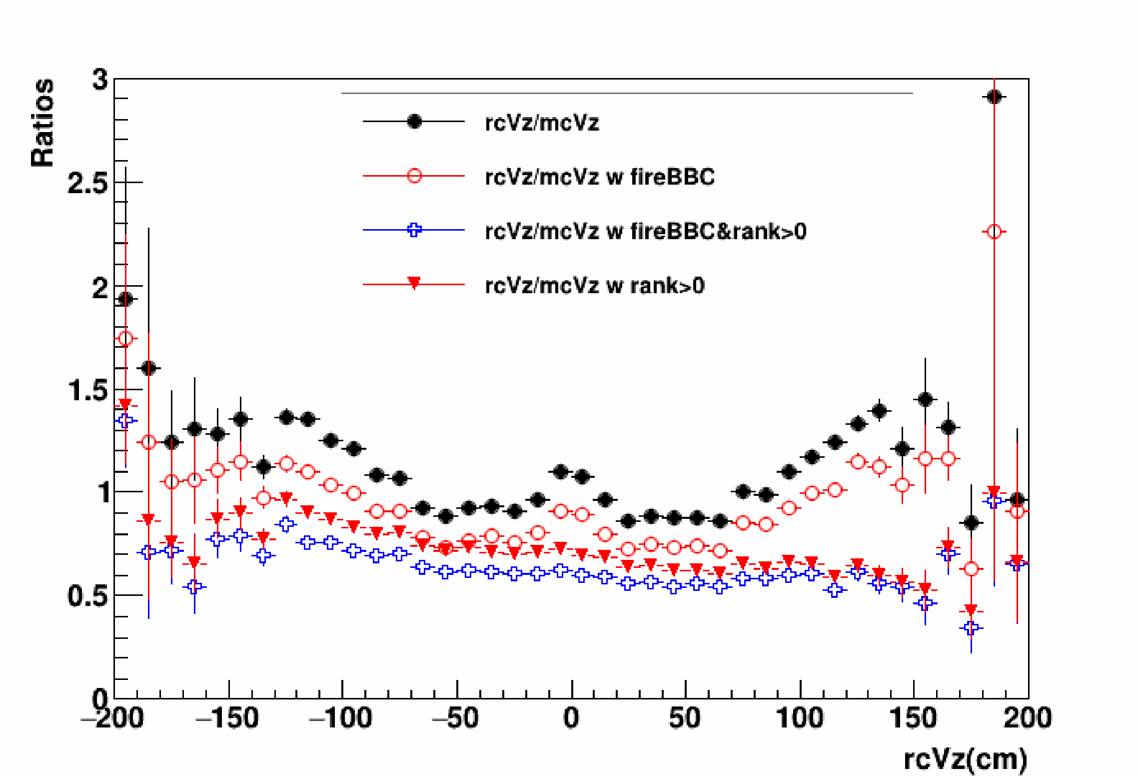

Figure 6: Ratio $\frac{rcVz}{mcVz}$ in the simulation

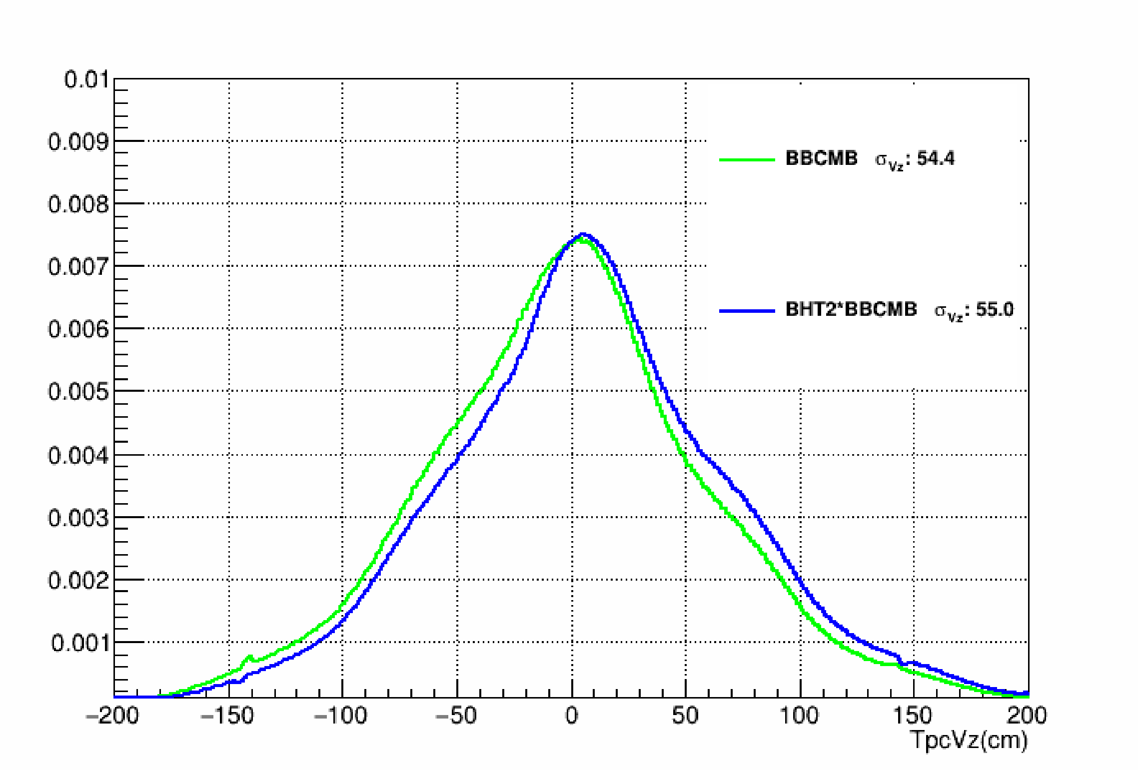

Figure 7: Vz distribution of BBCMB and BHT2 triggered events of Run15 pAu

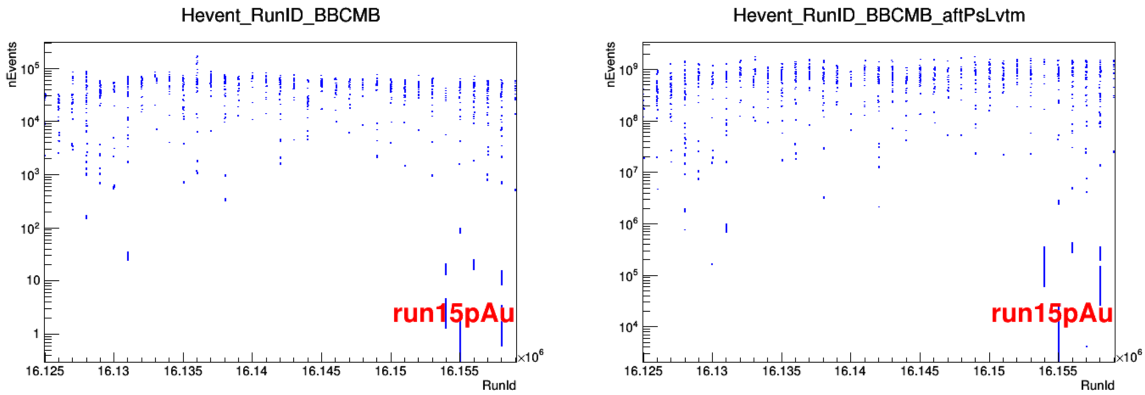

Figure 8: The left panel shows the number of recorded BBCMB events with both BBCMB trigger and BHT2*BBCMB trigger on-line vs Run number, the right panel shows the number of equivalent BBCMB events corresponding to the left panel vs Run number

The $N_{MB}^{eqv.} = 5.5211 \times 10^{11}$

5.3 In-bunch pileup correction

Due to the very high luminosity with 2015 p+p 200 GeV collisions, there might be more than one collisions happened during a bunch crossing, so we need to consider the contribution from the in-bunch pileup. Assuming that λ is the probability that one collision happens during a given bunch-crossing. Then the probability of that there are k collisions happen in a bunch-crossing would be:

$$P_k[\text{k collisions in a bunch-crossing}] = \frac{\lambda^k e^{-\lambda}}{k!}$$

and we would have: $P_0 = e^{-\lambda}$, $P_1 = \lambda e^{-\lambda}$, $P_2 = \frac{\lambda^2}{2} e^{-\lambda}$ and $P_3 = \frac{\lambda^3}{6} e^{-\lambda}$

The contribution of $k \geq 3$ is much smaller compared to k=1 and k=2, when the BBC is fired from collisions, we can only consider k=1 and k=2 cases. Let ϵ as the BBC single side fire efficiency($\epsilon = 0.9$).

- Then, for k=1, the probability of that two sides of BBC are fired:

$$P_{BBC}[k = 1] = P_1 * \epsilon^2$$

- Then, for k=2, two sides of BBC are fired can be the following cases:
    1. two collisions both fire two sides of BBC
    2. one collision fire two sides of BBC and another one fire only one side of BBC
    3. one collision fire two sides of BBC and another one fired nothing
    4. one collision fire only one side of BBC and the other collision fire the other side of BBC

Then, the probability of that two sides of BBC are fired:
$P_{BBC}[k = 2] = P_2 * [\epsilon^4 + 4 * \epsilon^3(1-\epsilon) + 2 * \epsilon^2(1-\epsilon)^2 + 2 * \epsilon^2(1-\epsilon)^2] = P_2 * [\epsilon^2(2-\epsilon)^2]$
So, among the BBC triggered events, fraction of k=2 events can be obtained by:

$$Fraction(k = 2) = \frac{P_{BBC}[k = 2]}{P_{BBC}[k = 1] + P_{BBC}[k = 2]} = \frac{P_2 * [\epsilon^2(2-\epsilon)^2]}{P_2 * [\epsilon^2(2-\epsilon)^2] + P_1 * \epsilon^2} = \frac{\lambda(2-\epsilon)^2}{2 + \lambda(2-\epsilon)^2}$$

If we assume the BBC rates are all due to the real collisions, then we would have:

$$\lambda \cong \frac{BBCRate/\epsilon^2}{9.383MHz * (102/120)}$$

A roughly estimation of the fraction of k=2: for the BBC rate at 0.5 MHz, 1.3 MHz, 2.5 MHz, $\lambda =$ 0.0774, 0.201, 0.387, the $Fraction(k = 2) = 5.2\%, 12.4\%, 21.5\%$.

Note that: The above estimation assumed the BBC rate from the real data are all coming from the real collisions.

5.3.1 How to quantify the contribution of in-bunch pile-up

The BBC rate in per bunch-crossing due to the real collisions should be the expectation of k=1 and k=2 collisions, then we have the following relation:

$$\frac{BBCRate}{9.838MHz * \frac{102}{120}} = 1 * P_1 * \epsilon^2 + 2 * P_2 * \epsilon^2(2-\epsilon)^2 + ... \cong \lambda e^{-\lambda}\epsilon^2 + \lambda^2 e^{-\lambda}\epsilon^2(2-\epsilon)^2$$

then, when λ is small and ϵ close to 1 we would have:

$$\frac{BBCRate/\epsilon^2}{9.838MHz * \frac{102}{120}} = \lambda e^{-\lambda} + \lambda^2 e^{-\lambda}(2-\epsilon)^2 \cong \lambda$$

Considering the strong correlation between BBC trigger and the VPD trigger, we can make use of the VPD trigger rate to calculate the corresponding BBC rate due to the real collision.

$$BBCRate = VPDRate * Slope = \frac{nVPDEvts * Prescale_{VPD}}{RunTime * LiveTime_{VPD}} * Slope, \text{ for a given run}$$

then, we would have:

$$\lambda \cong \frac{BBCRate/\epsilon^2}{9.838MHz * \frac{102}{120}} = \frac{nVPDEvts * Prescale_{VPD}}{RunTime * LiveTime_{VPD}} * Slope * \frac{1}{\epsilon^2} * \frac{1}{9.838MHz * \frac{102}{120}}$$

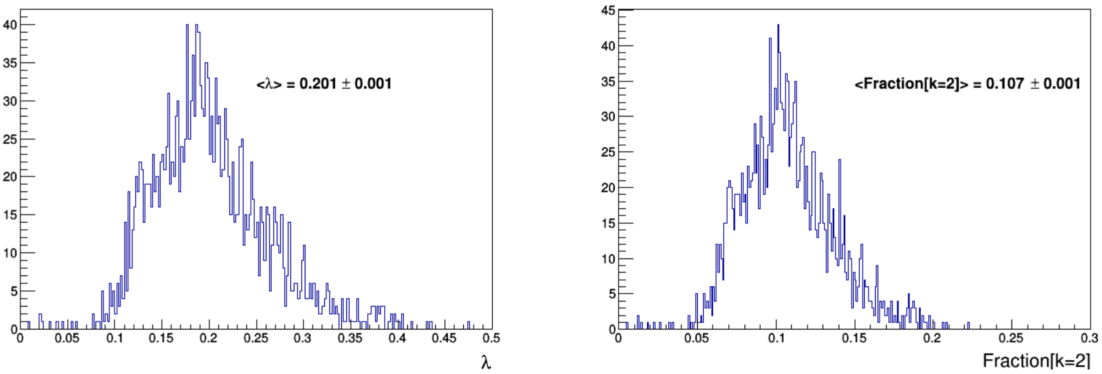

Figure 9: The left panel shows the λ distribution and the right panel shows the $fraction[k=2]$ distribution

and for each run, we could get a λ and a $Fraction[k=2]$, so to calculate the average of $Fraction[k=2]$ for all runs, we could do:

$$< Fraction[k=2] >= \frac{\sum_{firstRun}^{lastRun} eqv.MB[iRun] * Fraction(iRun)}{\sum_{firstRun}^{lastRun} eqv.MB[iRun]}$$

and the average λ and the average $Frac[k=2]$ are obtained as 0.201 ± 0.001 and 0.107 ± 0.001. Thus, the number of equivalent MB events should be corrected by:

$$N_{MB}^{eqv.,In-bunch-corr} = N_{MB}^{eqv.} * (1+ < Frac[k=2] >) = 2.7621 * 10^{12} * (1+0.107) = 3.06 \times 10^{12}$$

Given that there's a small difference in the total number of analyzed BHT2*BBC events between the study on raw yield (206.584M) and the study on the $N_{MB}^{eqv.}$ (211.8M), an additional scale factor of 206.584/211.8 is applied, yielding the final $N_{MB}^{eqv.,finale} = 2.98 \times 10^{12}$ for p+p.

Similar thing can be done for p+Au collisions. The following is the relavant figure:

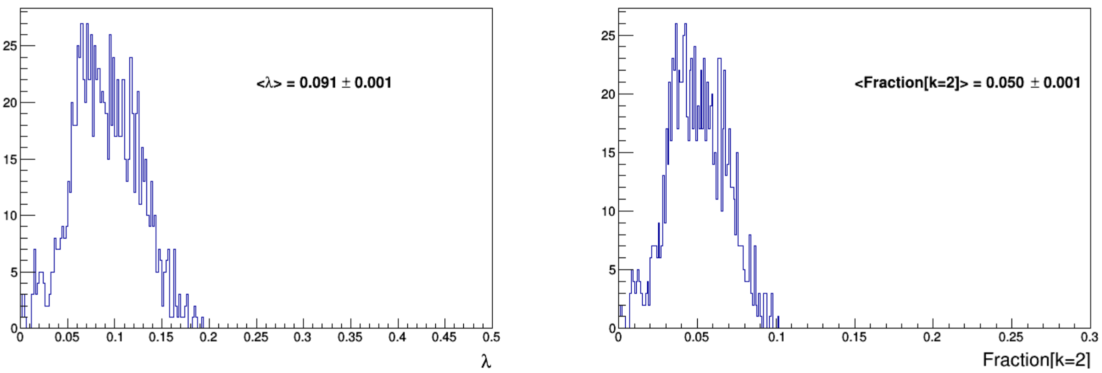

Figure 10: The left panel shows the λ distribution and the right panel shows the $fraction[k = 2]$ distribution

The in-bunch pileup correction factor for p+Au collision is $\langle Frac[k = 2]\rangle = 0.05 \pm 0.01$. The total number of BHT2*BBCMB events in the raw yield study and the $N_{MB}^{eqv.}$ study are 168.165M and 165.8M respectively. Therefore the final $N_{MB}^{eqv.,finale} = 5.88 \times 10^{11}$ for p+Au.

5.4 Trigger bias study

In our simulation, Pythia and HIJING is used as the event generator for p+p and p+Au collisions respectively.Then let the MC event go to STAR GEANT, and then mix the MC hits with those from the Zero-bias data. In this way, the trigger bias study is done under the environment same as the real data taking. And the Trigger bias definition is different for different method to calculate the equivalent MB events. In the Trigger Bias study, we present two results corresponding to the two different methods to calculate the equivalent MB events.

5.4.1 p+p

Simulation setup The event generator is Pythia8.162 +LHAPDF-6.1.4 (LHAPDF is a general purpose C++ interpolator, used for evaluating PDFs from discretised data files, detail document). And for the simulation, we have two kinds of events: MB only event and with J/ψ or Υ event. For the MB only event, the Pythia setting is "pythia8→Set("SoftQCD:minBias = on")". For the J/ψ or Υ event, a tunned settings named "STAR Heavy flavor tune" are used. And the details about the heavy flavor tune can be found at:STAR HF Tune

- Pythia8 + GEANT + Zero-Bias embedding

  Embed the simulated event into the Zero-bias triggered real data (daq files)

  The daq files are picked up from every 2 runs, cover full run ranges

- Library: SL16d

- Chain options for simulation production:
  "ry2015c geant gstar agml usexgeom Form(sdt%s,timestamp.Data())"

- Vertex setting:

  1. Vx and Vy: Get the time stamp based the run-number, and cast the time stamp to bfc, let it get the beam line shape from the database by itself. It will set the vx and vy to be same as in real data

  2. Vz: Set the Vz distribution with the Gaussian shape fitted from data

- Chain options used in the reconstruction step of simulation:

  fzin, gen$_T$, geomT, sim$_T$, TpcRS, sdtYYMMDD.HHMMSS, ry2015c, DbV20160418, pp2015c, btof, mtd ,mtdCalib,pp2pp, fmsDat, fmsPoint, fpsDat, BEmcChkStat, CorrX, OSpaceZ2, OGridLeak3D, -hitfilt, TpxClu, bbcSim, pxlFastSim,istFastSim, btofSim,

emcY2, emcSim, EEfs, mtdsim, TpcMixer, GeantOut, MiniMcMk, McAna, IdTruth, -in, useInTracker, -emcDY2

- with J/ψ or Υ filter:
  J/ψ event: $|y_{J/\psi}| < 1$, $|\eta_{e^+/e^-}| < 1$, $p_T(e^+/e^-) > 0.2$ GeV/c
  Υ event: $|y_\Upsilon| < 1$, $|\eta_{e^+/e^-}| < 1$, $p_T(e^+/e^-) > 0.2$GeV/c
  D_0 event: $|y_{D_0}| < 1$, $|\eta_{(K/\pi)}| < 1$, $p_T(K/\pi) > 0.2$ GeV/c

Result

- Luminosity in the simulation(Zero-bias) is weighted to what in the real data.
- Definition of BBC trigger: both BBC East and BBC West fired, denoted as "BBCAnd"
- Vertex cut: $|Vz| < 80cm$ (default vertex)
- dVzCut: $|rcVz - mcVz| < 1.5cm$
- Good Vertex: dVzCut and $Ranking > 0$

For the J/ψ or Υ cross-section calculation in this case:

$$\sigma_{J/\psi} = \frac{\sigma_{MB}}{N_{MB}^{eqv.}\epsilon_{MB}^{goodvtx}} * \frac{N_{J/\psi}^{raw}}{\epsilon_{J/\psi}^{Trig}\epsilon_{J/\psi}^{trk}\epsilon_{J/\psi}^{eID}} * \frac{\epsilon_{MB}^{BBC}\epsilon_{MB}^{goodvtx}}{\epsilon_{J/\psi}^{BBC}\epsilon_{J/\psi}^{goodvtx}}$$

As the $N_{MB}^{eqv.}$ is corrected by the in-bunch pile up effects($Frac[k=2]$), thus the corresponding ϵ_{MB}^{BBC}, $\epsilon_{J/\psi}^{BBC}$, $\epsilon_{MB}^{goodvtx}$, $\epsilon_{J/\psi}^{goodvtx}$ should also be corrected accordingly.

The BBC trigger efficiency can be corrected by:

$$<\epsilon>=\epsilon[k=1]*Frac[k=1]+\epsilon[k=2]*Frac[k=2] <\epsilon_{MB}^{BBC}>=\epsilon_{MB}^{BBC}[k=1]*Frack[k=1]+\epsilon_{MB}^{BBC}[k=2]*Frack[k=2]$$

and we have:

- $\epsilon_{MB}^{BBC}[k=1] = \epsilon_1^2$, and $\epsilon_{MB}^{BBC}[k=2] = \epsilon_1^2(2-\epsilon_1)^2$
- $\epsilon_{J/\psi}^{BBC}[k=1] = \epsilon_2^2$, and $\epsilon_{J/\psi+MB}^{BBC}[k=2] = \epsilon_1^2\epsilon_2^2 + [2\epsilon_1^2\epsilon_2(1-\epsilon_2) + 2\epsilon_2^2\epsilon_1(1-\epsilon_1)] + [\epsilon_1^2(1-\epsilon_2^2) + \epsilon_2^2(1-\epsilon_1^2)] + 2\epsilon_1(1-\epsilon_1)\epsilon_2(1-\epsilon_2) = (\epsilon_1+\epsilon_2-\epsilon_1\epsilon_2)^2$

Where ϵ_1 is BBC single side efficiency from the MB only event simulations and ϵ_2 is the BBC single side efficiency from Jpsi or Upsilon event simulations.

Note that for the BBC efficiency of J/ψ event, we can ignore the probability of 2 J/ψ produced in a bunch crossing, instead, we consider 1 J/ψ event + 1 MB event here.

FireType/EvtType	MBonly	J/ψ	Υ	D_0
BBCsingleFire	0.9278	0.9119	0.9038	0.9179
BBCdoubleFire	0.8603	0.8316	0.8166	0.8425

Table 1: Run15 pp BBC single fire and double fire efficiencies

And for the good vertex reconstruction efficiency. $\epsilon_{MB}^{goodvtx}$ will be canceled, so it doesn't need any further corrections.

And for the ZB data, the probabilities of k=0, k=1 and k=2 can be given by Poisson distributions: $P_0 = e^{-\lambda}$, $P_1 = \lambda e^{-\lambda}$, $P_2 = \frac{\lambda^2}{2}e^{-\lambda}$. Let the probability to produce a J/ψ in a event be $p_{J/\psi}$, $p_{J/\psi}$ should be $<< P_0, P_1, P_2$.

K/ϵ_{BBC}	ϵ_{MB}^{BBC}	$\epsilon_{MB+J/\psi}^{BBC}$	$\epsilon_{MB+\Upsilon}^{BBC}$	$\epsilon_{MB+D_0}^{BBC}$
K=1	0.8608	0.8316	0.8169	0.8425
K=2	0.9896	0.9873	0.9862	0.9882

Table 2: Run15 pp BBC efficiencies for K=1 and K=2

Since a MC J/ψ event is embedded into a Zero-Bias event, in principle, each event in these simulation should be:

$$1\ J\psi \text{ event} + 1 \text{ ZB event}$$

And for the $\epsilon_{J/\psi}^{goodvtx}$ in the PYTHIA+GEANT+ZeroBias simulation is from the total contribution of 1 J/ψ event + 1 ZB event(k=0, k=1, k=2). Thus the relative contributions of k=0, k=1, k=2 will be proportional to $p_{J/\psi} * p_0$:$p_{J/\psi} * p_1$:$p_{J/\psi} * p_2$, which is actually same as in the real data of our analysis. Thus $\epsilon_{J/\psi}^{goodvtx}$ can be obtained directly from the PYTHIA+GEANT+ZeroBias simulations.

$< \epsilon_{MB}^{BBC} >$	$< \epsilon_{J/\psi}^{BBC} >$	$< \epsilon_{\Upsilon}^{BBC} >$	$< \epsilon_{D_0}^{BBC} >$
0.8746	0.8483	0.8350	0.8582

Table 3: Run15 pp BBC efficiencies

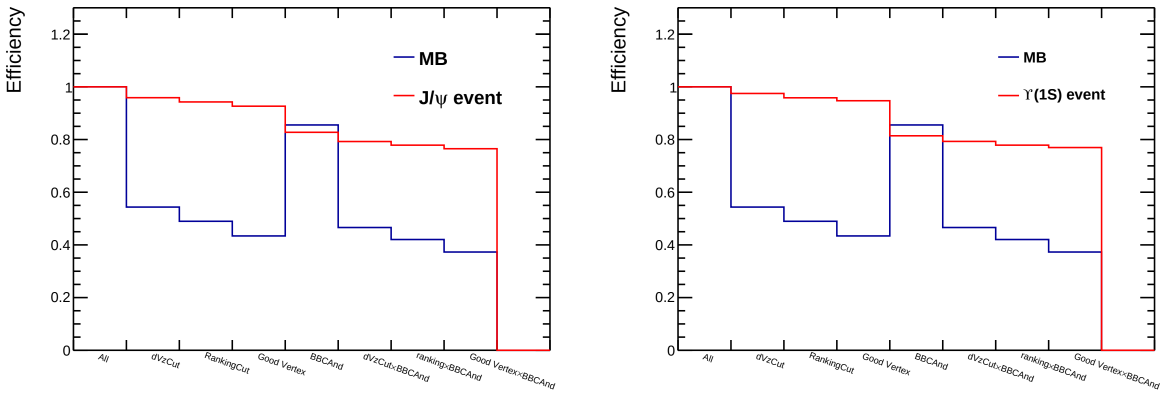

Figure 11: dVzCut: $|mcVz - rcVz| < 1.5$ cm cm; RankingCut: $ranking > 0$; good Vertex: dVzCut&RankingCut; BBCAnd: BBC both sides fired; we are using the default vertex (highest ranking)

$< \epsilon_{MB}^{goodVtx} >$	$< \epsilon_{J/\psi}^{goodVtx} >$	$< \epsilon_{\Upsilon}^{goodVtx} >$	$< \epsilon_{D_0}^{goodVtx} >$
0.4340	0.9266	0.9472	0.8487

Table 4: Run15 pp good Vertex efficiency

And the final trigger bias factors (while BBC as the Base trigger) are calculated and listed in Table. 5

	J/ψ	Υ	D_0
TrigBias	0.4829	0.4800	0.5211

Table 5: Run15 pp Trigger Bias $\frac{<\epsilon_{MB}^{BBC}><\epsilon_{MB}^{goodvtx}>}{<\epsilon_e xtpArticle^{BBC}><\epsilon_e xtpArticle^{goodvtx}>}$, Particle = J/ψ or Υ.

Contribution to global systematic uncertainty The TrigBias is calculated using another Pythia8 tuning "Tune:4Cx". More information about the Tune:4Cx can be found at: http://home.thep.lu.se/ torbjorn/pythia81html/Tunes.html.

	J/ψ	Υ
TrigBias	0.4816	0.4837

Table 6: Run15 pp Trigger Bias $\frac{<\epsilon_{MB}^{BBC}><\epsilon_{MB}^{goodvtx}>}{<\epsilon_e xtpArticle^{BBC}><\epsilon_e xtpArticle^{goodvtx}>}$, Particle = J/ψ or Υ.

Take the difference between the Trig-Bias results with HF-Tune and Tune:4Dx as the systematic uncertainty of Trig-Bias.

	J/ψ	Υ
TrigBias Sys.Error	2.7%	0.7%

Table 7: Systematic uncertainties of 2015 pp Trigger Bias of J/ψ or Υ.

5.4.2 p+Au

Simulation setup The event generator is HIJING + LHAPDF-6.1.4 (LHAPDF is a general purpose C++ interpolator, used for evaluating PDFs from discretised data files, detail document). And for the simulation, we have two kinds of events: MB only event and with D^0 event. (Quarkonium production is not available in HIJING simulator, D^0 is used to mimic the J/ψ events for the Trigger Bias study of Run15 pAu.

- Settings for the MB-only events in HIJING:
  hijing→SetImpact(0.0, 15.0); //Impact parameter (min, max) (fm)
  hijing→hiparnt().ihpr2(4)=0; //Jet quenching (1=yes/0=no)
  hijing→hiparnt().ihpr2(3)=0; //Hard scatering (heavy quark)
  hijing→hiparnt().ihpr2(18) = 1; // Turn on/off B production
  hijing→hiparnt().hipr1(10) = 2.0; // p_T jet
  hijing→hiparnt().ihpr2(8) = 10; // Max number of jets /nucleon
  hijing→hiparnt().ihpr2(11) = 1; // Set baryon production
  hijing→hiparnt().ihpr2(12) = 1; // Turn on/off decay of particles
  hijing→hiparnt().hipr1(7) = 5.35; // Set B production
  hijing→hiparnt().ihpr2(21) = 1; //Enable to track all particles
- Settings for the D^0 events in HIJING:
  hijing→SetImpact(0.0, 15.0); //Impact parameter (min, max) (fm)
  hijing→hiparnt().ihpr2(4)=0; //Jet quenching (1=yes/0=no)
  hijing→hiparnt().ihpr2(3)=0; //Hard scatering (heavy quark)
  hijing→hiparnt().ihpr2(18) = 1; // Turn on/off B production
  hijing→hiparnt().hipr1(10) = 2.0; // p T jet
  hijing→hiparnt().ihpr2(8) = 10; // Max number of jets /nucleon
  hijing→hiparnt().ihpr2(11) = 1; // Set baryon production
  hijing→hiparnt().ihpr2(12) = 1; // Turn on/off decay of particles
  hijing→hiparnt().hipr1(7) = 5.35; // Set B production
  hijing→hiparnt().ihpr2(21) = 1; //Enable to track all particles
- HIJING + GEANT + Zero-Bias embedding
  Embed the simulated event into the Zero-bias triggered real data (daq files)
  The daq files are picked up from every 2 runs, cover full run ranges
- Library: SL16d
- Chain options for simulation production:
  "ry2015c geant gstar agml usexgeom Form(sdt%s,timestamp.Data())"

- Vertex setting:
  1. Vx and Vy: Get the time stamp based the run-number, and cast the time stamp to bfc, let it get the beam line shape from the database by itself. It will set the vx and vy to be same as in real data
  2. Vz: Set the Vz distribution with the Gaussian shape fitted from data
- Chain options used in the reconstruction step of simulation:

  fzin, gen$_T$, geomT, sim$_T$, TpcRS, sdtYYMMDD.HHMMSS, ry2015c, DbV20160418, pp2015c, btof, mtd ,mtdCalib,pp2pp, fmsDat, fmsPoint, fpsDat, BEmcChkStat, CorrX, OSpaceZ2, OGridLeak3D, -hitfilt, TpxClu, bbcSim, pxlFastSim,istFastSim, btofSim, emcY2, emcSim, EEfs, mtdsim, TpcMixer, GeantOut, MiniMcMk, McAna, IdTruth, -in, useInTracker, -emcDY2

- with J/ψ or Υ filter:

  J/ψ event: $|y_{J/\psi}| < 1$, $|\eta_{e^+/e^-}| < 1$, $p_T(e^+/e^-) > 0.2$ GeV/c

  Υ event: $|y_\Upsilon| < 1$, $|\eta_{e^+/e^-}| < 1$, $p_T(e^+/e^-) > 0.2$GeV/c

  D_0 event: $|y_{D_0}| < 1$, $|\eta_{(K/\pi)}| < 1$, $p_T(K/\pi) > 0.2$ GeV/c

Result After considering the in-bunch pileup contribution, the BBC trigger efficiency can be corrected by:

$$< \epsilon >= \epsilon[k=1]*Frac[k=1]+\epsilon[k=2]*Frac[k=2] < \epsilon_{MB}^{BBC} >= \epsilon_{MB}^{BBC}[k=1]*Frack[k=1]+\epsilon_{MB}^{BBC}[k=2]*Frack[k=2]$$

K/ϵ_{BBC}	ϵ_{MB}^{BBC}	$\epsilon_{MB+D_0}^{BBC}$
K=1	0.8355	0.8823
K=2	0.9829	0.9865

Table 8: Run15 pAu BBC efficiencies for K=1 and K=2

and we have:

- $\epsilon_{MB}^{BBC}[k=1] = \epsilon_E(MB) * \epsilon_W(MB)$
- $\epsilon_{MB}^{BBC}[k=2] = \epsilon_E(MB) * \epsilon_W(MB) * (2 - \epsilon_E(MB))(2 - \epsilon_W(MB))$
- $\epsilon_{D_0}^{BBC}[k=1] = \epsilon_E(D_0) * \epsilon_W(D_0)$
- $\epsilon_{D_0+MB}^{BBC}[k=2]$
  $= \epsilon_E(MB)*\epsilon_W(MB)*\epsilon_E(D_0)*\epsilon_W(D_0) + \epsilon_E(MB)*\epsilon_W(MB)*\epsilon_E(D_0)*(1-\epsilon_W(D_0)) + \epsilon_E(MB)*\epsilon_W(MB)*(1-\epsilon_E(D_0))*\epsilon_W(D_0) + \epsilon_E(MB)*(1-\epsilon_W(MB))*\epsilon_E(D_0)*\epsilon_W(D_0) + (1-\epsilon_E(MB))*\epsilon_W(MB)*\epsilon_E(D_0)*\epsilon_W(D_0) + \epsilon_E(MB)*\epsilon_W(MB)*(1-\epsilon_E(D_0))*(1-\epsilon_W(D_0)) + (1-\epsilon_E(MB))*(1-\epsilon_W(MB))*\epsilon_E(D_0)*\epsilon_W(D_0) + \epsilon_E(MB)*(1-\epsilon_W(MB))*(1-\epsilon_E(D_0))*\epsilon_W(D_0) + (1-\epsilon_E(MB))*\epsilon_W(MB)*\epsilon_E(D_0)*(1-\epsilon_W(D_0))$
  $= \epsilon_E(MB)*\epsilon_W(MB)*\epsilon_E(D_0)*\epsilon_W(D_0)$ - $\epsilon_E(MB)*\epsilon_W(MB)(\epsilon_E(D_0)+\epsilon_W(D_0))$ - $(\epsilon_E(MB)+\epsilon_W(MB))*\epsilon_E(D_0)*\epsilon_W(D_0) + \epsilon_E(MB)*\epsilon_W(MB) + \epsilon_E(D_0)*\epsilon_W(D_0) + \epsilon_E(MB)*\epsilon_W(D_0) + \epsilon_W(MB)*\epsilon_E(D_0)$

Where $\epsilon_E(MB), \epsilon_W(MB), \epsilon_E(D_0), \epsilon_W(D_0)$ is BBC single side efficiencies from the MB only or the D_0 event simulations. Note that for the BBC efficiency of D_0 event, we can ignore the probability of 2 D_0 produced in a bunch crossing, instead, we consider 1 D_0 event + 1 MB event here.

$< \epsilon_{MB}^{BBC} >$	$< \epsilon_{D_0}^{BBC} >$
0.8428	0.8874

Table 9: Run15 pAu BBC efficiencies

$< \epsilon_{MB}^{goodVtx} >$	$< \epsilon_{D_0}^{goodVtx} >$
0.5464	0.9268

Table 10: Run15 pAu good Vertex efficiency

	D_0
TrigBias	0.5599

Table 11: Run15 pAu Trigger Bias $\frac{<\epsilon_{MB}^{BBC}><\epsilon_{MB}^{goodvtx}>}{<\epsilon_extpArticle^{BBC}><\epsilon_extpArticle^{goodvtx}>}$, Particle $= D_0$.

5.5 Data Driven $n\sigma_e$ Efficiency

The STAR embedding does not provide acceptable simulation on the $n\sigma_e$ (see Embedding QA appendix), therefore the $n\sigma_e$ efficiency is extracted from data with photonic electron pairs. In this analysis, the photonic electron pairs are selected by requiring $M_{ee} < 0.24$GeV/c^2 and DCA$_{ee} < 1$ cm on top of basic tracking quality and kinematics cuts. The mean and width of $n\sigma_e$ distribution are extracted from this sample as functions of momentum (p). Both mean and width show asymptotic behavior towards constant. Therefore, functions are extrapolated over $p > 20$ GeV/c with constant fits in $3 < p < 20$GeV/c. With these functions, and given $n\sigma_e$ cuts and reconstructed p of each track, we can calculate the probability of the track being selected, which is by definition the $n\sigma_e$ efficiency. The following shows how the momentum range is binned and Gaussian fit results in each bin for both p+p and p+Au:

p+p

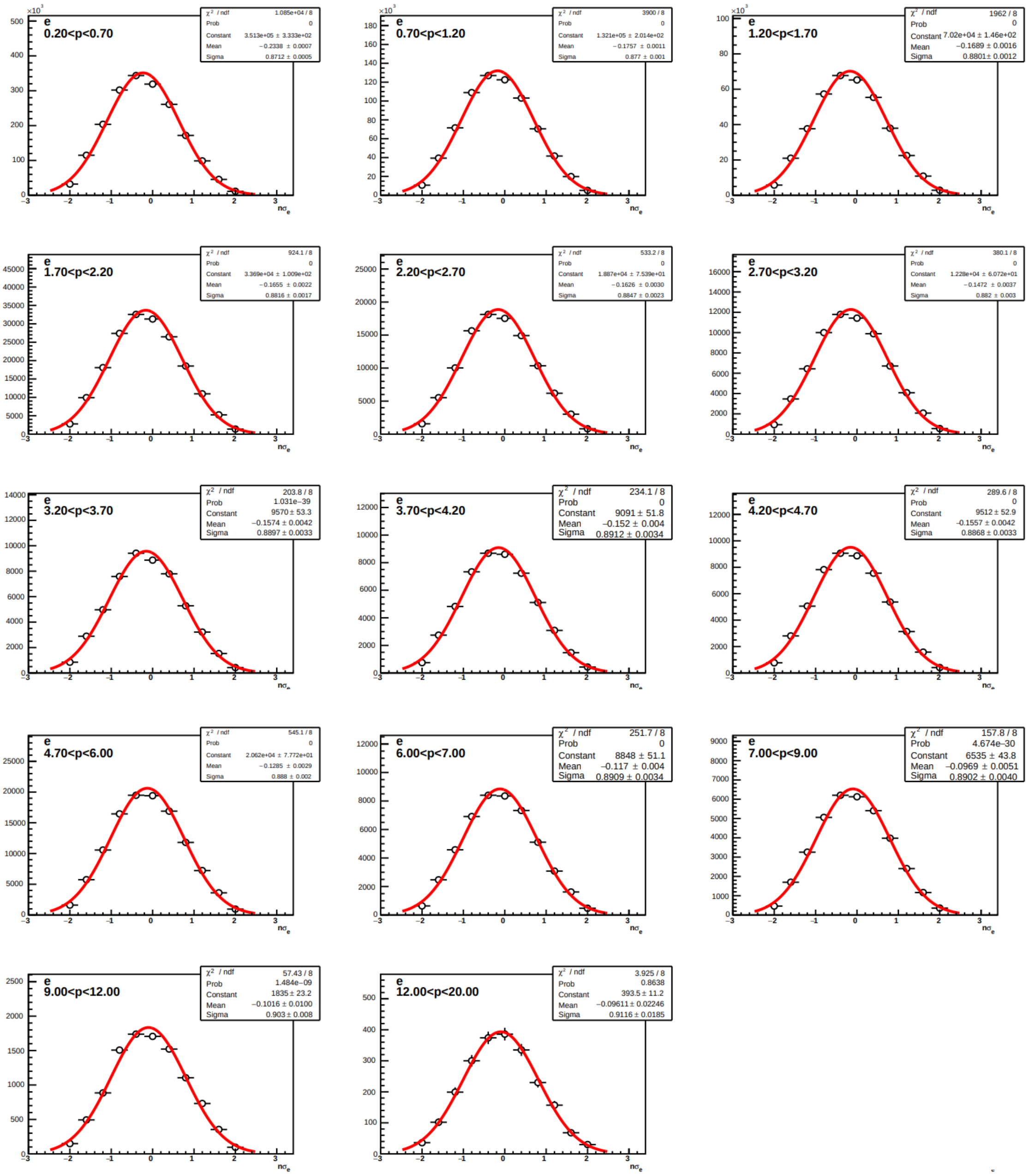
e 0.20<p<0.70
e 0.70<p<1.20
e 1.20<p<1.70
e 1.70<p<2.20
e 2.20<p<2.70
e 2.70<p<3.20
e 3.20<p<3.70
e 3.70<p<4.20
e 4.20<p<4.70
e 4.70<p<6.00
e 6.00<p<7.00
e 7.00<p<9.00
e 9.00<p<12.00
e 12.00<p<20.00

p+Au

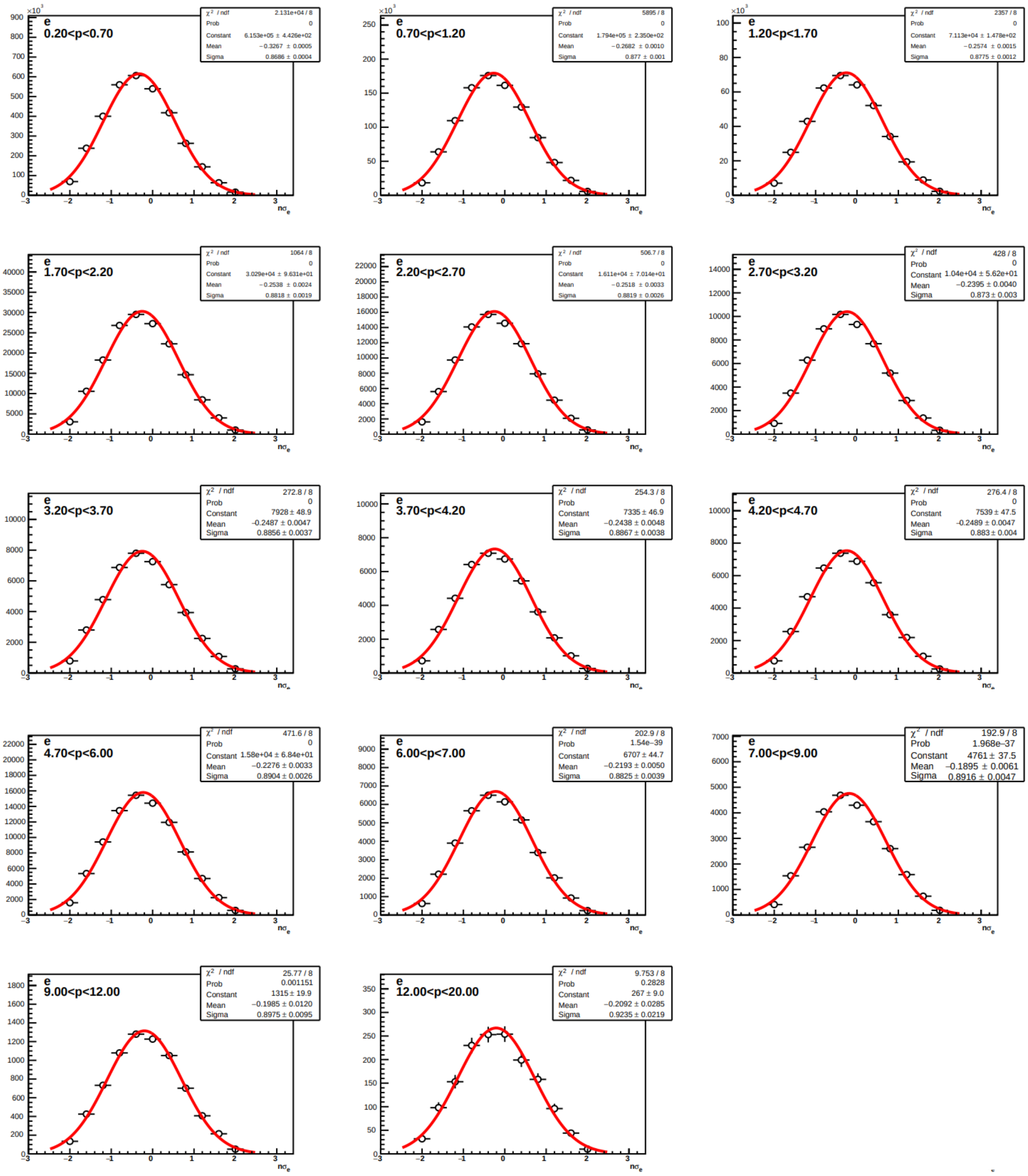

5.6 Single $e^{\pm}$ Efficiencies and p$_T$ Smearing Templates in Embedding

The single $e^{\pm}$ efficiencies are extracted from embedding to be utilized in EvtGen, in order to implement a more realistic decay model. All cuts mentioned in the "Event and Track Selection" section is applied based on embedding result, with one exception of the data driven $n\sigma_e$ efficiency implementation. The other cuts will accept or reject the events/tracks, while the $n\sigma_e$ distribution extracted from the previous section provides the $n\sigma_e$ efficiency as a function of $e^{\pm}$ reconstructed momentum and serve as weighting fators. Only the prompt daughter $e^{\pm}$s (before interacting with detector materials) are included, i.e. scattering electrons are not included.

The following is a list of cuts used in this analysis of different category:

Tracking: nHitsFit, nHitsDedx, nHitsRatio, DCA, nσ_e, η, p$_T$

Electron Identification: e/p, deposited energy

Trigger electron: Adc0, Dsmadc, trigger p_T

Cuts are combined into groups for convenience. The groups are named by “TPC” cuts, “EID” cuts and “Trigger” cuts (short as “TRG”).

1. “TPC” includes all cuts that have non-negligible φ dependence and must exclude cuts that directly depend on reconstructed momentum (p_T^{RC}): nHitsFit, nHitsDedx, nHitsRatio, DCA, η

2. “TRG” includes the only 3 trigger related cuts: Adc0, Dsmadc

3. “EID” includes the rest of the cuts (deposited energy in EMC tower e, e/p, nσ_e), must have positive p_T)

Such grouping is mainly for the following consideration:

1) All cuts that could influence “p_T smearing” and “additional smearing” are contained in a single group (TPC)

2) All cuts whose variable directly depend on on p_T^{RC} are contained in a single group (EID)

3) All cuts that has φ dependence are contained in a signle group (TPC)

4) All cuts that reject positrons and electrons differently are contained in a signle group (TPC)

The following are the definition of efficiencies. The kinematics variable p_T, η and φ are all in MC level.

1. The TPC have p_T, η and φ dependence, and electrons and positrons are treated seperately. The definition is as follows:

$\epsilon_{\pm}^{TPC}(p_T, \eta, \varphi) = \frac{N_{\pm}^{TPC}(p_T,\eta,\varphi)}{N_{\pm}^{MC}(p_T,\eta,\varphi)}$

where the $N_{\pm}^{MC}$ is the number of MC electron/positron, and $N_{\pm}^{TPC}$ is the number of electron/positron that passed TPC cuts. The following plots show the dependency of TPC efficiency on p_T, η and φ. Significant difference is observed in φ dependence. These are purely for demonstration purposes since they are integrated over 2 out of 3 designed variable (p_T, η and φ).

p+p

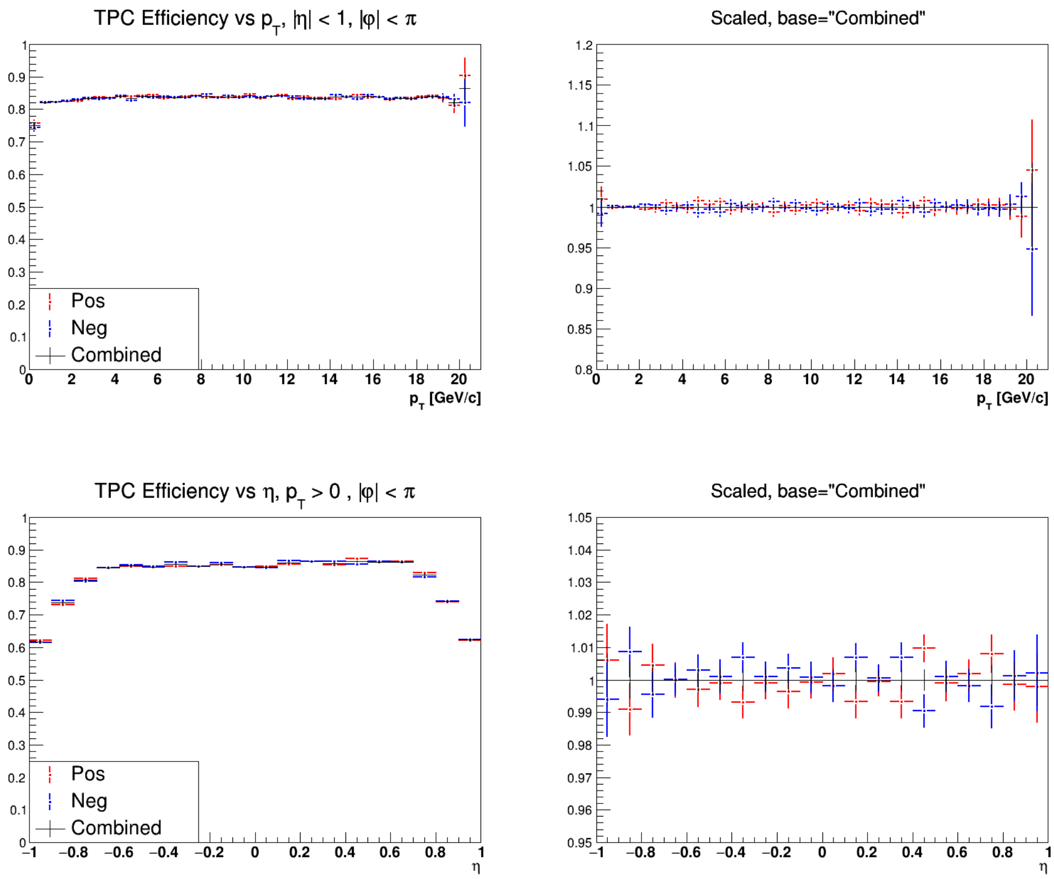

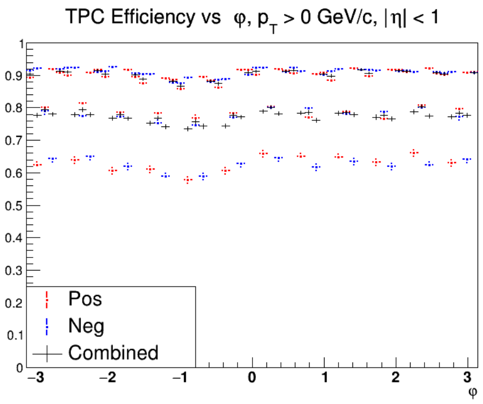
TPC Efficiency vs φ, p_T > 0 GeV/c, |η| < 1
Pos
Neg
Combined
φ

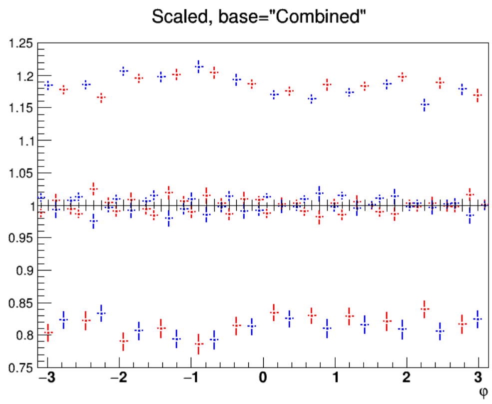
Scaled, base="Combined"
φ

p+Au

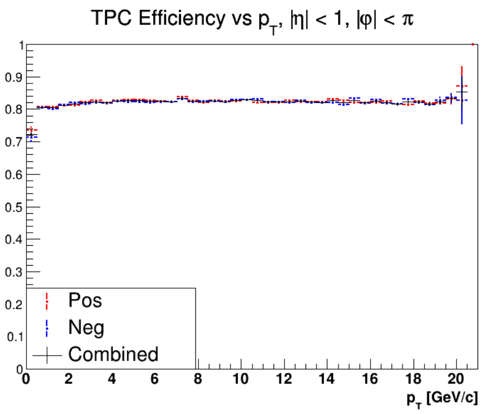
TPC Efficiency vs p_T, |η| < 1, |φ| < π
Pos
Neg
Combined
p_T [GeV/c]

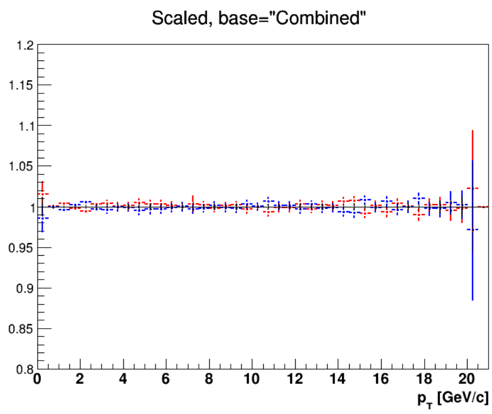
Scaled, base="Combined"
p_T [GeV/c]

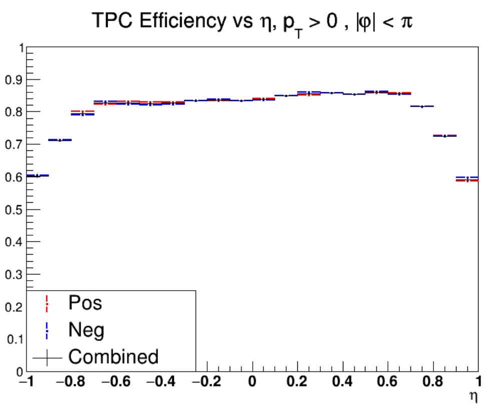
TPC Efficiency vs η, p_T > 0 , |φ| < π
Pos
Neg
Combined
η

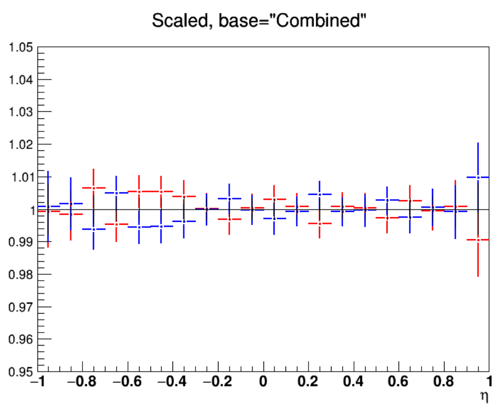
Scaled, base="Combined"
η

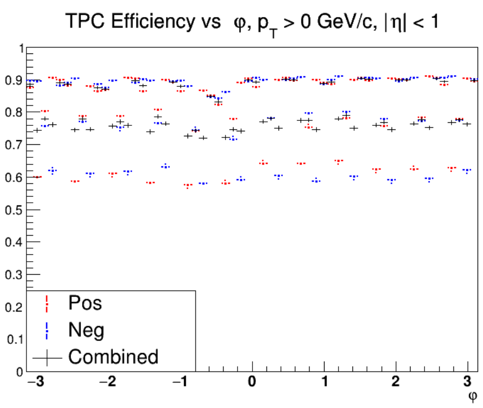
TPC Efficiency vs φ, p_T > 0 GeV/c, |η| < 1
Pos
Neg
Combined
φ

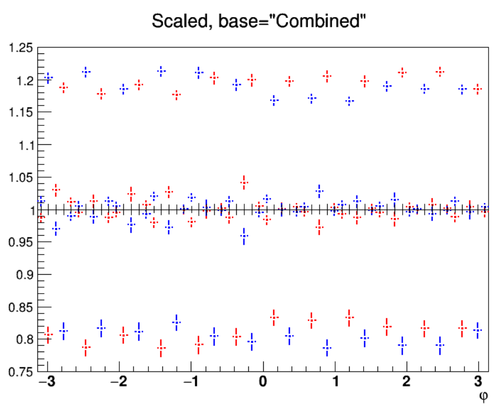
Scaled, base="Combined"
φ

2. The EID efficiency is calculated separately for 3 “types” of $e^{\pm}$: 1) Triggered, short as TRG (pass TPC, EID and TRG); 2) Non-triggered, short as !TRG or NTR (pass TPC, EID while rejected by TRG); 3) the union of the previous 2, short as ALL (pass TPC and EID). The efficiencies are defined as follows:

2.1 TRG: $\epsilon^{EID,TRG}(\mathrm{p}_T, \eta) = \frac{N_e^{TPC,EID,TRG}(p_T,\eta)}{N_e^{TPC}(p_T,\eta)}$

2.2 !TRG: $\epsilon^{EID,!TRG}(\mathrm{p}_T, \eta) = \frac{N_e^{TPC,EID,!TRG}(p_T,\eta)}{N_e^{TPC}(p_T,\eta)}$

2.3 ALL: $\epsilon^{EID}(\mathrm{p}_T, \eta) = \frac{N_e^{TPC,EID}(p_T,\eta)}{N_e^{TPC}(p_T,\eta)}$

The following plots show the dependency of EID efficiencies on p_T and η. These are purely for demonstration purposes since they are integrated over 1 out of 2 designed variable (p_T and η).

p+p

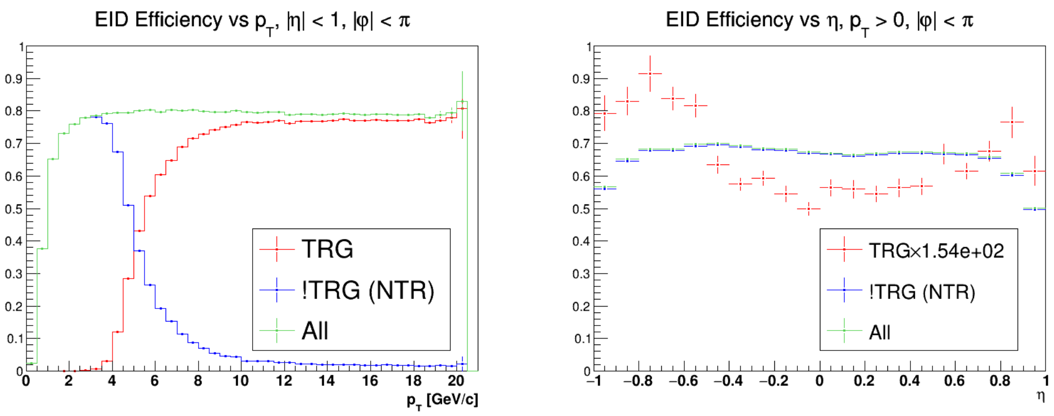

p+Au

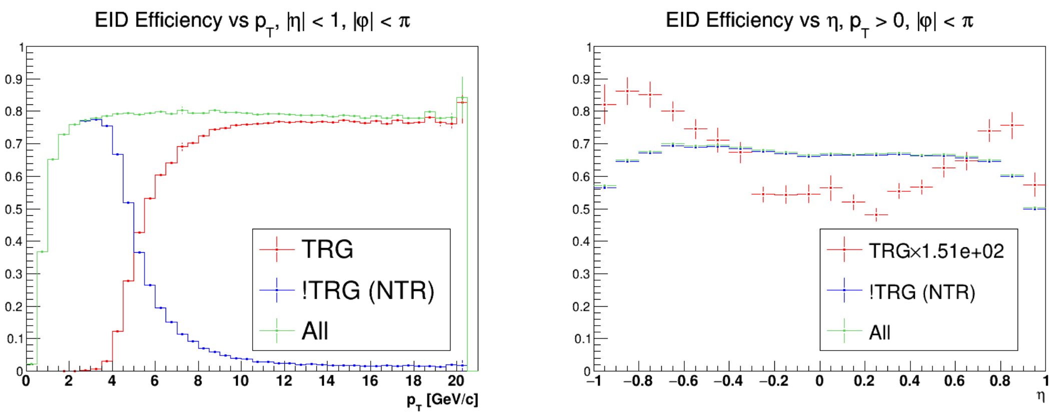

The distributions of $\frac{p_T^{RC}}{p_T^{MC}} - 1$ are extracted separately for the aforementioned 3 types of electrons in different $e^{\pm}$ MC p_T bins. They will be used as $e^{\pm}$ p_T smearing templates in the next step where EvtGen is utilized. The following plots show the templates for $e^{\pm}$ with MC p_T between 0.5 to 12.5 GeV/c for p+p and p+Au collisions.

5.7 J/ψ Reconstruction in EvtGen and J/ψ Efficiency

The single $e^{\pm}$ efficiencies and p_T smearing templates are fed into EvtGen. A straight forward J/ψ reconstruction process is listed below:

1. EvtGen decays a J/ψ into di-electron pairs. We have access to their MC level momentum information.

2. The di-electron pair (e_1, e_2) can be detected in the following combination of $e^{\pm}$:

1) e_1 - TRG, e_2 - !TRG

2) e_1 - !TRG, e_2 - TRG

3) e_1 - TRG, e_2 - TRG

3. All 3 cases are taken into account for each J/ψ decay. In each case, both e_1 and e_2 obtain a smeared p_T according to template corresponds to its type (TRG, !TRG), and then be used to reconstruct J/ψ. The RC J/ψ is weighted by the multiplication of RC efficiency of both daughter. Afterwards, like in real data, basic kinematics cut are applied (on p_T and η) to accept or reject the RC J/ψ. It's worth noting that, although all 3 cases contribute to the RC J/ψ counts, they contributes to different kinematics range due to the difference in the $e^{\pm}$ smearing templates used in each case.

Alternatively, (e_1, e_2) can be detected in another combination:

1) e_1 - TRG, e_2 - ALL

2) e_1 - ALL, e_2 - TRG

3) e_1 - TRG, e_2 - TRG

Here, instead of summing up all 3 cases, one needs to subtract 3) from then sum of 1) and 2). In the "Choice of Decay Model" section, we will see that both combinations can reproduce the embedding J/ψ efficiency in the p_T range of interest (belowe 12 GeV/c), while in the high p_T range the **TRG+All** combination has less bias in high p_T range compared to the **TRG+!TRG**. Therefore the **TRG+All** combination is chosen in this analysis.

The J/ψ RC efficiency is then calculated by making a ratio of number of RC J/ψ falls in a mass window (2.6<mass<3.35 GeV/c^2) against MC J/ψ on the entire mass spectrum. It's worth noting that the embedding MC J/ψ does not have a single value mass, but a very narrow Breit-Wigner peak at the J/ψ mean mass. The EvtGen is also set up to produce same MC J/ψ mass distribution for consistency.

5.8 Signal Extraction

All cut mentioned in the "Event and Track Selection" are applied in signal extraction for real data. The $e^{\pm}$ in real data are paired into unlike-sign (**US**) and like-sign (**LS**) pairs. The LS is a good estimation of the uncorrelated combinatorial background contribution in US. It's worth noting that, in embedding, such a combinatorial background is zero by construction since pairs are included only and if only those pairs are the prompt daughters of the same J/ψ. The **US-LS** histogras are main subjects of study in the raw signal extraction section. It is integrated over φ and $|y| <1$, and has p_T and pair mass dependence. Parctically speaking, the **US-LS** is considered as mass distributions in 6 wide p_T bins, with the bin edge of 4, 5, 6, 7, 8, 10 and 12 GeV/c.

5.8.1 Special Treatment of Low Effective Counts Bins

ROOT uses $\sqrt{N}$ as the symmetric uncertainty of N counts bins by default, assuming they are in Poisson distribution with large statistics. Therefore, low effective counts bins need special treatment to compensate for underestimation of uncertainty. The unified confidence interval [μ_1, μ_2] of 90% and 95% for the mean of a Poisson variable given n observed events is listed below:

[Ref https://pdg.lbl.gov/2023/reviews/contents_sports.html Table 40.4]

	$1-\alpha = 90\%$		$1-\alpha = 95\%$	
n	μ_1	μ_2	μ_1	μ_2
0	0.00	2.44	0.00	3.09
1	0.11	4.36	0.05	5.14
2	0.53	5.91	0.36	6.72
3	1.10	7.42	0.82	8.25
4	1.47	8.60	1.37	9.76
5	1.84	9.99	1.84	11.26
6	2.21	11.47	2.21	12.75
7	3.56	12.53	2.58	13.81
8	3.96	13.99	2.94	15.29
9	4.36	15.30	4.36	16.77
10	5.50	16.50	4.75	17.82

The upper and lower limits are asymmetric. The 90% and 95% confidence interval is comparable to 2σ and 1.64σ width in Gaussian respectively. In terms of the interval limits, slight inconsistency can be found between 90% and 95% after scaling the deviation $|\mu_1 - n|, |\mu_2 - n|$ (from mean to the limits), to Gaussian 1σ equivalent, $\sqrt{n}$. Therefore, the arithmetic average of the deviationsare calculated. In the following figure, the points of $|\mu_1 - n|, |\mu_2 - n|$ are the aformentioned average. These average values are fit to the quadratic function separately. For simplicity, the average of the 2 fit functions $f_{mid}(n)$ is assigned to be the half width of a symmetric confidence interval centered at n.

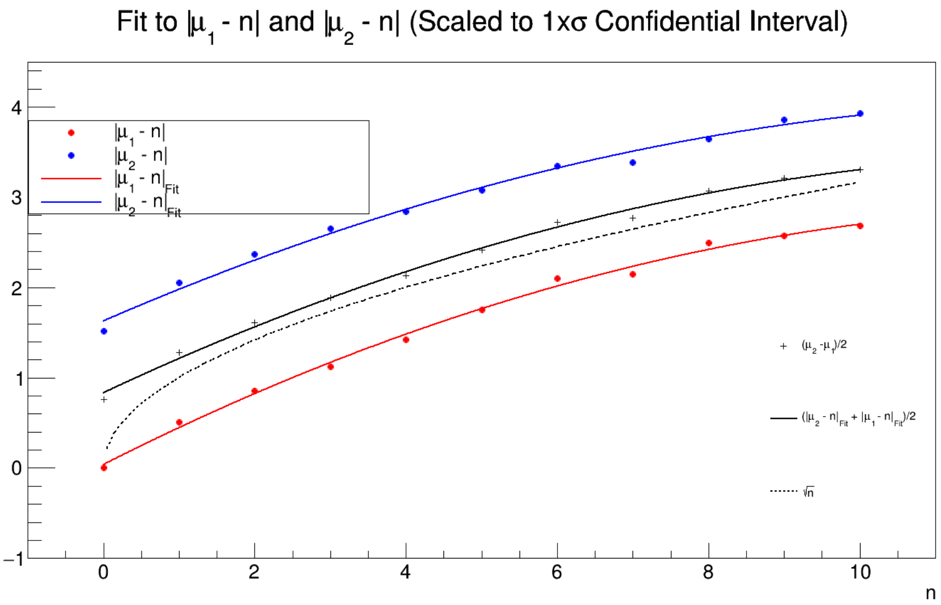

This will enable treatment to non-integer effective counts bins due to weighting. The "$\sqrt{n}$" curve and the original half width $\frac{\mu_2-\mu_1}{2}$ points are also plotted for comparison. The correction will compensate the underestimation of statistic uncertainties. The "effective counts" is defined by $N = (\frac{C}{err})^2$, where **C** is the bin content and **err** is the bin error. If N≤10, $f_{mid}(N)$ is assigned to be the corrected uncertainty for this bin; when N>10 the difference is small so no treatment is applied.

This special treatment is applied to **US** and **LS** after they are integrated over φ and $|y|$ <1 and rebinned in p$_T$ and mass axis. Then **LS**s is subtracted from **US**s, yielding **US-LS**s, which are the histograms studied in the following subsections.

5.8.2 Raw Yield Estimation

The aforementioned **US-LS** histograms are fit to functions with 2 contributions: signal (**SIG**) + residual background (**ResBG**). The **SIG** is the normalized RC mass distribution from EvtGen, with a scale factor N_{SIG} for normalization; the **ResBG** is arbitrary and chosen to be a exponential function $N_{ResBG} \times e^{-bM_{e^+e^-}}$, where N_{ResBG} is for normalization. The number of free parameters in those fits is 3: N_{SIG}, N_{ResBG}, and b. The fit range is set to be $1.5 < M_{e^+e^-} < 4.5GeV/c^2$. The fit options used are: 1) **I**, fit the integral of the function in the bin instead of the function value at bin center; 2) **M**, attempt to find a better local minimum near the previous convergence. The following plots show the mass fit in each p$_T$ bin. (Note: the plots shown are after additional smearing, or more precisely "additionally smeared fit")

p+p

Trigger p$_T$ 4.3 GeV/c

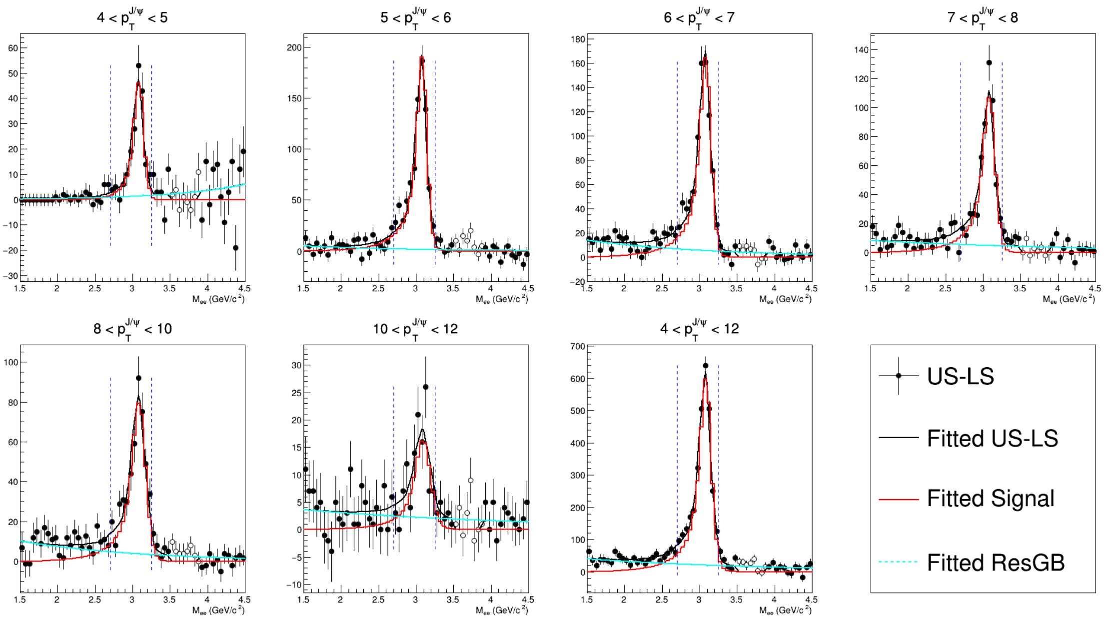

Trigger p_T 3.5 GeV/c

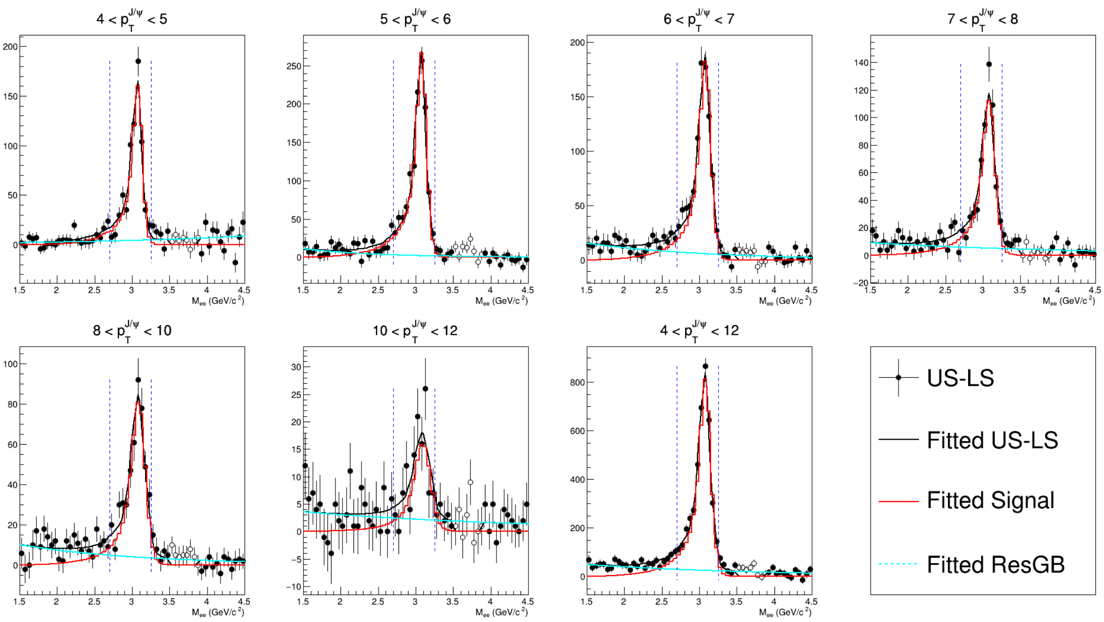

p+Au

Trigger p_T 4.3 GeV/c

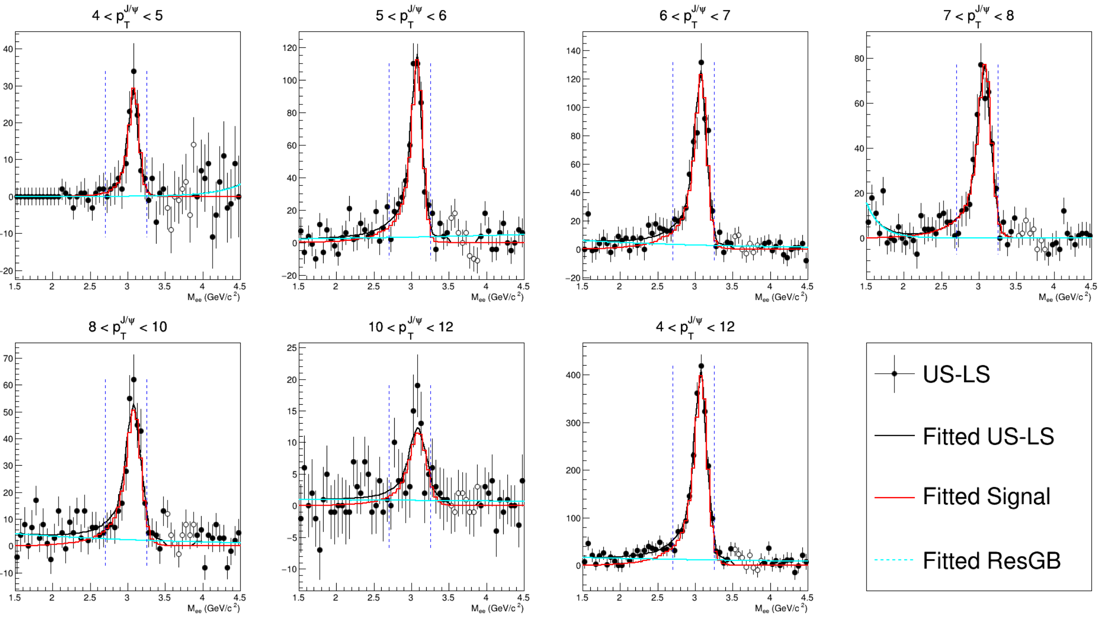

Trigger p_T 3.5 GeV/c

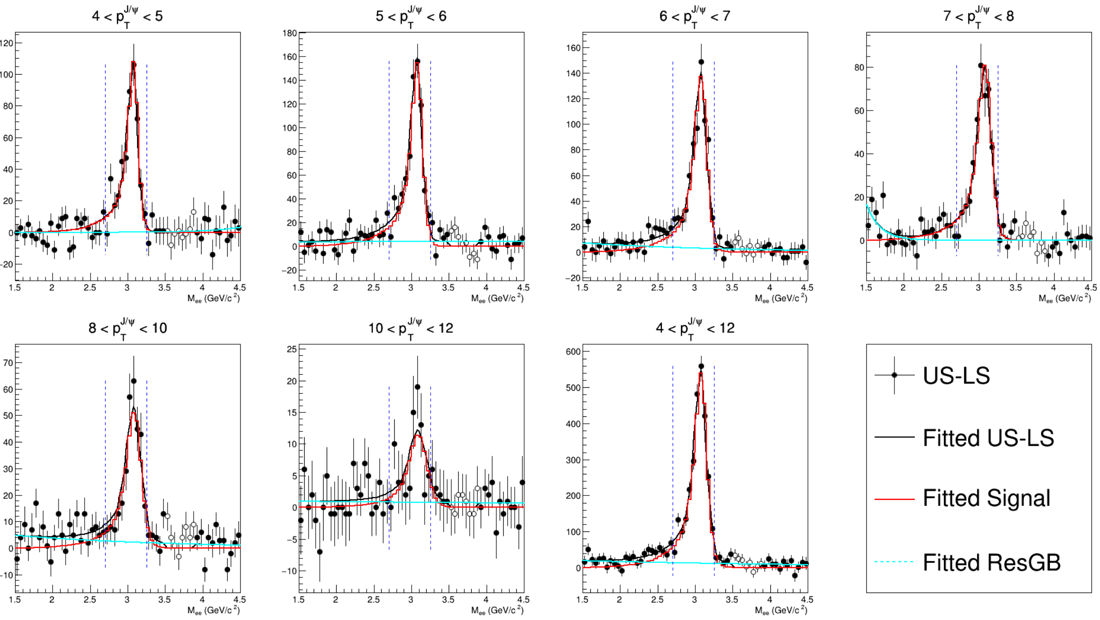

The raw yield is estimated by subtracting the integral of resulting fit function's **ResBG** part from the integral of **US-LS**, within the mass window of 2.7 to 3.25 GeV/c^2.

5.9 Additional Smearing and Parameter Optimization for the Momentum Resolution

As mentioned before, the embedding has overestimated the momentum resolution of $e^{\pm}$ tracks. Additional smearing is aimmed at providing a more realistic momentum resolution.

The resolution in η and φ are reasonably well-simulated therefore only the resolution in transverse momentum is additionally smeared.

5.9.1 Parameterization of RC Momentum Resolution in Embedding

In this analysis, the $e^{\pm}$ p_T resolution in embedding is characterized by the distribution of $\frac{p_T^{RC}}{p_T^{MC}} - 1$. A comparison is made between positrons and electrons in this distribution, and they are consistent within uncertainty. The positrons and electrons are combined for better precision. The following plots demonstrates the embedding $\frac{p_T^{RC}}{p_T^{MC}} - 1$ for electrons and positrons in p+p and p+Au collisions. Comparisons are made in finer p$_T$ bins but only the integrated ones are shown:

p+p

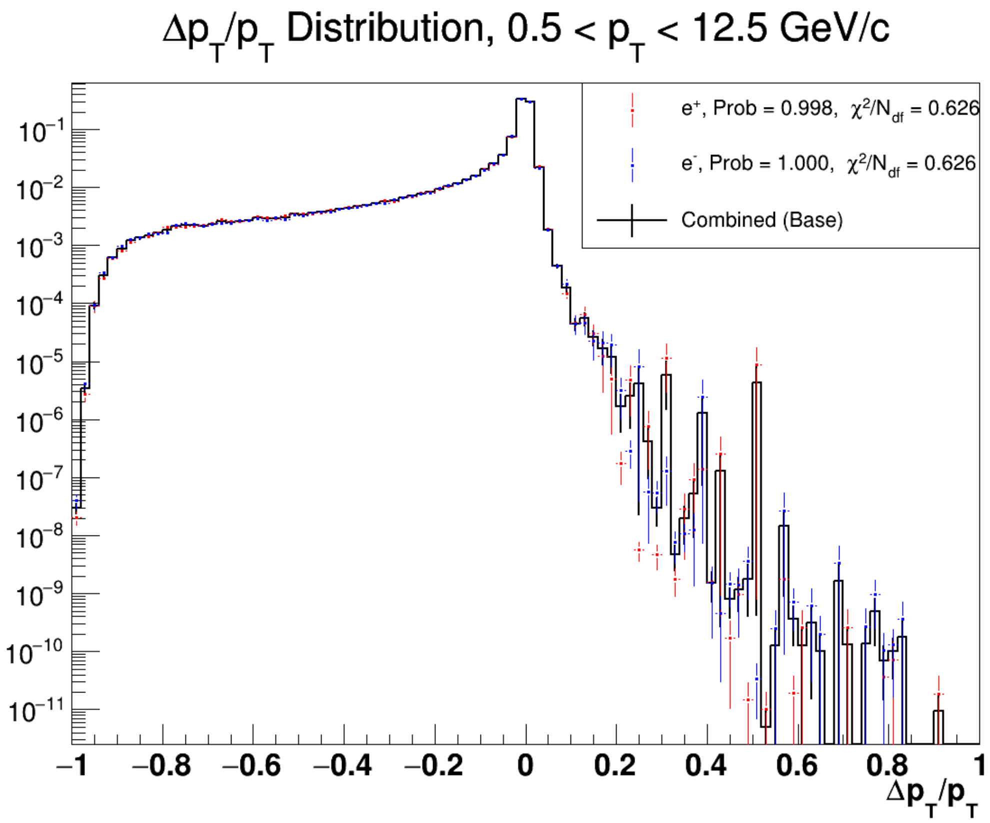

p+Au

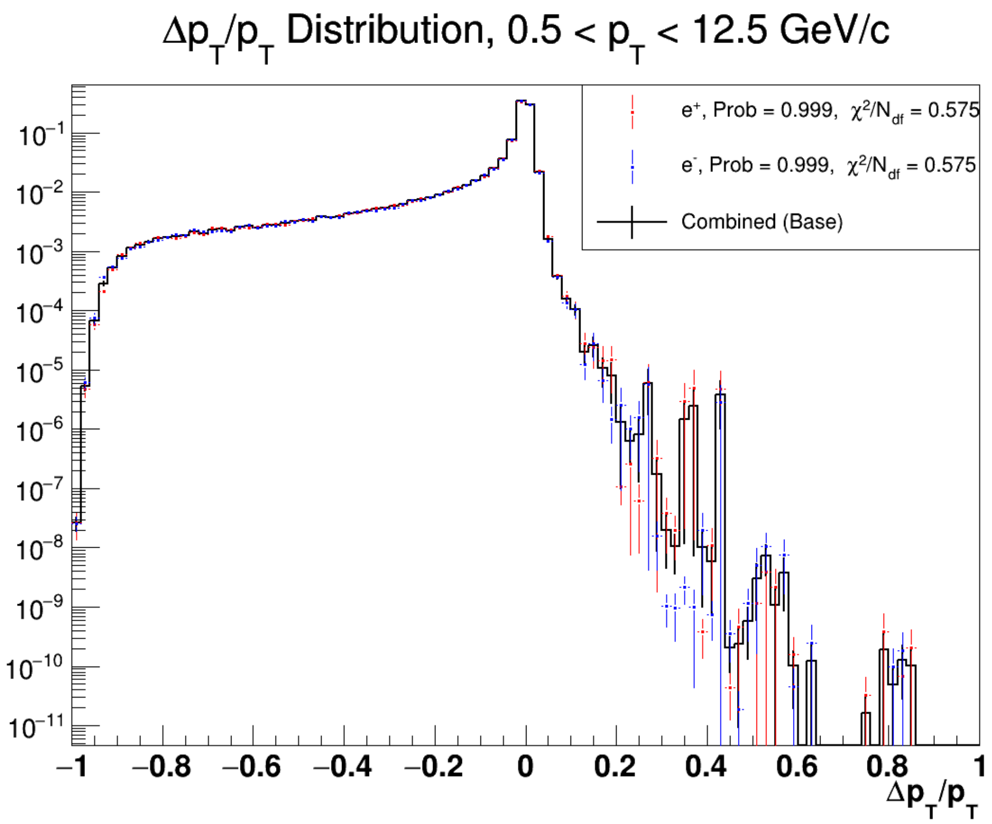

Near $\frac{p_T^{RC}}{p_T^{MC}} - 1 = 0$ peak area, this distribution at different p_T^{MC} (p_T^{MC} bins) presents itself as a Gaussian. Therefore, distributions at different p_T^{MC} are fit to Gaussian and the width of Gaussian as a function of p_T^{MC} is extracted from this series of fit. This function can be well described by the following empirical formula: $f(p_T) = \sqrt{(ap_T)^2 + b^2}$, where p_T is short for p_T^{MC} while a and b are parameters.

The fit range of aforementioned Gaussian fit for each p_T^{MC} bin is decided by a prior of $f(p_T)$ and the following empirical formula: $x_{min} = -1.5 \times f(p_T$, $x_{max} = 2.0 \times f(p_T$. Essentially, this range includes the -1.5σ to 2.0σ region of the prior. The fit is conducted in an iterative manner, until the prior of $f(p_T)$ is consistent with the resulting one. The selection of the scaling factors of -1.5 and 2.0 is arbitrary but carefully treated. It is intended to be as wide as possible, while within this fit range the distribution has been guaranteed to be Gaussian. The ratio of histogram against the fit function is consistent to 1 within fit range and starts to deviate from 1 when going outside. The following are the Gaussian fit for each p_T bin:

The following 2 plots demonstrate the fit for the width function in p+p and p+Au collisions:

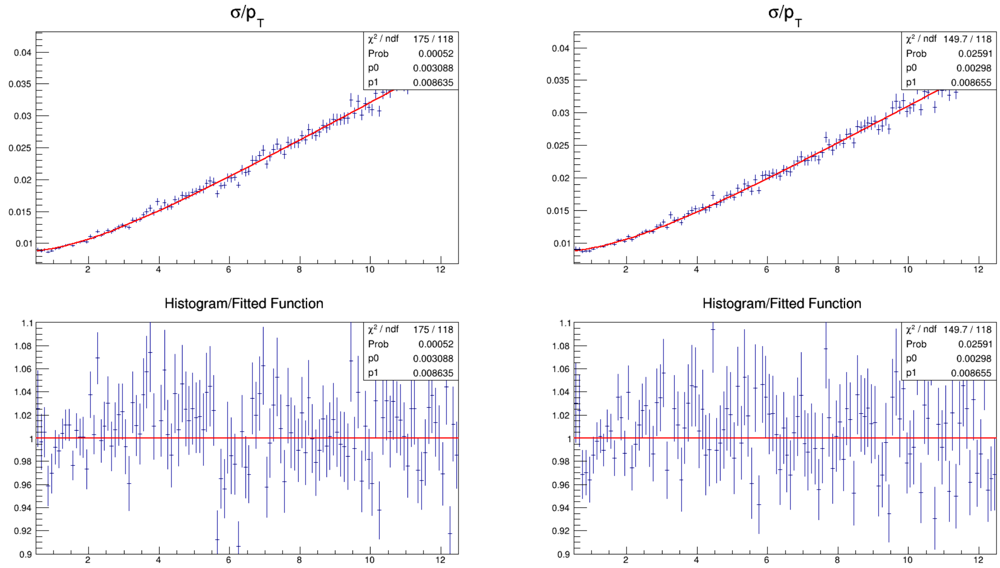

5.9.2 Procedure of Additional Smearing

In embedding, the fit parameter a in the width function is varied to construct the additional smearing: a is varied to $a' = a \times (1 + iStep \times 0.03)$ while b is kept the same in $f(p_T) = \sqrt{(ap_T)^2 + b^2}$ (iStep = 0, 1, 2, ... 99). The new $f'(p_T)$ represents a new momentum resolution as a function of MC p$_T$. Therefore, $\frac{f'(p_T)}{f(p_T)} = \frac{\frac{p_T^{RC'} - p_T^{MC}}{p_T^{MC}}}{\frac{p_T^{RC} - p_T^{MC}}{p_T^{MC}}} = \frac{p_T^{RC'} - p_T^{MC}}{p_T^{RC} - p_T^{MC}}$, yielding $p_T^{RC'} = \frac{f'(p_T)}{f(p_T)} \times p_T^{RC} + (1 - \frac{f'(p_T)}{f(p_T)}) \times p_T^{MC}$, where $p_T^{RC'}$ is assigned to be the additional smeared RC p_T, whenever the original p_T^{RC} presents, both in embedding and EvtGen. I.e, the EID efficiencies and the smearing templates of 3 types (TRG, NTR, All) of electrons will obtain dependence on **iStep**. As a result, the RC J/ψ in embedding as well as in EvtGen also depend on **iStep**, and **iStep=0** corresponds to “no additional smearing”.

5.9.3 Optimization of Parameter a

The J/ψ mass resolution is influenced by the momentum resolution. Therefore, one can attempt to match the RC mass distribution to the real data while varying $a'(iStep)$. The optimized $a'(iStep)$ is defined to be the one provides most consistency RC mass distribution. The exact approach is described below:

0) Generate the templates at different $a'(iStep)$, $iStep = 0, 1, 2, 3, \ldots$ 99

1) Conduct a series of “Signal Extraction” with each templates from step 0)

2) Record the fit χ^2 as a function of $\frac{\Delta a}{a} = iStep \times 0.03$. The χ^2 describes how well the simulation is consistent with data

3) Fit the χ^2 vs $\frac{\Delta a}{a}$ to a 4^{th} order polynomial function in order to avoid fluctuations

4) Find the minimum of the fit function χ^2_{min} and corresponding $(\frac{\Delta a}{a})_{min}$ in range

5) Use the closest integer to $(\frac{\Delta a}{a})_{min}$ obtained in the 4) to be the optimized $(\frac{\Delta a}{a})_{opt}$

6) The lower/upper confidence interval of $(\frac{\Delta a}{a})_{min}$ is determined by the x (or $\frac{\Delta a}{a}$) coordinate of the closest intersection of y (or χ^2) $= \chi^2_{min} + z^2$ and the χ^2 fit function on the left/right side of $(\frac{\Delta a}{a})_{min}$, where z is the confidence level value. I.e., $z = 1$ in this formula has the equivalent statistical significance with 1σ in Gaussian. The confidence interval is assigned to be an asymmetric uncertainty.

$(\frac{\Delta a}{a})_{min}$ as well as the uncertainties are obtained in individual p$_T$ bins and the p$_T$ integrated bin. $z = 1, 2$ are both calculated, represented by thin and thick error bars (boxes) for the individual p$_T$ bins (p$_T$ integrated bin)

The fit result of the parameters are also monitored by looking at the fit parameters (N_{Sig}, N_{Res}, b_{exp}) vs $\frac{\Delta a}{a}$. Intuitively, they should present themselves as continous functions.

N_{Sig}, N_{Res}, b_{exp} vs $\frac{\Delta a}{a}$ and χ^2 vs $\frac{\Delta a}{a}$ are shown as below:

p+p

Trigger p_T = 4.3 GeV/c

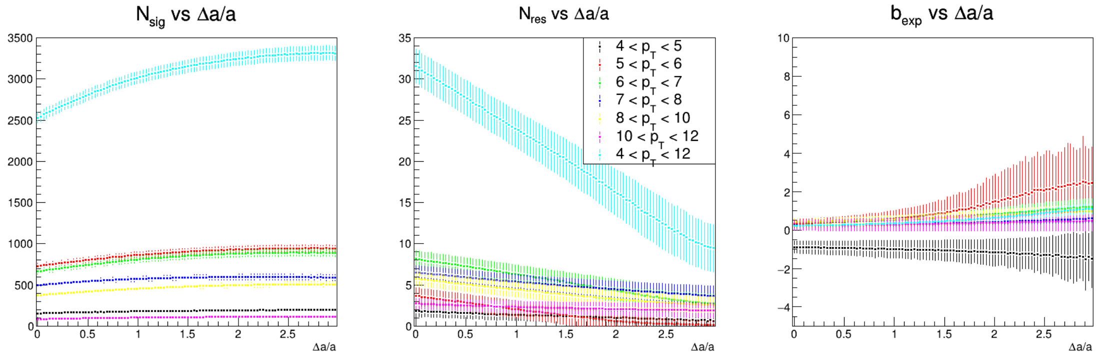

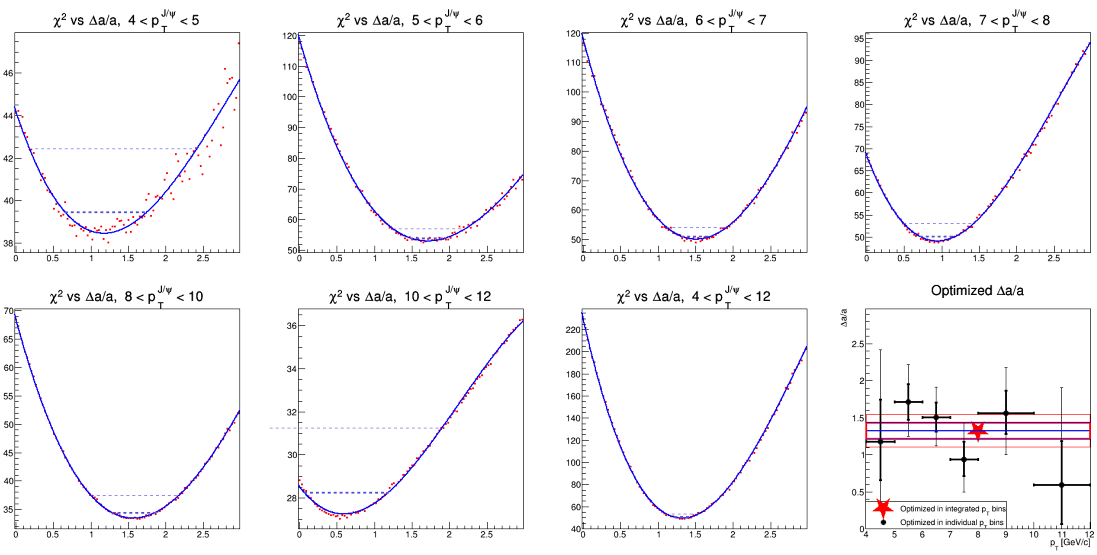

Trigger p_T = 3.5 GeV/c

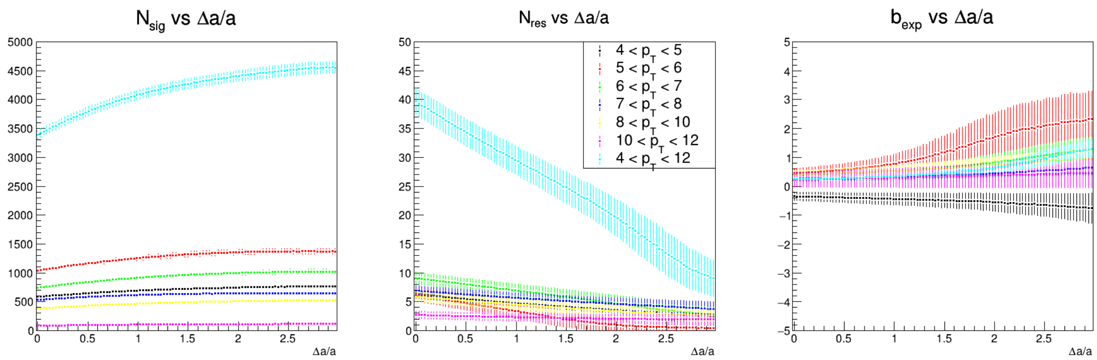

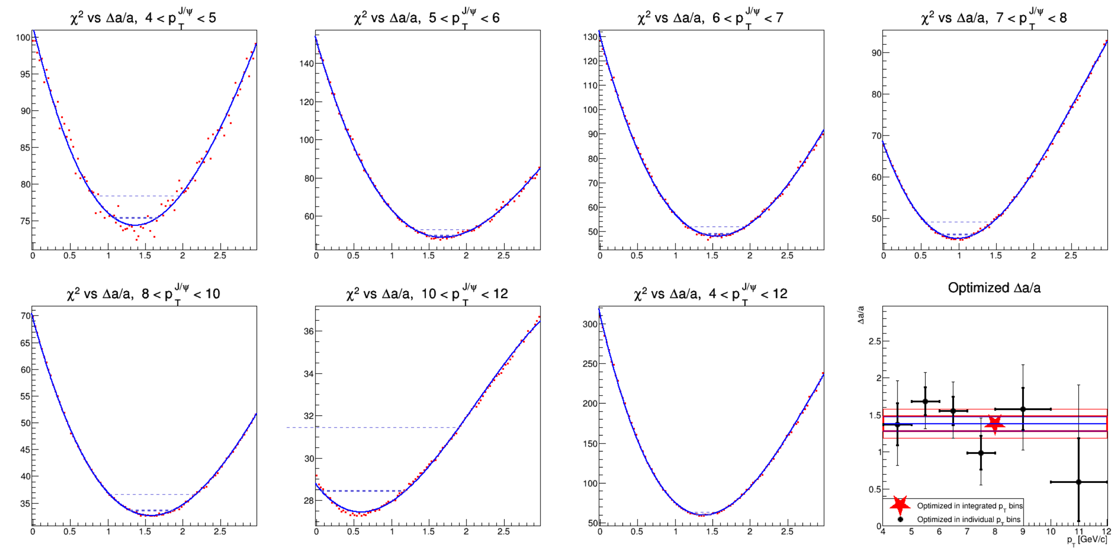

p+Au

Trigger $p_T = 4.3$ GeV/c

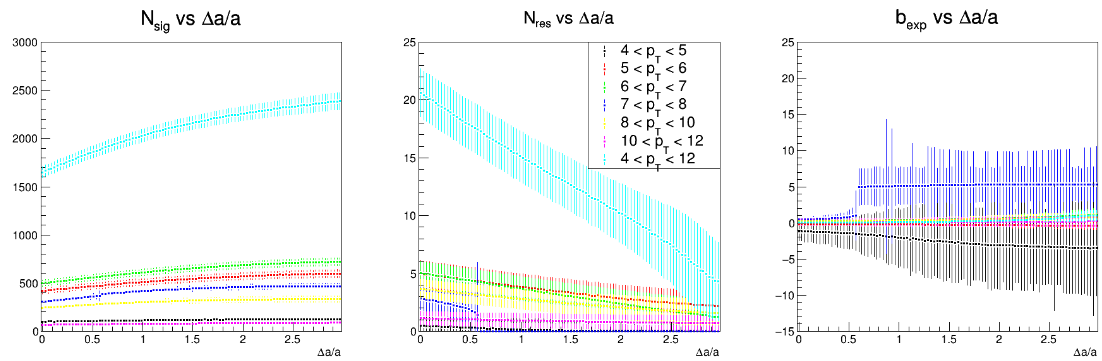

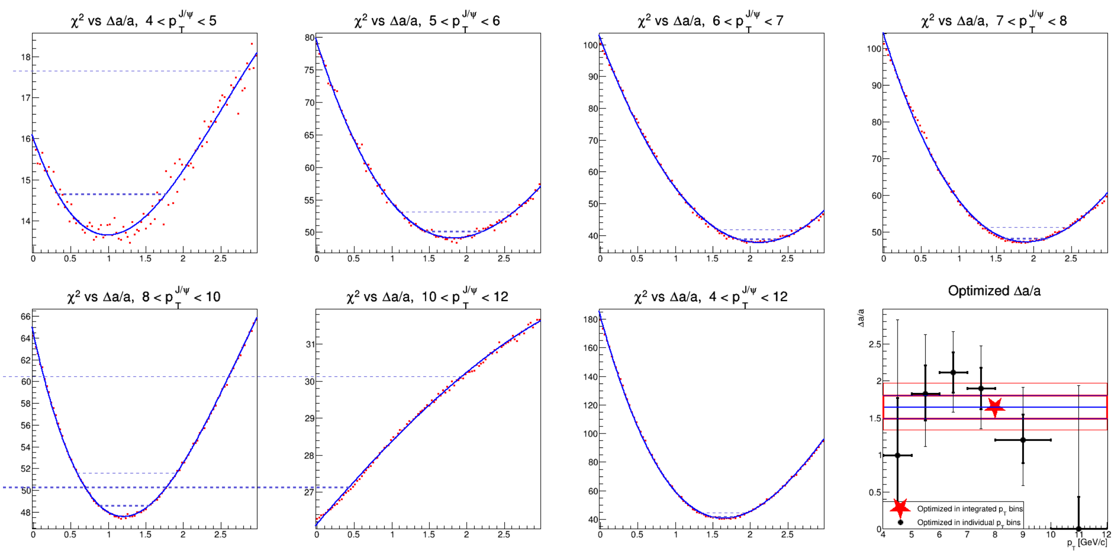

Trigger $p_T = 3.5$ GeV/c

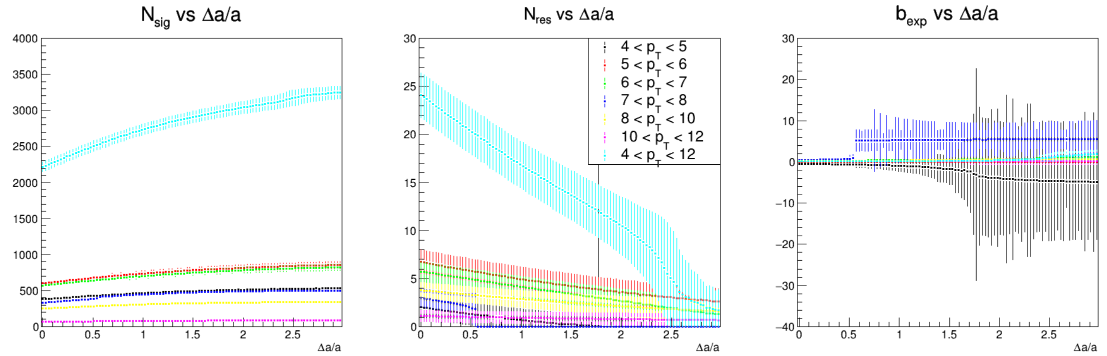

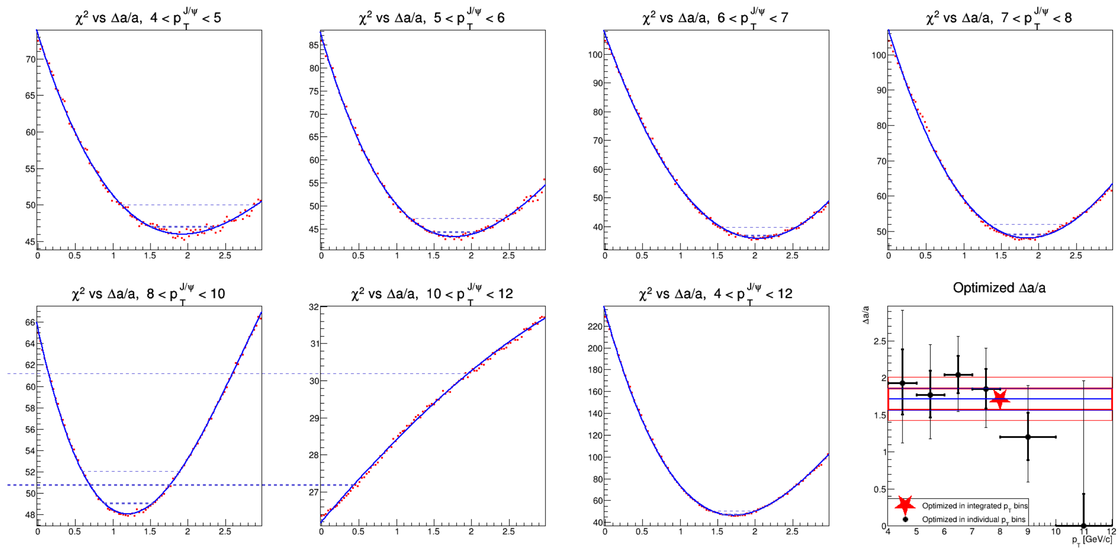

$(\frac{\Delta a}{a})_{opt}$ vs p$_T$ is statistically flat, and consistent with the one with the p$_T$ integrated one. Therefore the p$_T$ integrated $(\frac{\Delta a}{a})_{opt}$ is used as the optimized parameter without p$_T$ dependence. Then in each individual p$_T$ bins, with the p$_T$ integrated $(\frac{\Delta a}{a})_{opt}$, the J/$\psi$ RC efficiency with additional smearing can be calculated, and the raw yield extracted by templates with additional smearing is picked out from the series of "Signal Extraction" result in 1).

5.10 Physics Results

With the raw yield extracted by templates with additional smearing, J/ψ RC efficiency with additional smearing, one can calculate the physics results of this analysis. The physics results include the differential cross Section in p+p collisions, the invariant yield in p+Au collisions, and the nuclear modification factor R_extpA. .

5.10.1 The Differential Cross Section in p+p Collisions and the Invariant Yield p+Au Collisions

As a reminder, the electron trigger p$_T$ cut used to reconstuct J/ψ for calculating the p+p cross section and p+Au invariant yield is 4.3 GeV/c.

Recap: the p$_T$ differentiated yield per unit rapidity is calculated by the following formula:

$$\frac{d^2N}{dp_T dy} = \frac{1}{\Delta p_T \Delta y} \cdot \frac{1}{N_{MB}^{eqv}\epsilon_{MB}^{gvtx}} \cdot \frac{\epsilon_{MB}^{BBC}\epsilon_{MB}^{gvtx}}{\epsilon_{J/\psi}^{BBC}\epsilon_{J/\psi}^{gvtx}} \cdot \frac{N_{J/\psi}^{raw}}{\epsilon_{J/\psi}^{RC}}$$

where:

$\Delta y = 2$ corresponds to the rapidity acceptance $|y| < 1$

N_{MB}^{eqv} is the equivalent number of MB events

ϵ_X^{gvtx} is the good vertex efficiency of X (X = MB, J/ψ)

$\frac{\epsilon^{BBC}_{MB}\epsilon^{gvtx}_{MB}}{\epsilon^{BBC}_{J/\psi}\epsilon^{gvtx}_{J/\psi}}$ is the trigger bias factor, in which ϵ^{BBC}_{X} is the beam-beam counter efficiency of X (X = MB, J/ψ)

$N^{raw}_{J/\psi}$ is the raw yield of J/ψ

$\epsilon^{RC}_{J/\psi}$ is the J/ψ reconstruction efficiency

p$_T$ Position Determination Due to the nature of binned data, the choice of x being equal to the bin center and subsituting this value to calculate $\frac{d^2N}{dp_T dy}$ is an approximation. $\frac{d^2N}{dp_T dy}$ is chosen to be held untouched while a p$_T$ shift technique is applied, in which a shifted p$'_T$ is assigned to be x coordinate in order to make the integral of $f(p_T)$ equals the product of bin width and $f(p'_T)$ in each p$_T$ bin, where $f(p_T)$ is an emperical fit funtion of $\frac{d^2N}{dp_T dy}$ vs p$_T$. The p$_T$ shift is conducted in a iterative manner as described below:

0) The starting point is the set of uncorrected p$_T$, denoted by $S_0 = \{p^{(n_{bin})}_{T,0} | n_{bin} = 0, 1, 2, 3, 4, 5\}$ where n_{bin} is the bin index. The uncorrected p$_T$ is simply the bin center of each p$_T$ bin.

1) In the i^{th} iteration (i = 1, 2, 3, 4...), use $S_{i-1} = \{p^{(n_{bin})}_{T,i-1} | n_{bin} = 0, 1, 2, 3, 4, 5\}$ as the x coordinates in $(p_T, \frac{d^2N}{dp_T dy})$. Fit the set of points $\{(p_T, \frac{d^2N}{dp_T dy})\}$ to $f(p_T) = N \cdot p_T \cdot (1 + (\frac{p_T}{A})^2)^{-n}$. This essentially maintains the integrated yield in this p$_T$ bin invariant. The resulting function in this iteration is denoted by $f_i(p_T)$.

2) Solve for the root of $p^{n_{bin}}_{T,i}$ in the equation below in each p$_T$ bin:

$$\int_{l(n_{bin})}^{h(n_{bin})} f_i(p_T)\, dp_T = Width(n_{bin}) \cdot f_i(p^{(n_{bin})}_{T,i})$$

where $l(n_{bin})$, $h(n_{bin})$ and $Width(n_{bin})$ is the lower bound, higher bound and bin width of the p$_T$ bin with index n_{bin}. This constructs a map from $p^{n_{bin}}_{T,i-1}$ towards $p^{n_{bin}}_{T,i}$

3) Loop over step 1) and 2), until the resulting fit function is consistent with the previous iteration. The criteria is arbitrary, but set to "all parameters and their fit errors are identical up to 6 digits". Denote this iteration has an index of $i = N$

4) The procedure converges in the iteration of $i = N - 1$, therefore $S_{N-1} = S_k, \forall k > N - 1, k \in \mathbb{Z}$is the set of shifted p$_T$ assigned.

The shifted p$_T$ values in each p$_T$ bin are listed in the following table.

The first 2 columns are obtained with the electron trigger p$_T$ cut at 4.3 GeV/c. These 2 columns participate in the calculations of the final physics results of the differential cross section in p+p collisions and the invariant yield in p+Au collisions.

Such values were also extracted with the electron p$_T$ cut at 3.5 GeV/c, but not shown in this table. Similar to the 4.3 GeV/c case, for the 3.5 GeV/c case the difference in the p$_T$ position between p+p and p+Au is negligible. Therefore when calculating R$_e xtpA$, the 1/p$_T$ term, which converts the yield into invariant yield, is considered to cancel out after taking the p+Au/p+p ratio. The arithmetic average of the p$_T$ positions in p+p and p+Au and are the assigned to be the visual p$_T$ positions.

Assigned p$_T$ [GeV/c]			
p$_T$ Range [GeV/c]	p+p	p+Au	R$_e xtpA$
4 - 5	4.44182	4.44449	4.44745
5 - 6	5.44484	5.44643	5.44802
6 - 7	6.44896	6.44987	6.45060
7 - 8	7.45312	7.45361	7.45379
8 - 10	8.83719	8.83778	8.83684
10 - 12	10.86037	10.86004	10.85800

Calculate the Invariant Yield The invariant yield is calculated by the following formular:

$$\frac{d^2N}{2\pi p_T dp_T dy} = \frac{d^2N}{dp_T dy} \cdot \frac{1}{2\pi p_T}$$

where p$_T$ on the right hand side is the shifted p$_T$ assigned in the table above. For p+p collisions, the invariant yield is converted into differential cross section by multiplying the non-single diffractive (**NSD**) cross section in p+p collisions $\sigma_{pp}^{NSD} = 30.0 \pm 2.4mb$ at 200 GeV:

$$\frac{d^2\sigma}{2\pi p_T dp_T dy} = \frac{d^2 N}{2\pi p_T dp_T dy} \cdot \sigma_{pp}^{NSD}$$

The following plots show the differential cross-section in p+p and the invariant yield in p+Au collisions.

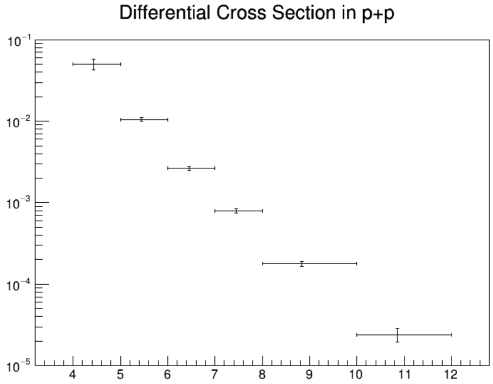

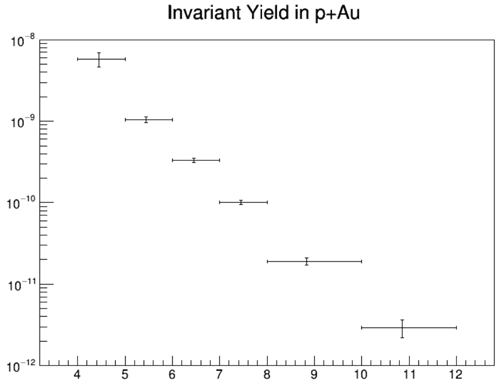

5.10.2 Nuclear Modification Factor R$_e xtpA$

The nuclear modification factor is calculated with the following formula:

$$R_e xtpA = \frac{1}{\langle N_{coll} \rangle / \sigma_{pp}^{inel.}} \cdot \frac{(\frac{d^2 N}{2\pi p_T dp_T dy})_e xtpA}{(\frac{d^2\sigma}{2\pi p_T dp_T dy})_{pp}}$$

where $\sigma_{pp}^{inel.} = 42mb$ is the inelastic cross-section of nucleon-nucleon collisions at 200 GeV in p+p collisions, and $\langle N_{coll} \rangle = 4.7 \pm 0.3$ is the average number of binary nucleon-nucleon collisions.

As a reminder, the electron trigger p$_T$ cut used to reconstruct J/ψ for calculating the R$_e xtpA$ is 3.5 GeV/c. Therefore, the cross section in p+p collisions and invariant yield in p+Au collisions used to calculate R$_e xtpA$ are different from the their stand-alone physics result. The resulting R$_e xtpA$ is shown as below:

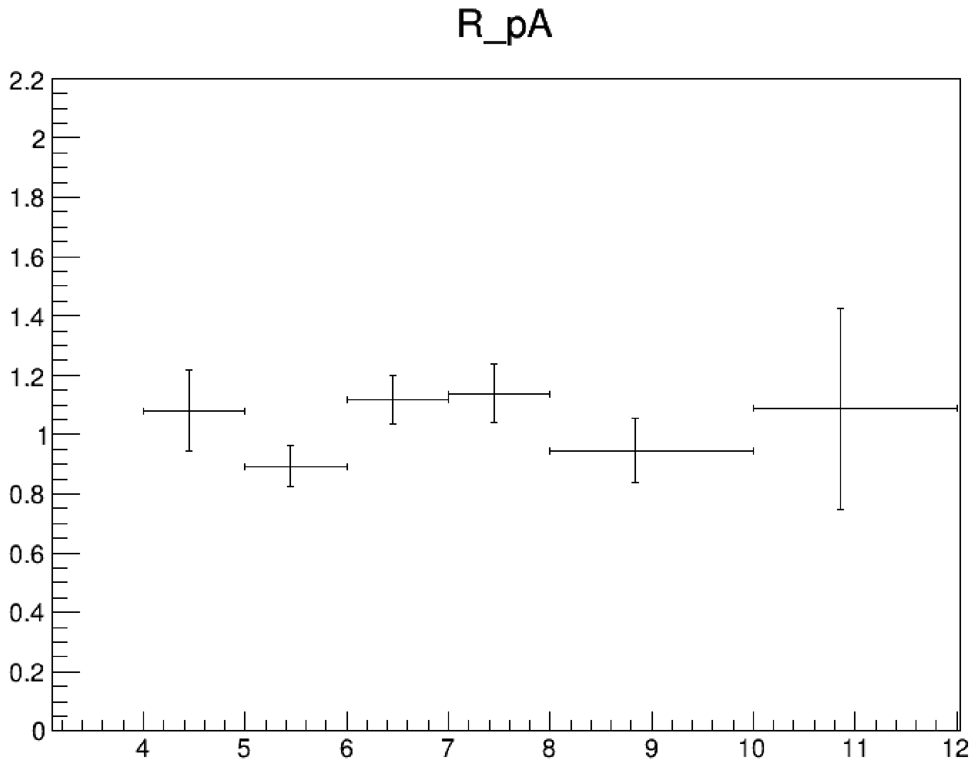

6 Systematic Uncertainties

The systematic uncertainty is estimated separately for the three physics results: p+p cross section, p+Au invariant yield, and R$_{e}xtpA$, but they estimated in a same way.

Four aspects are included in the systematic uncertainties and each of them will be discussed:

1. Tracking
2. Electron identification
3. Electron triggering
4. Raw yield extraction

The contributions from them are assumed to be uncorrelated with each other.

6.1 Treatment of Undersampling

Each contribution of the systematic uncertainty is estimated by varying cut(s) or parameter. One can reconstuct J/ψ with the varied cut(s) or parameter and calculate the corresponding varied physics result. The systematic uncertainty contribution is related to the difference between the default physics result and each one of the varied results. In this analysis, some cut(s) only has one of variation. In this case, if the deviation is smaller than the quadrature difference between the statistical uncertainty of the default physics result and the varied one, this contribution is assigned to be 0 due to the fact that the deviation is suppressed by and most likely due to statistical fluctuation.

6.2 Independent Contribution from Each of the 4 Aspects

Details of each contribution is discussed.

1. Tracking The tracking quality cuts could be highly correlated. Therefore, three tracking quality cuts (nHitsFit, nHitsDedx, and DCA) are varied simultaneously in order to avoid any overestimation. There's only 1 set of variation and the undersampling is considered.

2. Electron identification The 2 electron identification cuts are selections by 2 independent detector subsystems. Therefore the related 2 cuts ($n\sigma_e$ and e/p) are varied separately. One variation is conducted to each cut and undersampling is considered for each of them. The total contribution from electron identification is the quadrature sum of the 2.

3. Electron triggering It is independent from other factors. One ($Adc0$) of the related cuts is varied to a single variation and undersampling is considered.

4. Raw yield extraction The raw yield is extracted by a fit procedure. The fit range, the integral mass window cut, the mass bin width, the fit function of contribution of residual background, and how the signal integral is calculated ("semi bin-counting" or "fit integral"), are arbitrarily chosen. The arbitrarity of these factors as well as the uncertainty of the additional smearing parameter cover the "raw yield extraction" aspect of systematic uncertainty. They are assumed to be correlated.

The fit range has 4 variations.

The mass window cut has 4 variations.

The mass binning and the form of the form of the fit function of the residual background contribution has 1 variation each, separately.

In terms of the signal integral, pure bin counting itself is an 0-biased and 0-variance estimator when no background presents. In our case, one can either integrate over the signal contribution in the fit function (fit integral), or integrate over the signal+background histogram and subtract the integral of the fit function of the residual background contribution (semi bin-counting). The semi bin-counting is chosen to be the default value under an uneducated and intuitive guess that it is less biased compared to fit integral, nevertheless the difference between them is assigned as one of the contribution.

The optimized parameter ($\frac{\Delta a}{a}$) is varied from $(\frac{\Delta a}{a})_{opt}$ to the asigned lower and upper confidence interval boundary at confidence level value $z = 1$.

Among the 13 correlated variations, the maximum deviation from the default value in each p_T bin is assigned to be the total contribution from raw yield extraction as a conservative estimation.

The following plots show the relative deviations as a function of p_T for different variations:

p+p Cross Section

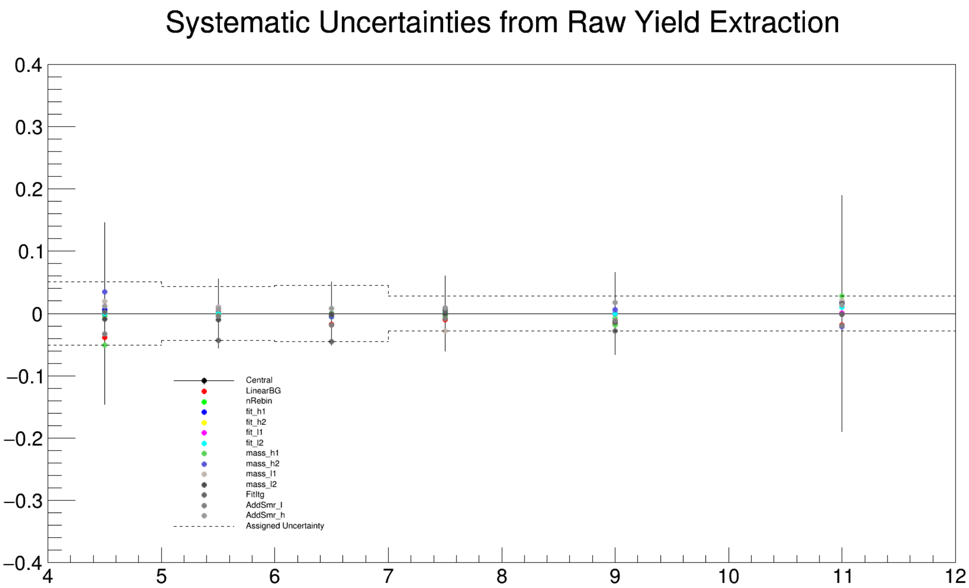

p+Au Invariant Yield

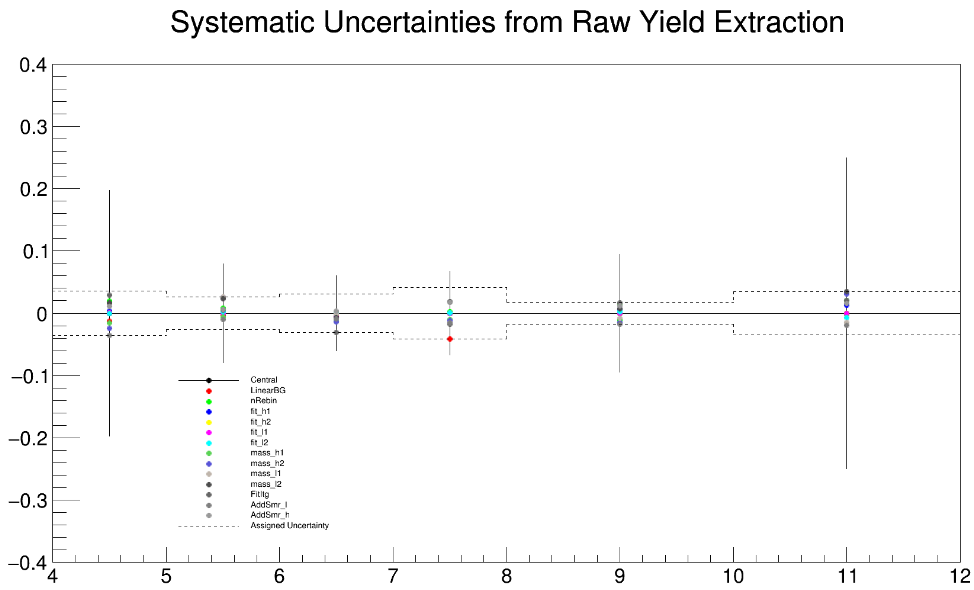

$\mathbf{R}_e xtpA$

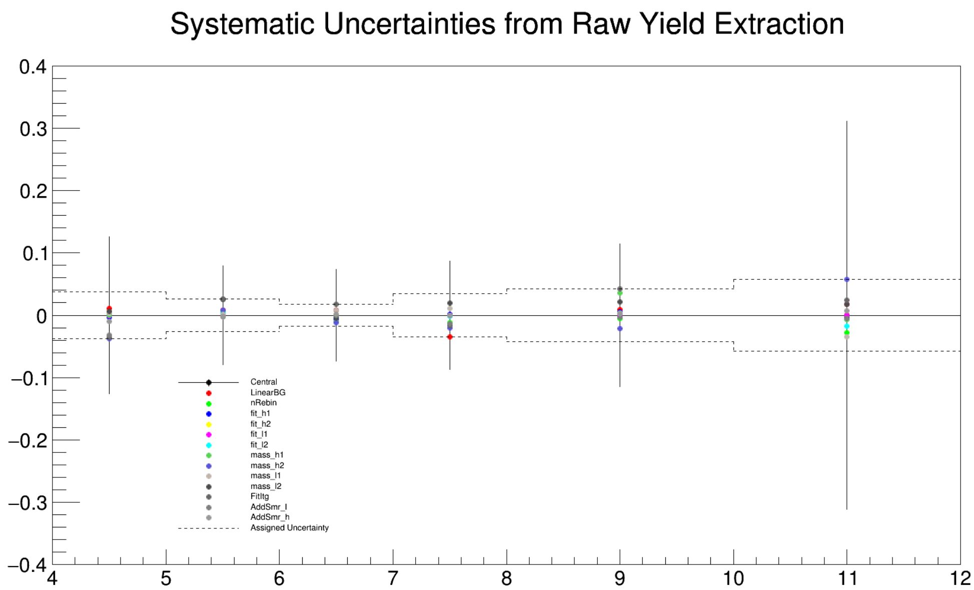

6.3 The Total Systematic Uncertainty

The total systematic uncertainty is the quadrature sum of the independent contributions from the aforementioned 4 aspects.

The following is a summary table of all variations.

Variable Name	Default	Variation(s)
Tracking Quality (Simultaneously)		
nHitsFit	$[20, \infty)$	$[25, \infty)$
nHitsDedx	$[10, \infty)$	$[15, \infty)$
DCA	$[0, 1.5)$	$[0, 1.4)$
Electron Identification (Separately)		
$n\sigma_e$	$(1.5, 2.5)$	$(-1.7, 2.5)$
$\frac{E}{p}$	$(0.5, 2.5)$	$(0.6, 2.4)$
Electron Triggering		
Adc0	$[300, \infty)$	$[316, \infty)$
Raw Yield Extraction (Choose Maximum)		
Fit Range	$[1.5, 4.5]$	$[1.5, 4.5 \pm 0.05]$, $[1.5 \pm 0.05.4.5]$
Mass Window	$[2.70, 3.25]$	$[2.70, 3.25 \pm 0.05]$, $[2.70 \pm 0.05, 3.25]$
Mass Bin Width	0.05 GeV/c^2	0.025 GeV/c^2
$f_{ResBG}(M_{e^+e^-})$	$A \cdot e^{-b \cdot M_{e^+e^-}}$	$a + b \cdot M_{e^+e^-}$
Signal Integral Method	semi bin-counting	fit integral
Parameter in Addtional Smearing	$(\frac{\Delta a}{a})_{opt}$	lower and upper confidence interval limits

The following plots show the independent contributions and the quadrature sum as a function of p_T for different variations. Note that in the EID contribution, each subject is independent from each other. Henceforth they are effectively 2 independent contrubutions to the total systematic uncertainty. For convenience, both of them are presented in this plot as independent contributions.

p+p Cross Section

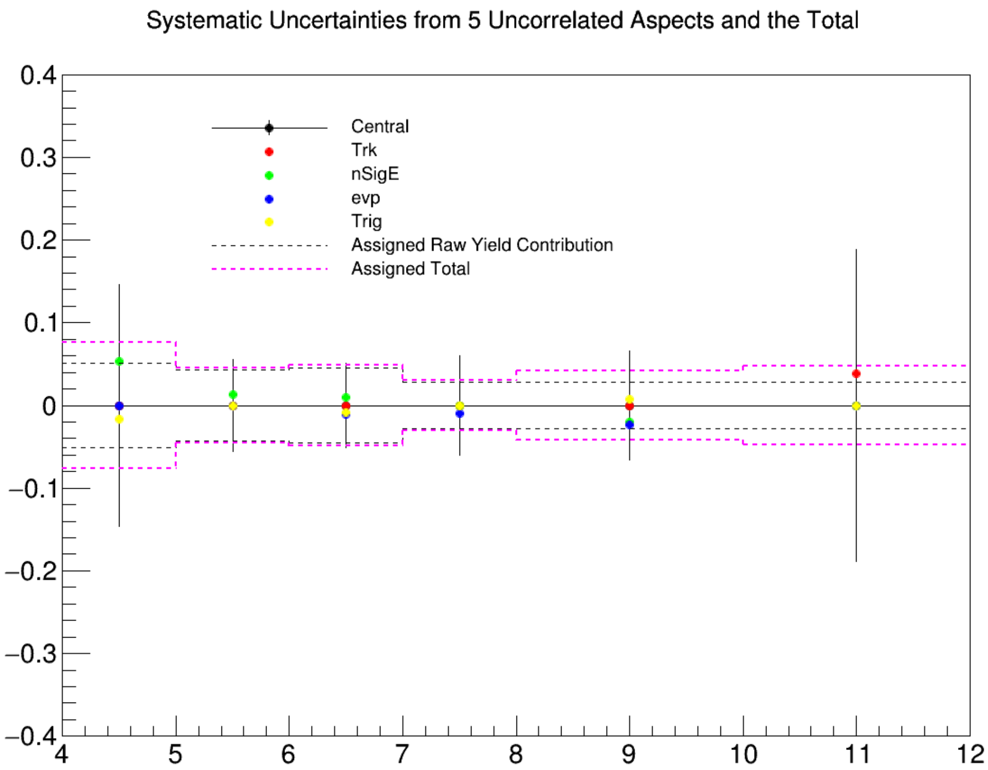

p+Au Invariant Yield

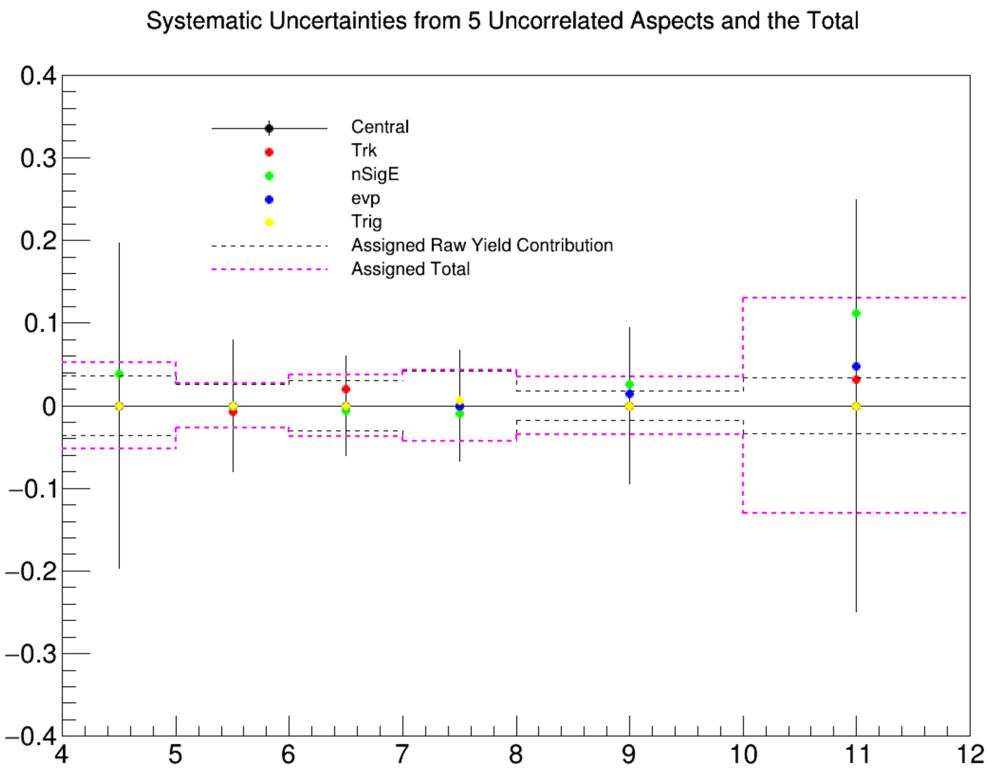

$\mathbf{R}_e xtpA$

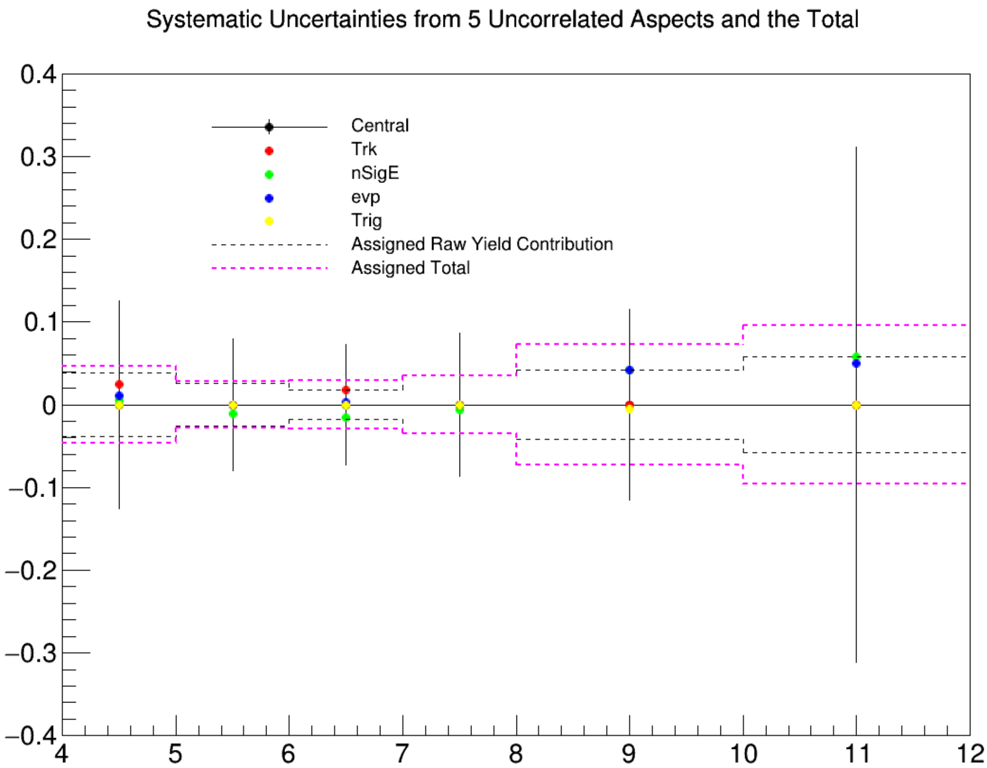

The three physics results (cross section in p+p collisions, invariant yield in p+Au collisions, and the $\mathrm{R}_e xtpA$ with error bars representing statistical uncertainty and boxes representing systematic uncertainty are presented as follows:

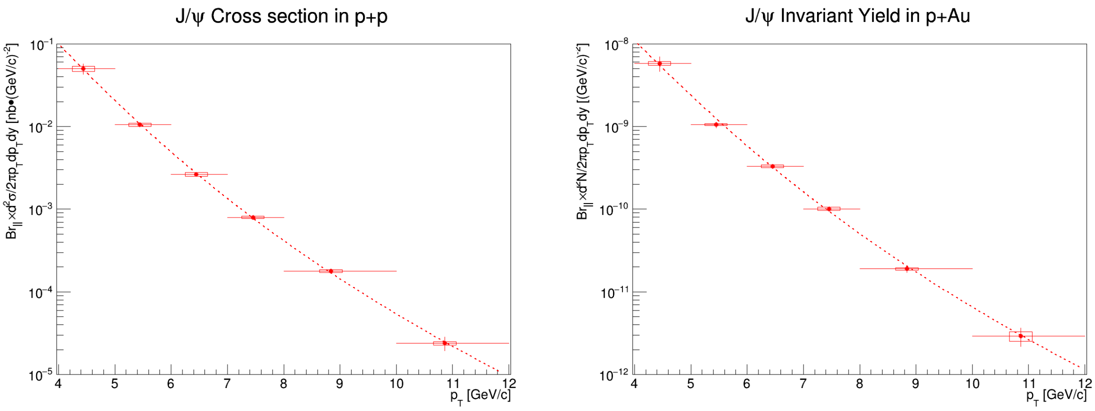

Figure 12: The dashed line is a function derived from the aformentioned fit function to the yield in p+p and p+Au, $f(p_T) = N \cdot p_T \cdot (1+(\frac{p_T}{A})^2)^{-n}$, by factoring out the p$_T$ term and multiplying the N parameter by $\frac{\sigma_{pp}^{NSD}}{2\pi}$ and $\frac{1}{2\pi}$, respectively

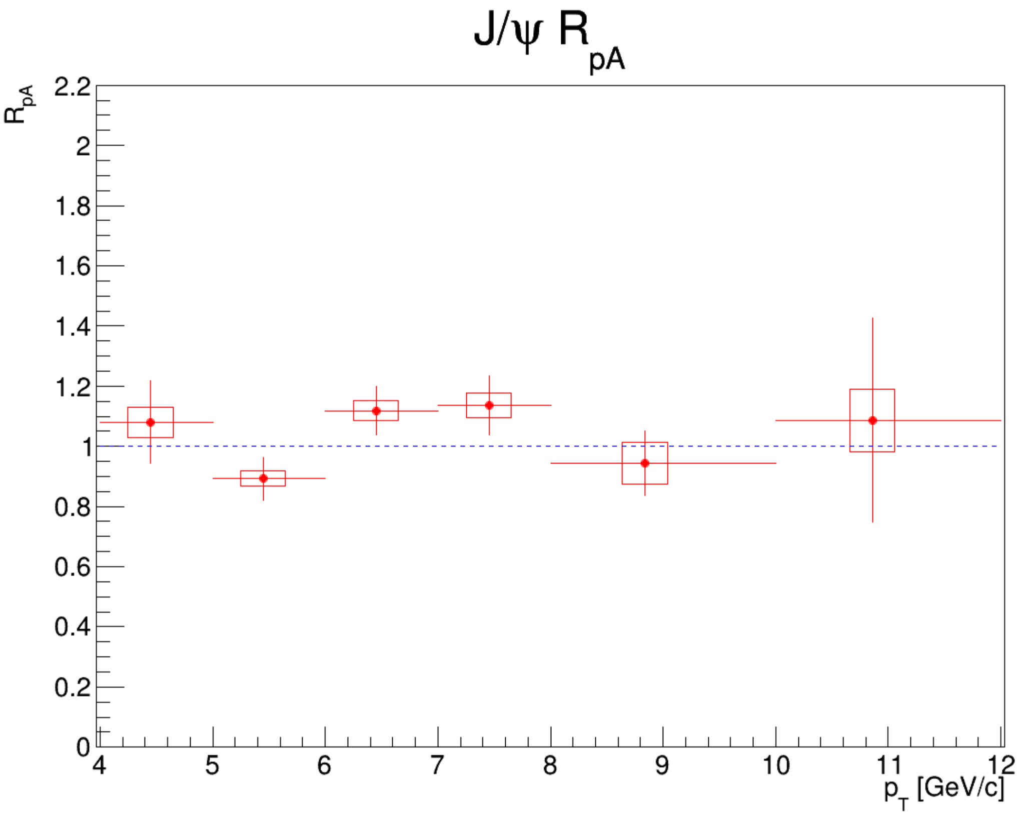

Figure 13: The blue dashed line represents unity

7 Appendices

Most of the appendix is temporarily removed to speed up compilation.

7.1 Embedding QA Plots

The distributions for single electrons in data are compared to those in embedding. These distributions are corresponding to those electrons from J/ψ candidates without selection in J/ψ transverse momentum (p_T), rapidity (y) or mass. The P values of Kolmogorov–Smirnov test between data and RC (original embedding) are calculated and shown in the titles. Trigger electron and non-trigger electron are shown in different plots. Comparisons in both p+p and p+Au collisions are made. In p+p, additional histograms with additional smearing and folding with evtGen models are also present, as a side proof for the rigorousness of the additional smearing procedure.

Basic Kinematics

$\mathbf{p}_T$ [GeV/c^2]

Triggered, p+p:

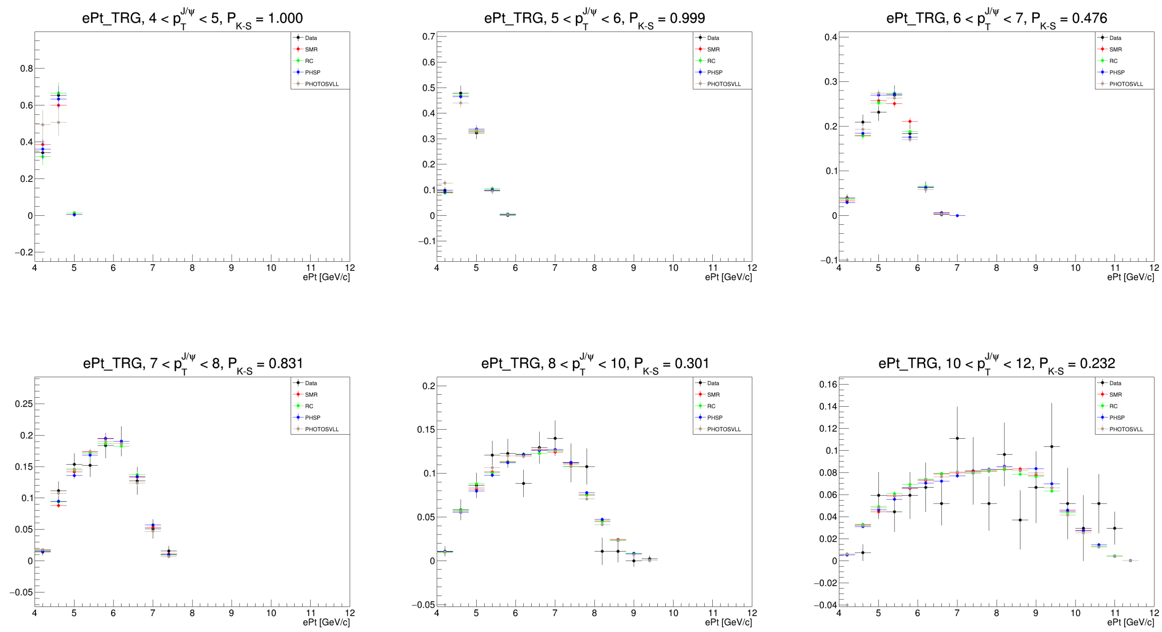

Non-triggered, p+p:

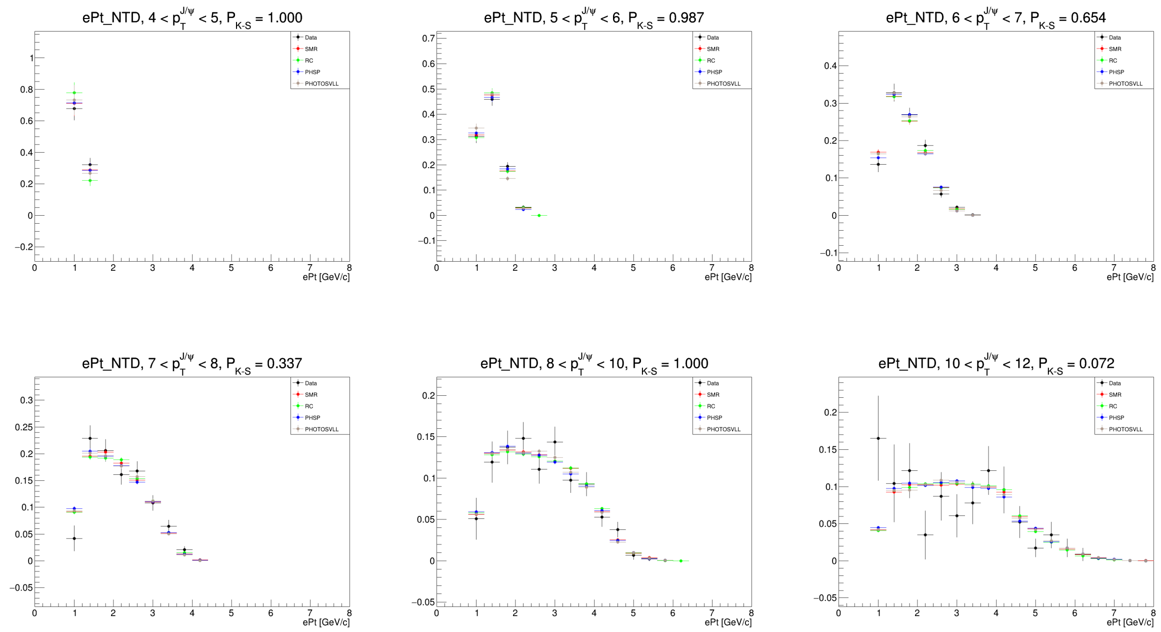

Triggered, p+Au:

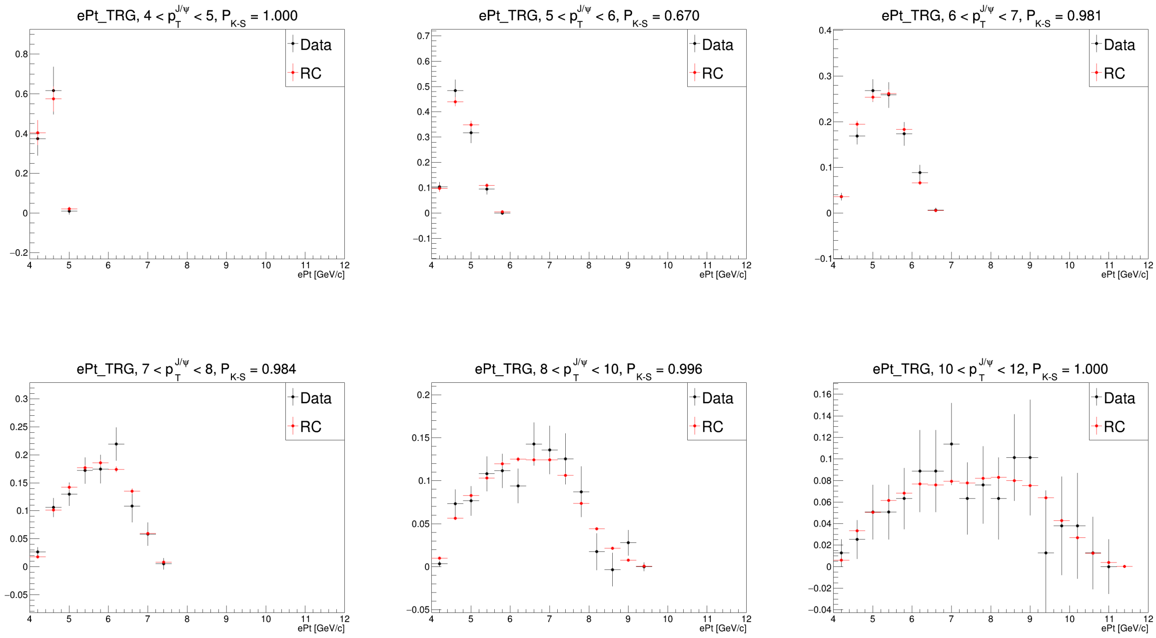

Non-triggered, p+Au:

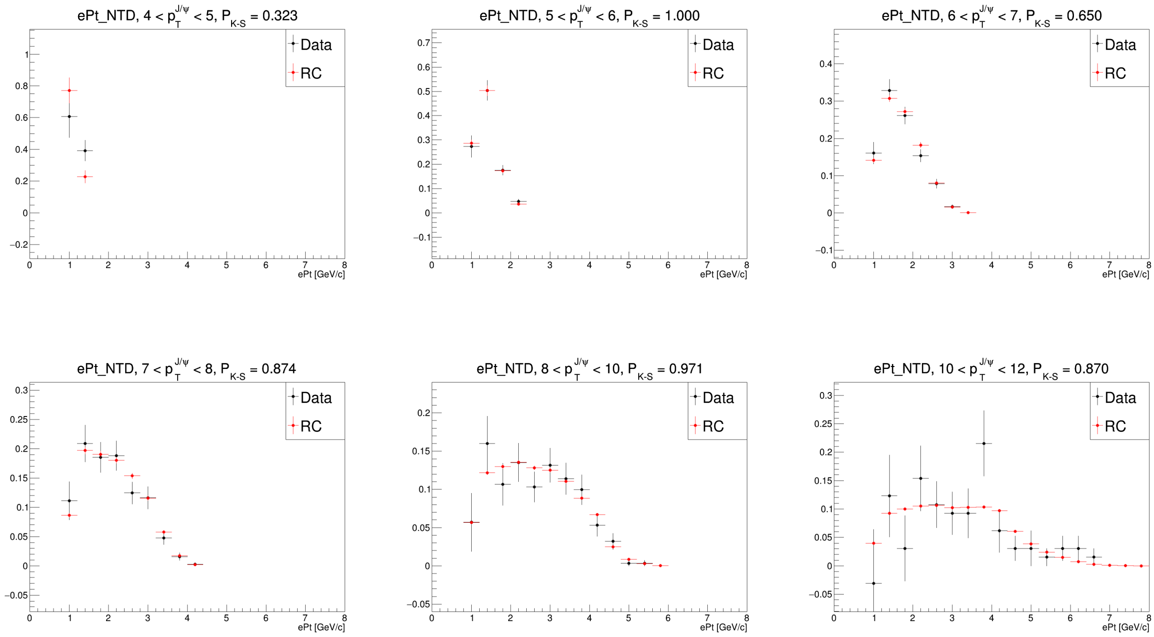

Pseudorapidity (η)

Triggered, p+p:

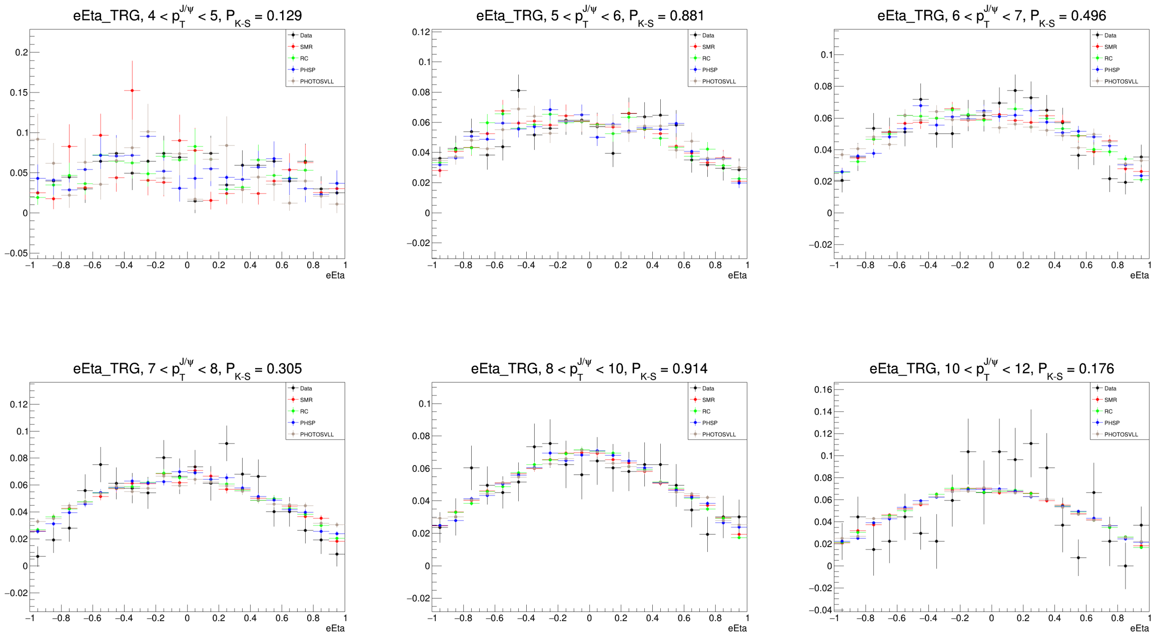

Non-triggered, p+p:

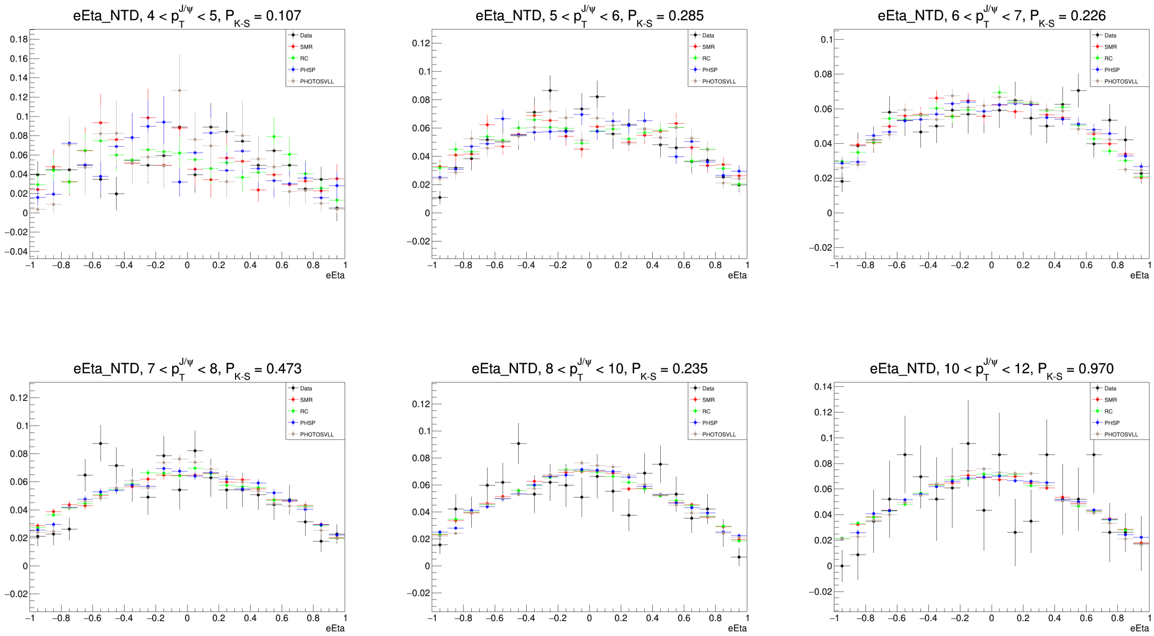

Triggered, p+Au:

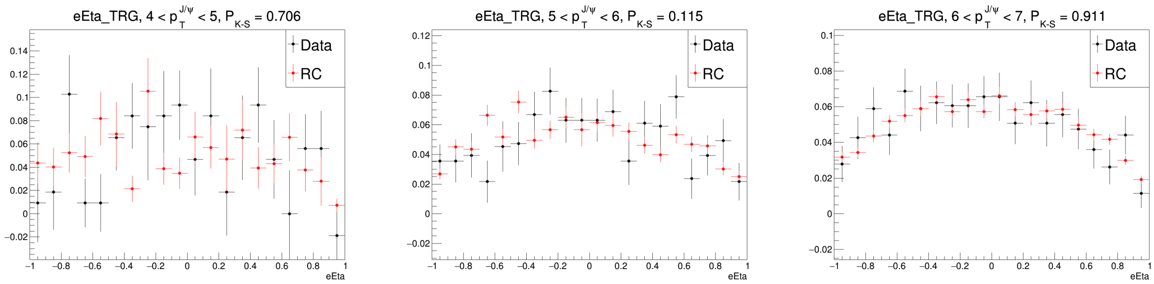

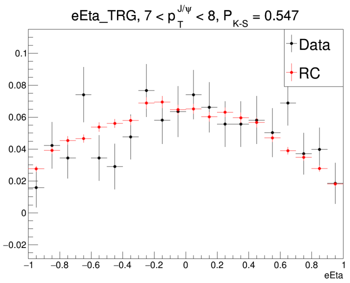

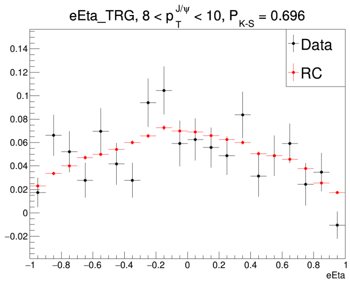

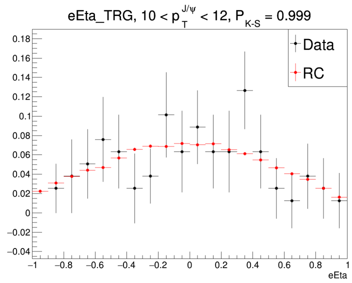

Non-triggered, p+Au:

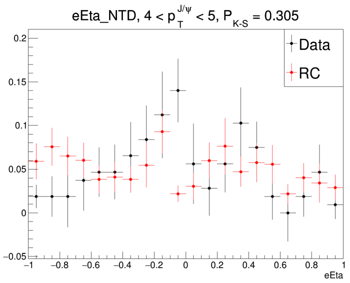

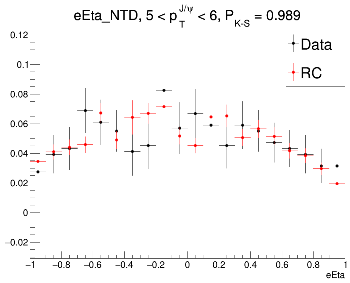

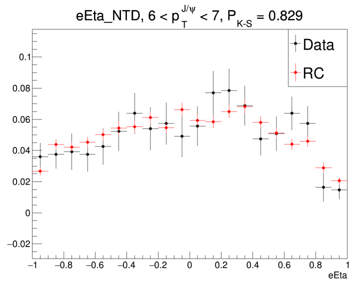

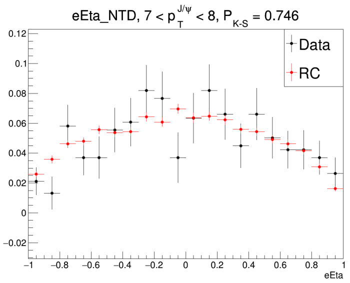

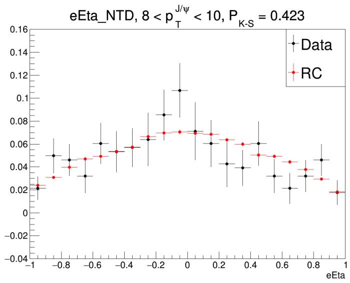

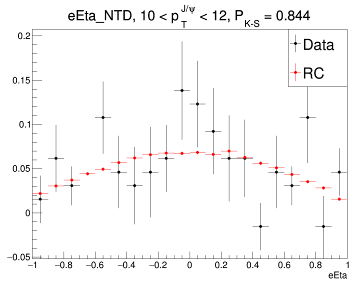

ϕ

Triggered, p+p:

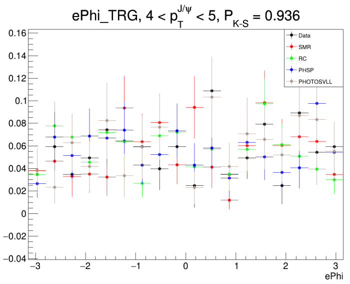

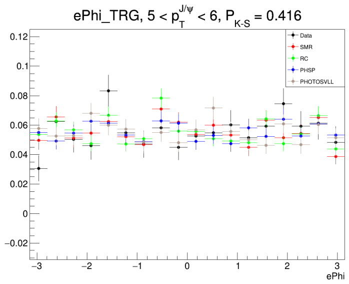

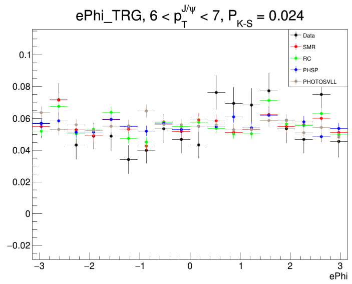

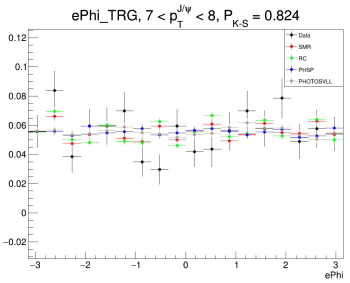

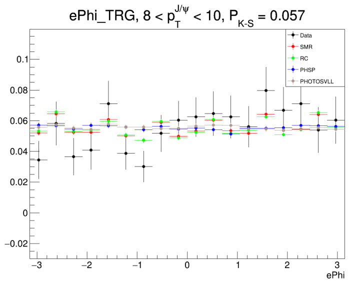

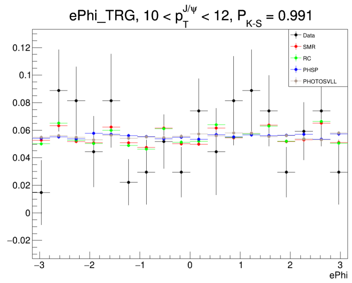

Non-triggered, p+p:

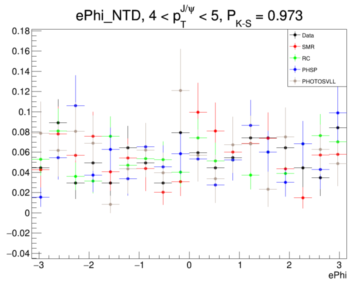

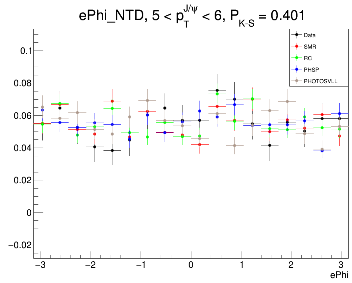

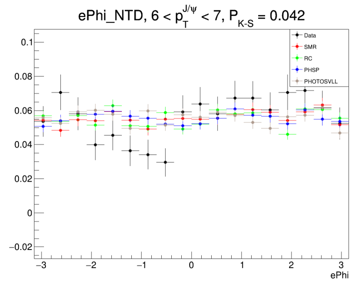

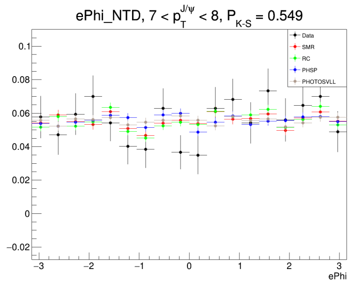

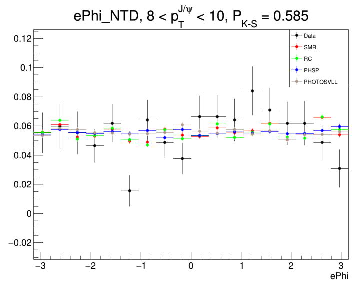

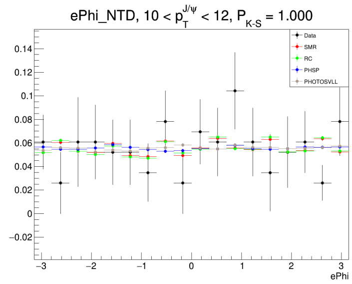

Triggered, p+Au:

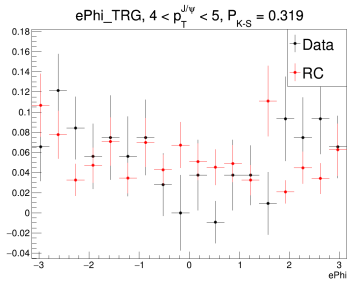

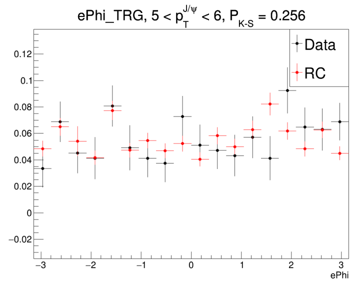

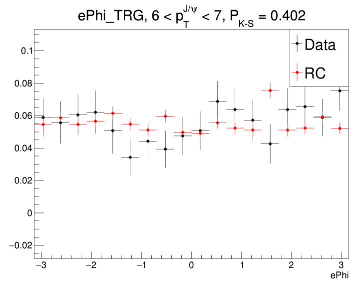

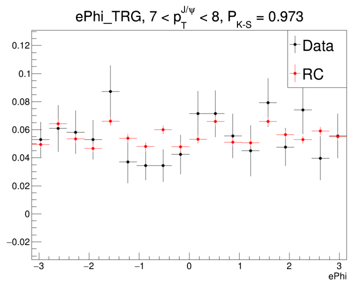

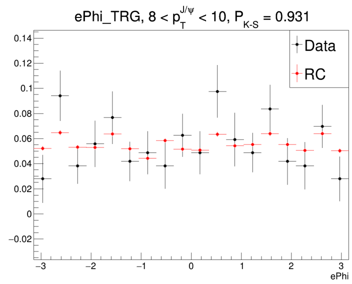

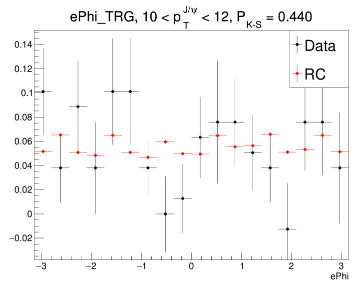

Non-triggered, p+Au:

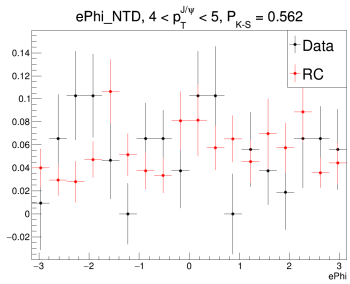

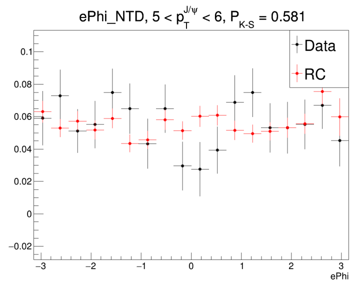

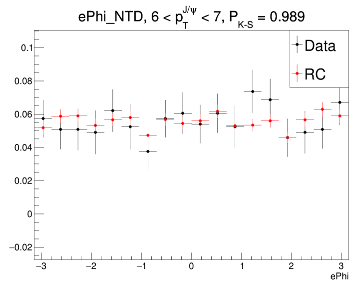

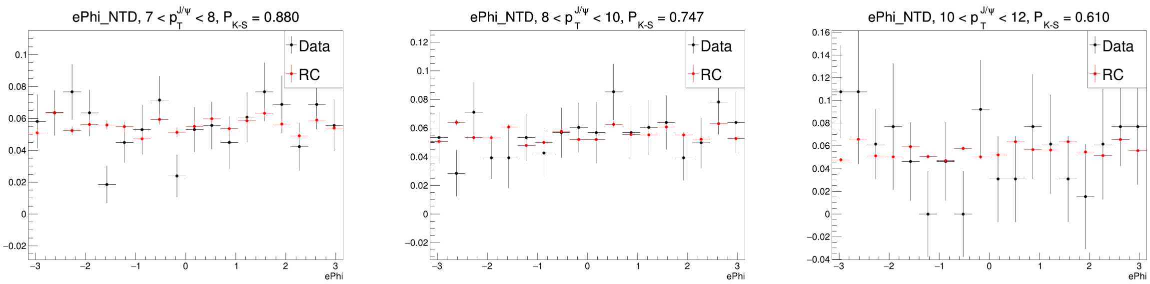

Tracking Quality

Distance of Closest Approach (DCA) [cm]

Triggered, p+p:

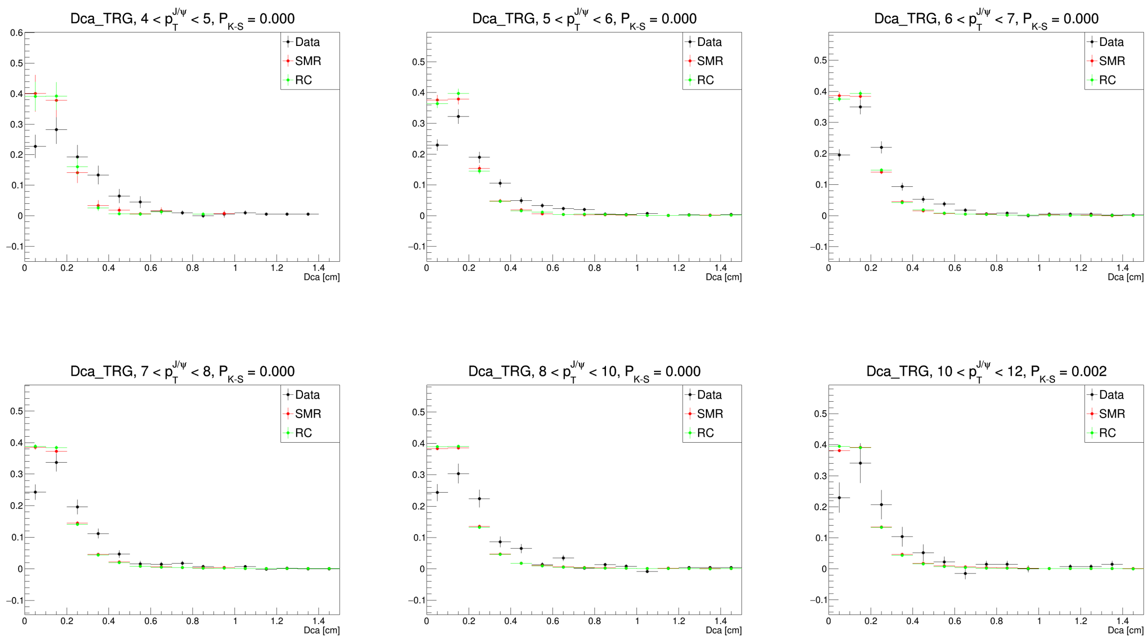

Non-triggered, p+p:

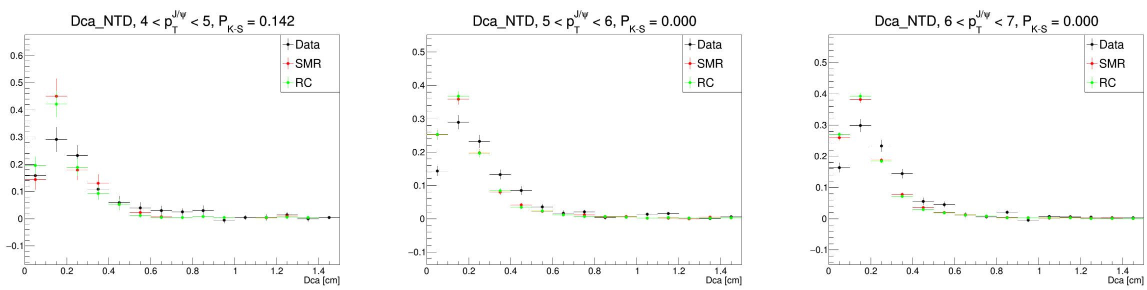

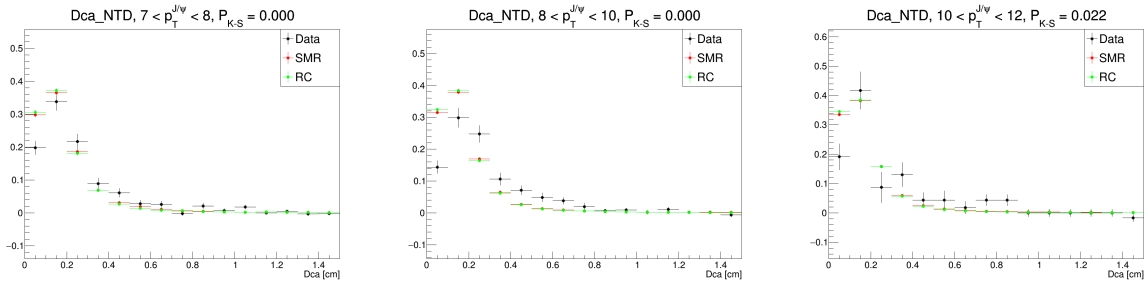

Triggered, p+Au:

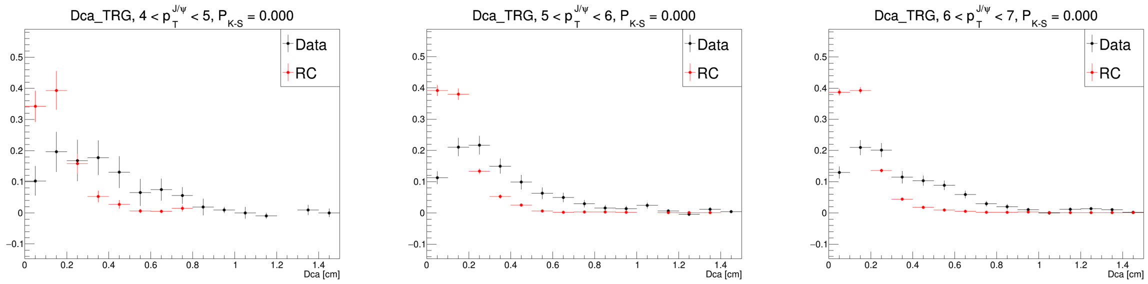

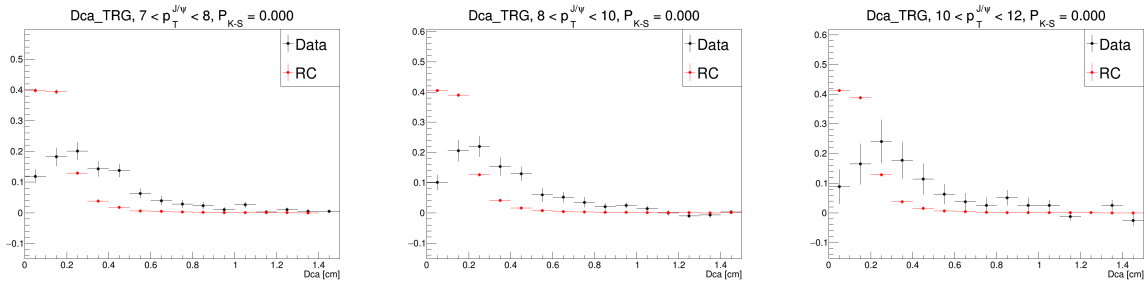

Non-triggered, p+Au:

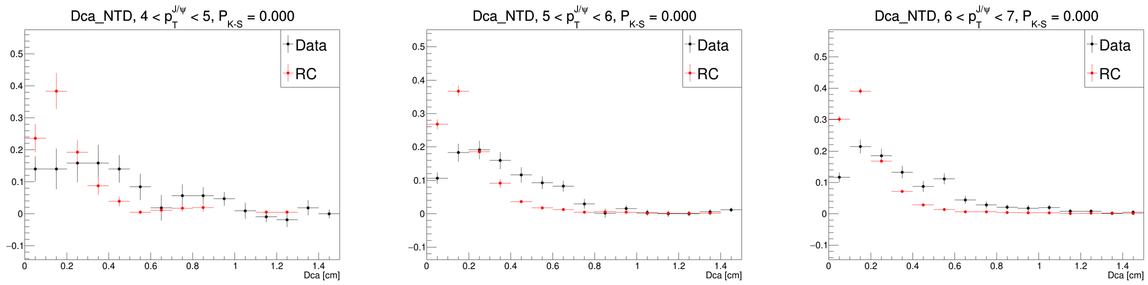

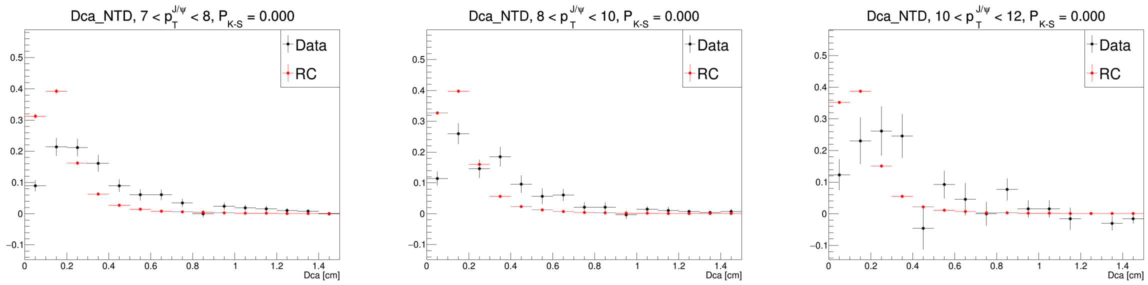

nHitsFit

Triggered, p+p:

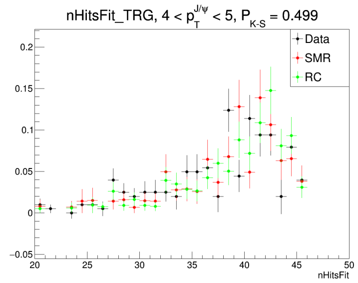

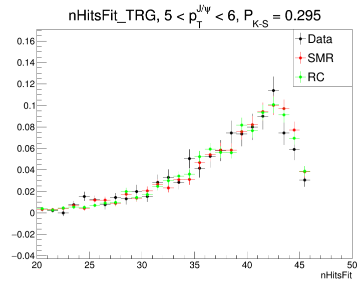

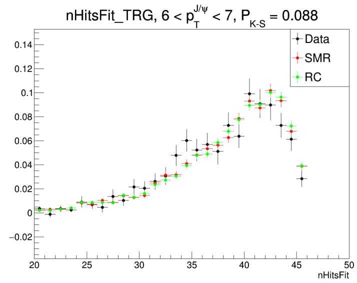

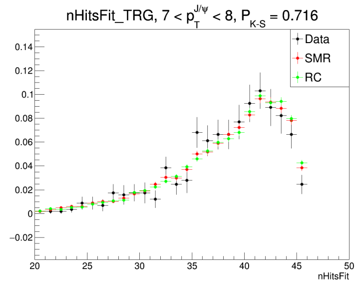

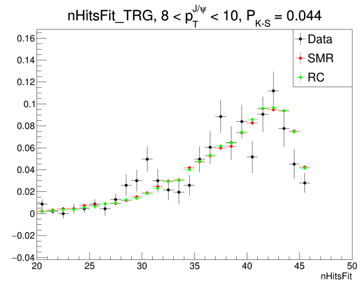

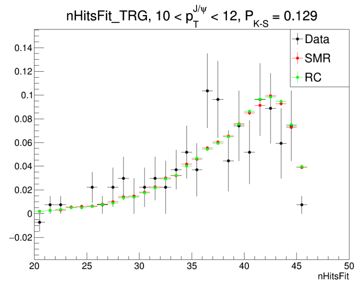

Non-triggered, p+p:

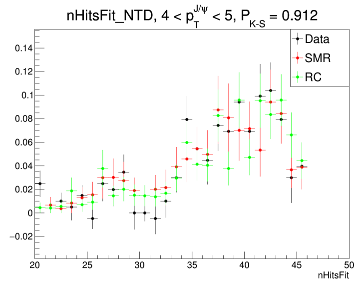

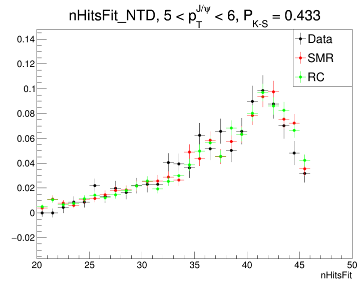

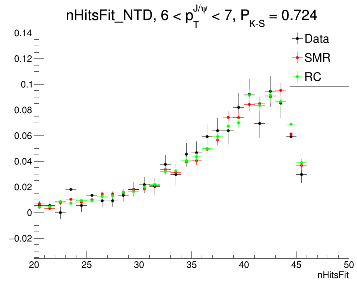

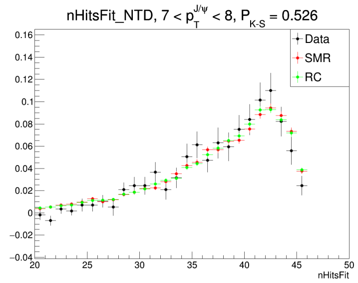

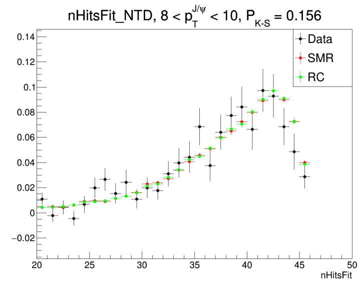

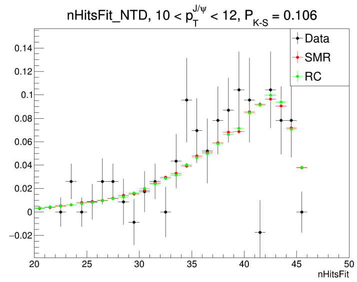

Triggered, p+Au:

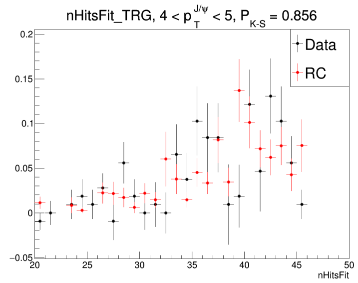

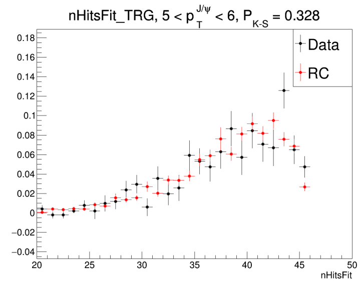

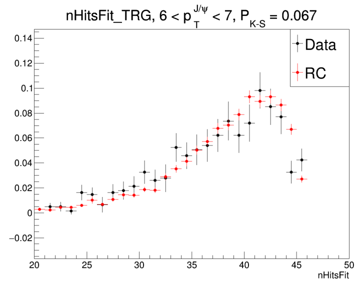

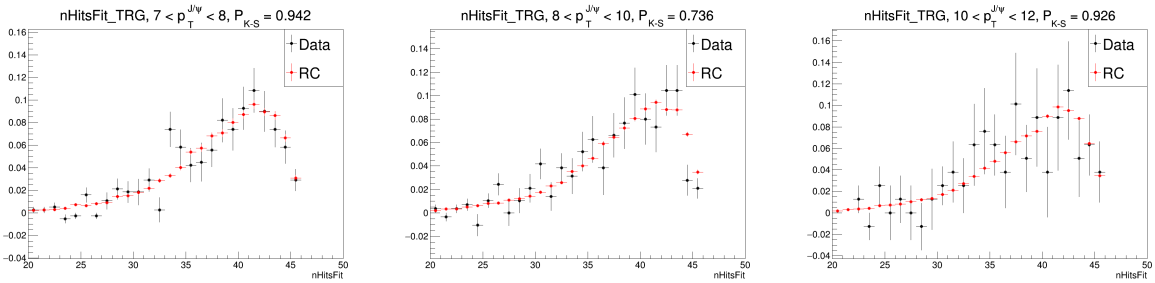

Non-triggered, p+Au:

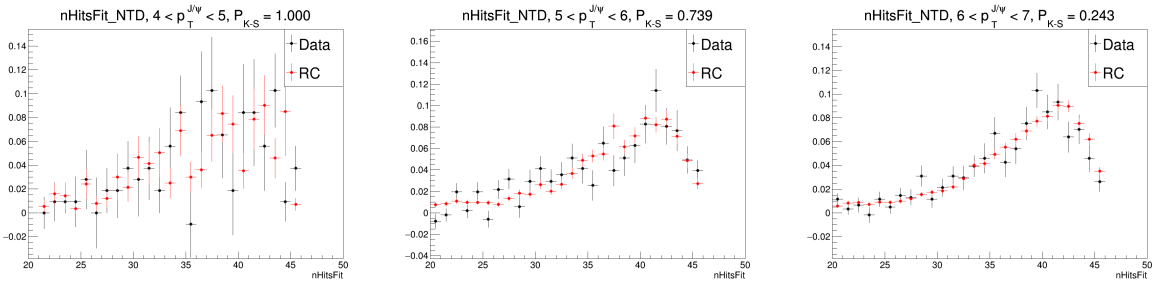

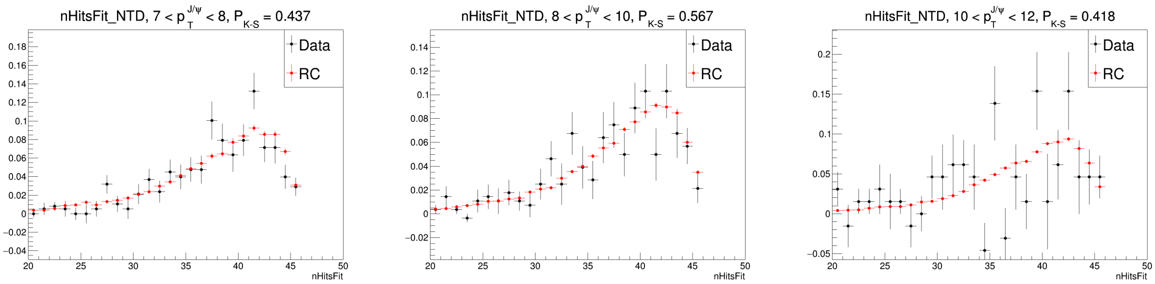

nHitsDedx

Triggered, p+p:

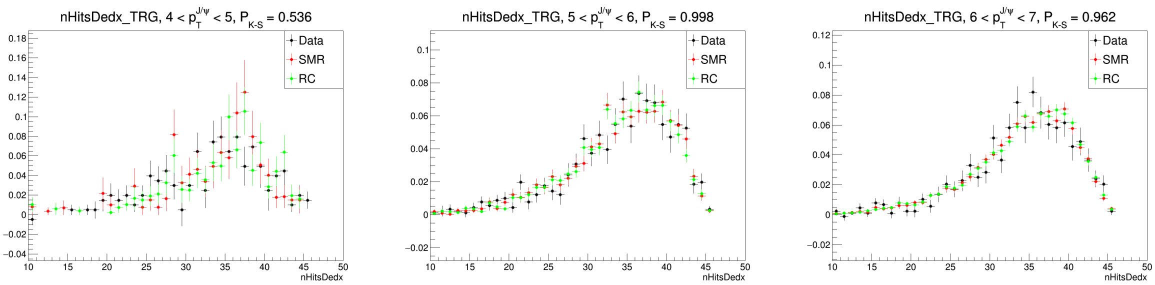

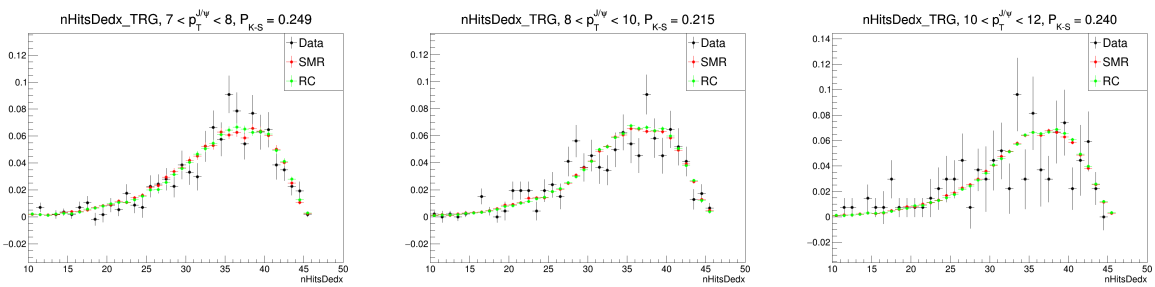

Non-triggered, p+p:

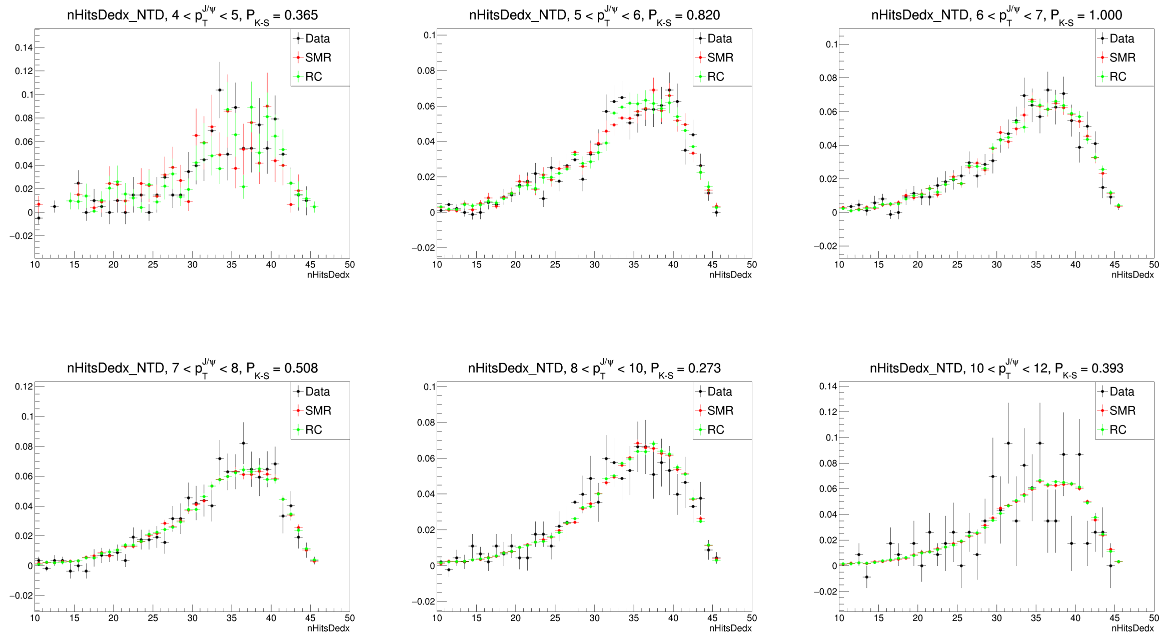

Triggered, p+Au:

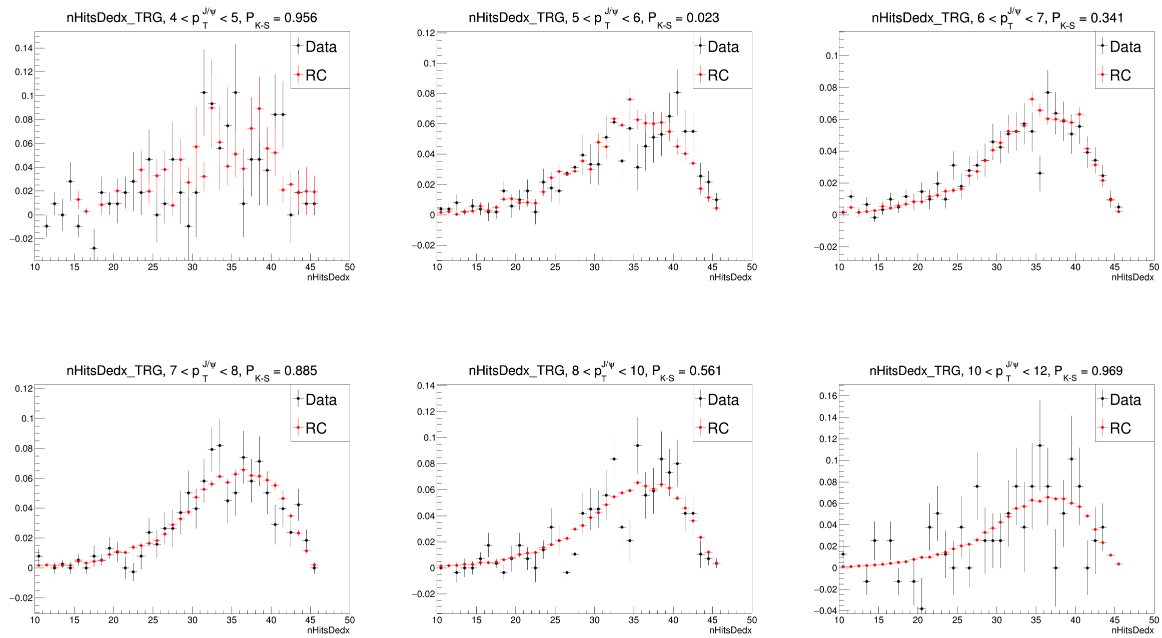

Non-triggered, p+Au:

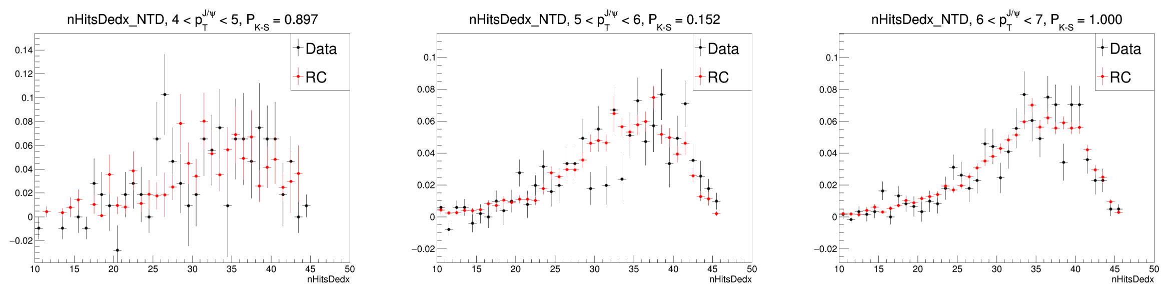

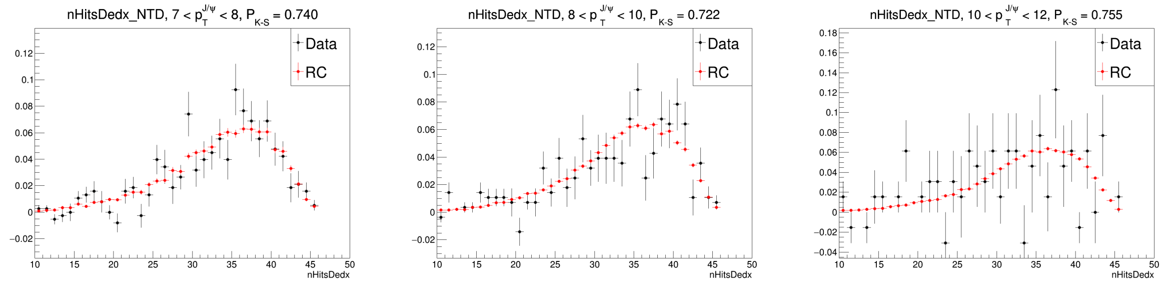

$\mathbf{n}\sigma_e$

Triggered, p+p:

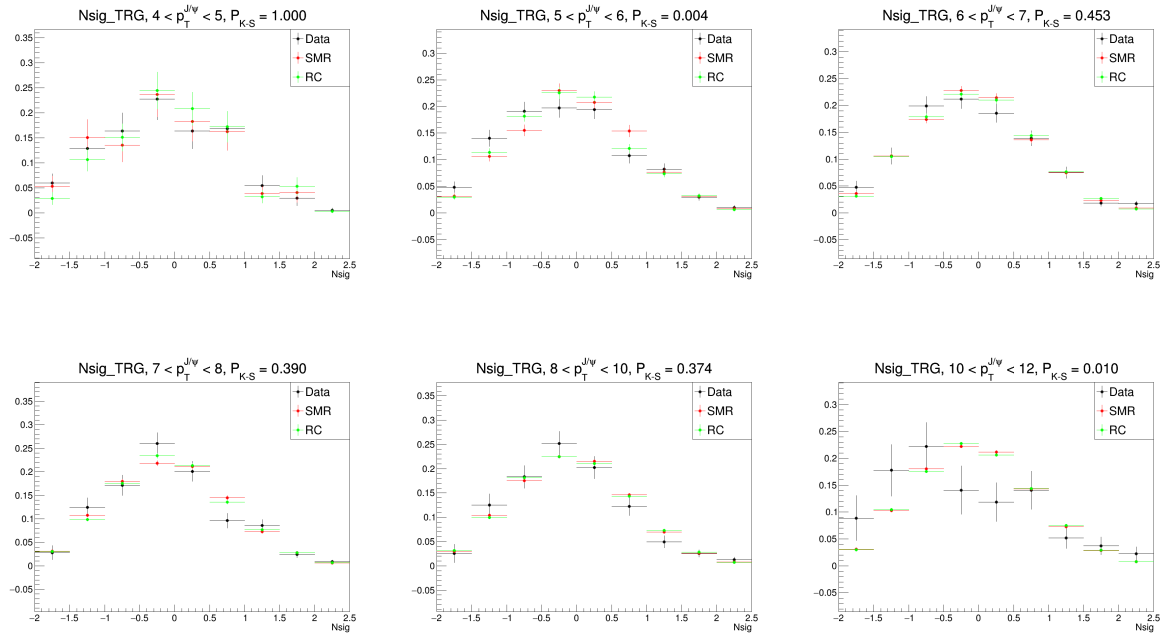

Non-triggered, p+p:

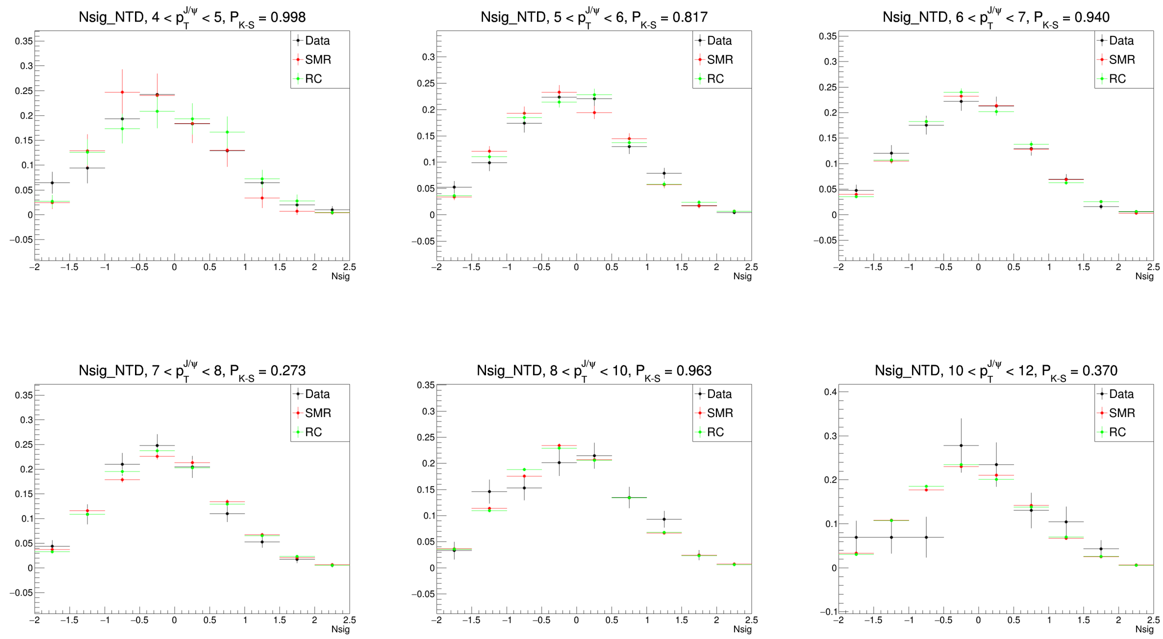

Triggered, p+Au:

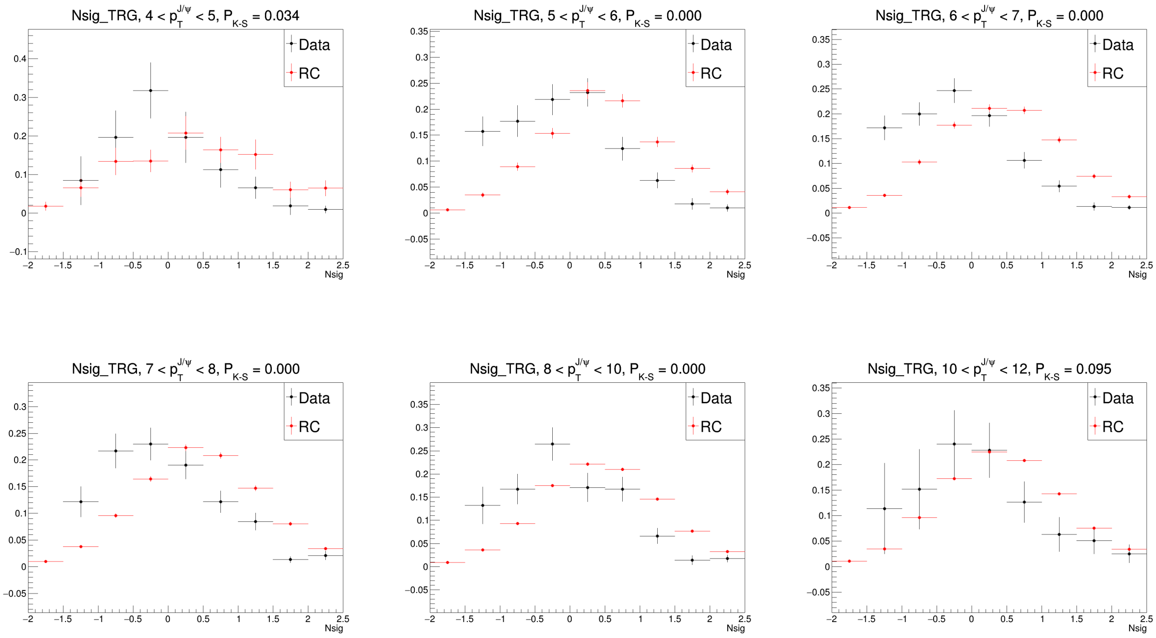

Non-triggered, p+Au:

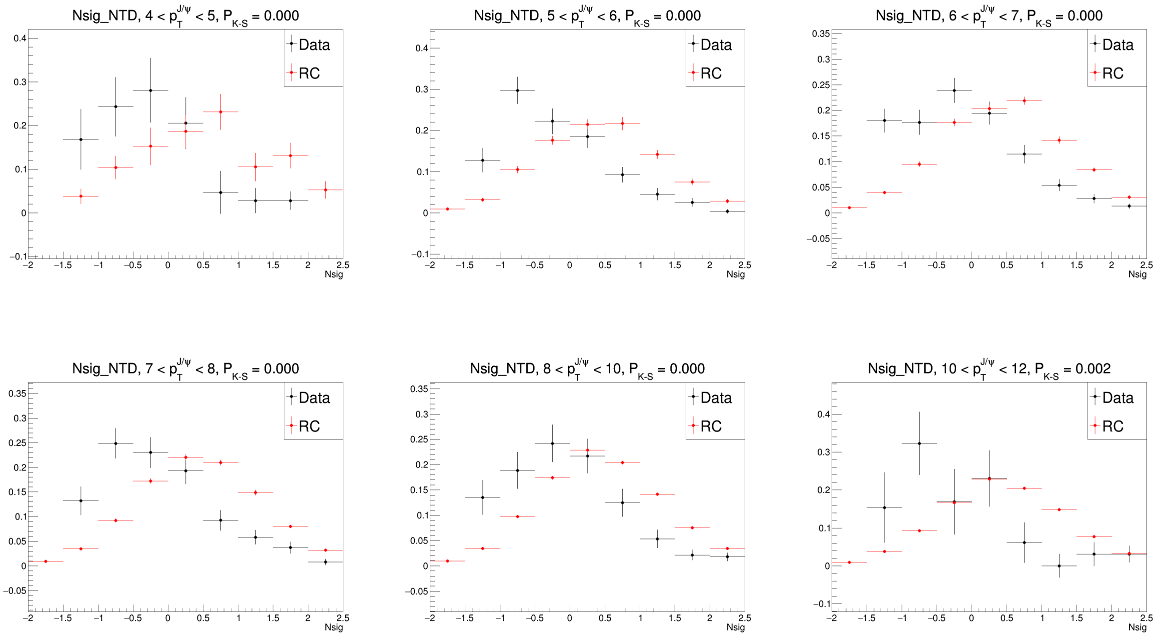

Others

e/p [c]

Triggered, p+p:

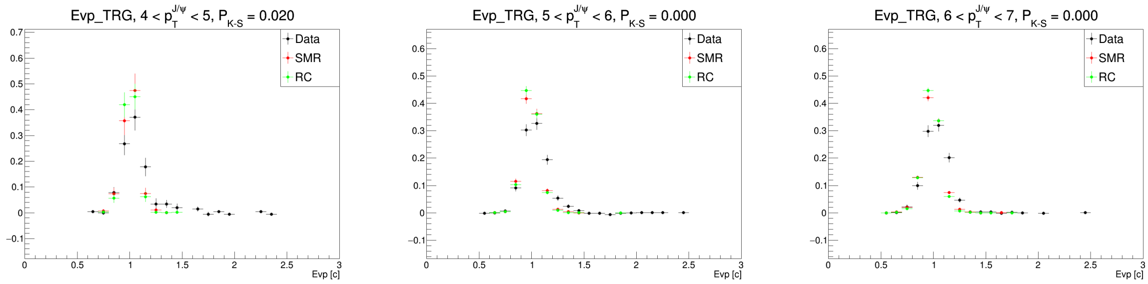

Non-triggered, p+p:

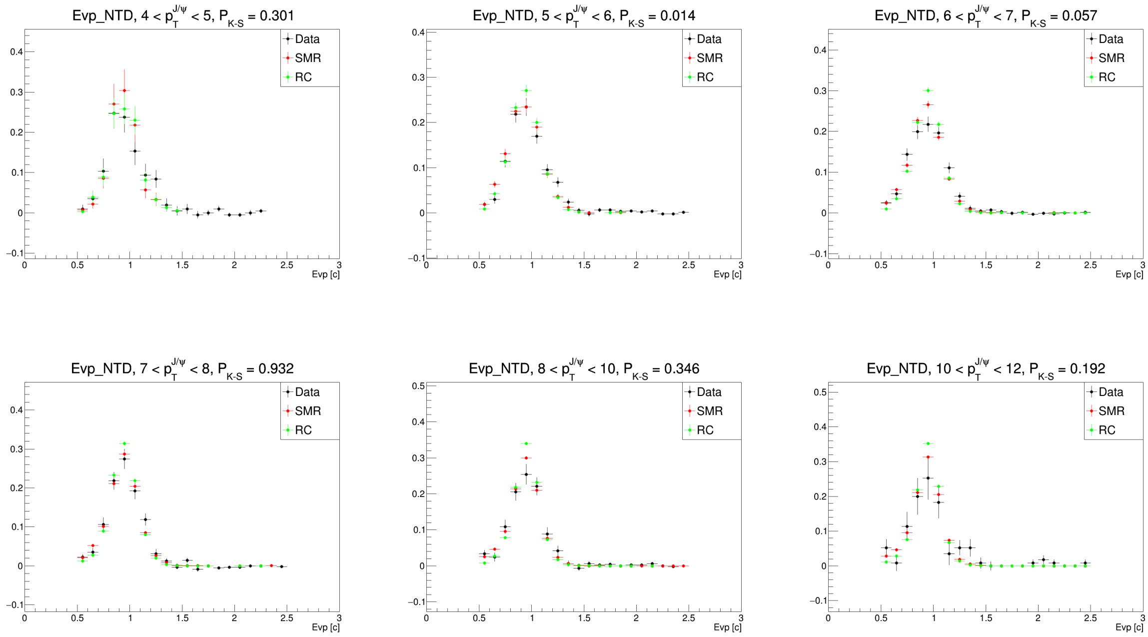

Triggered, p+Au:

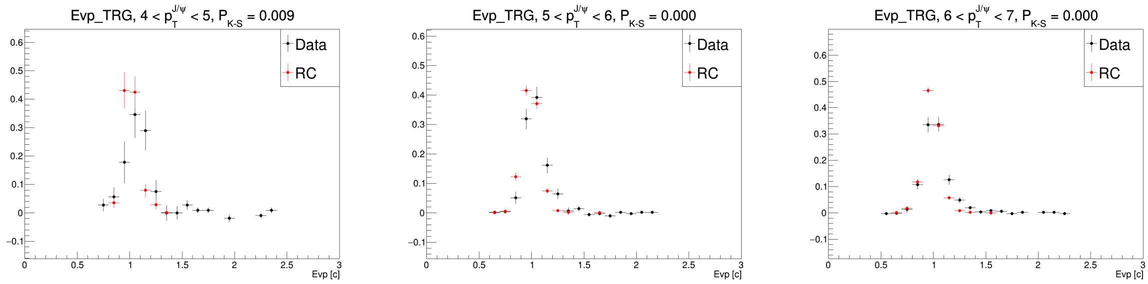

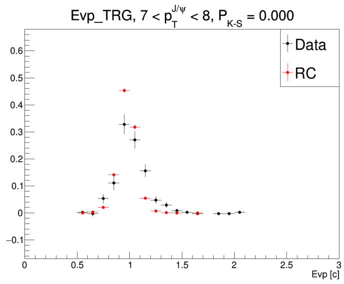

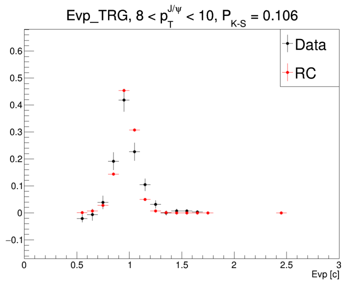

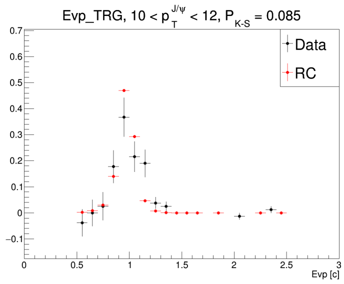

Non-triggered, p+Au:

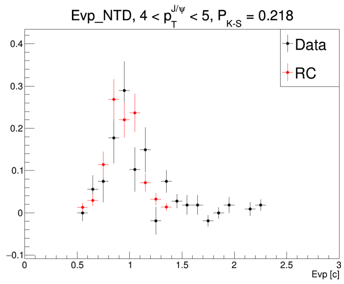

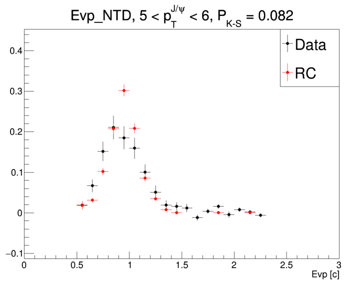

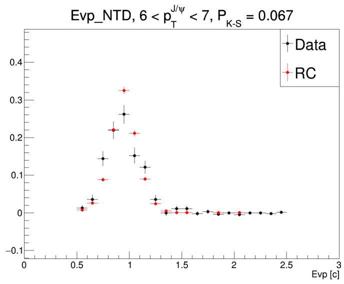

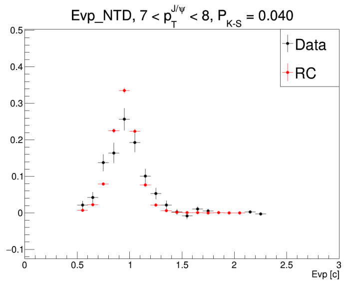

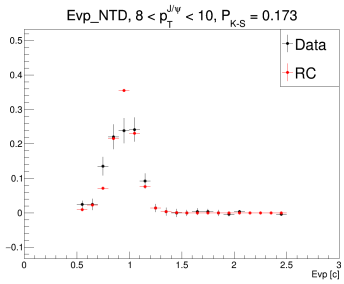

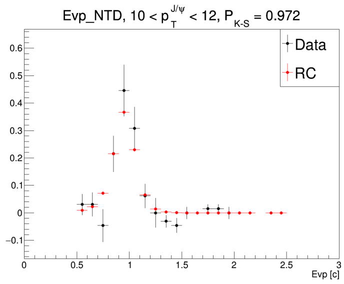

Adc0

Triggered, p+p:

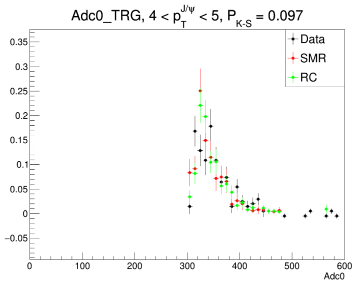

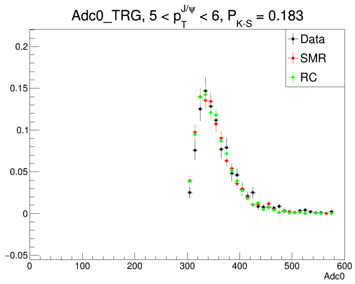

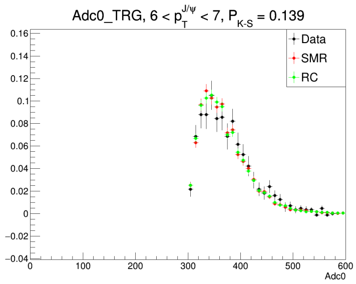

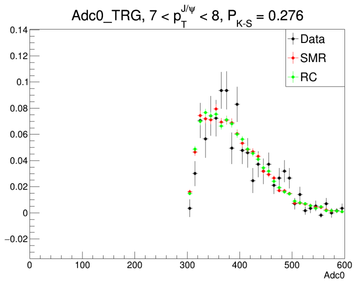

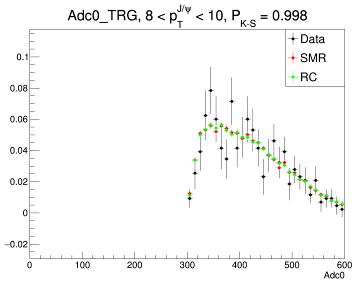

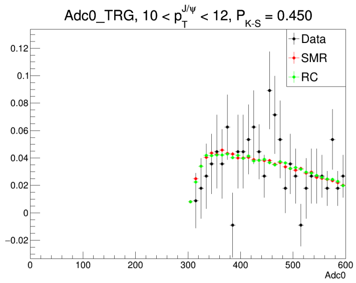

Non-triggered, p+p:

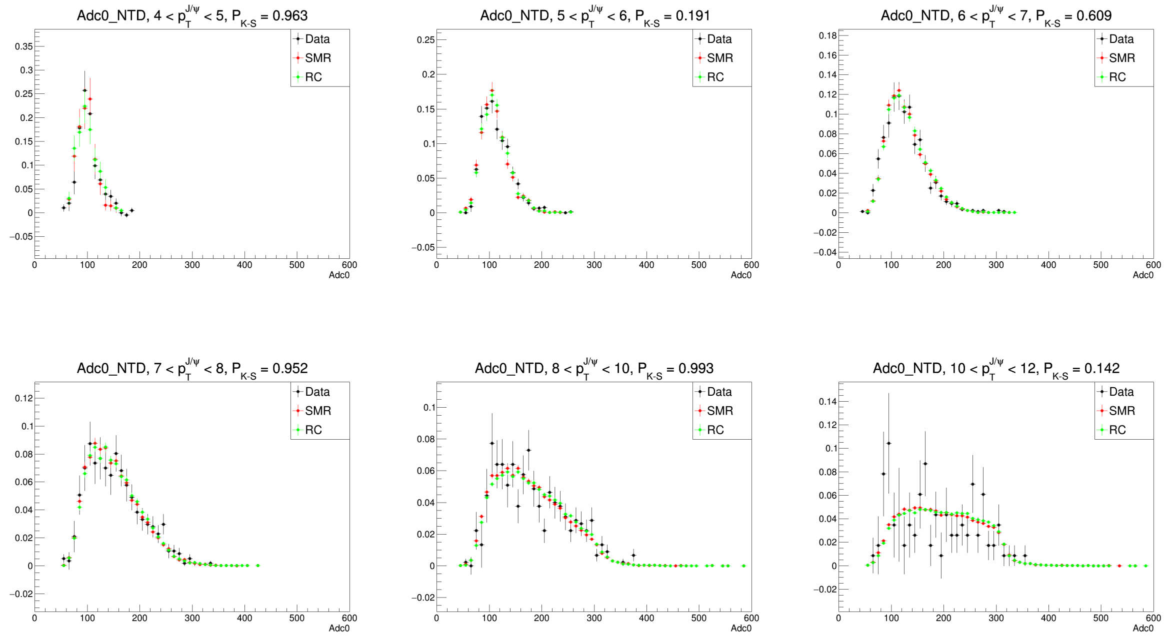

Triggered, p+Au:

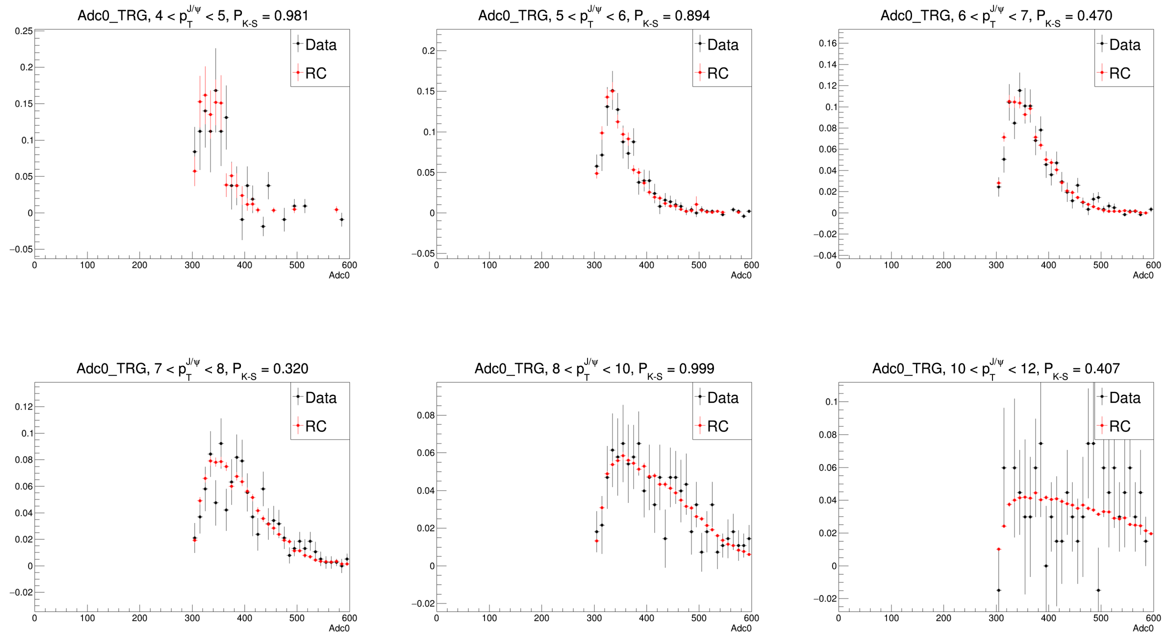

Non-triggered, p+Au:

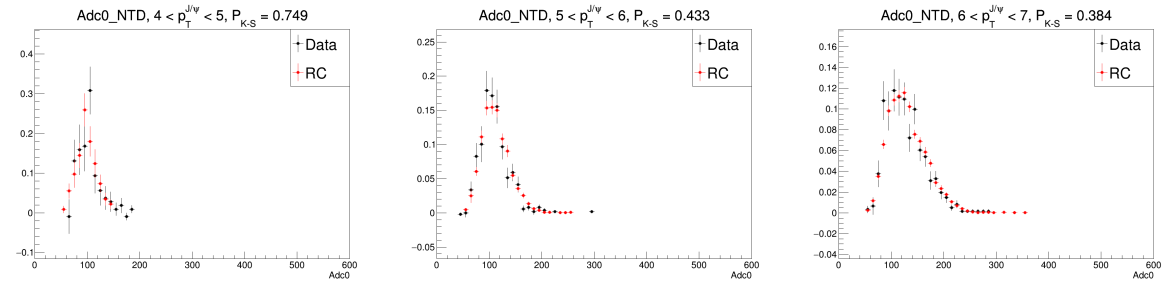

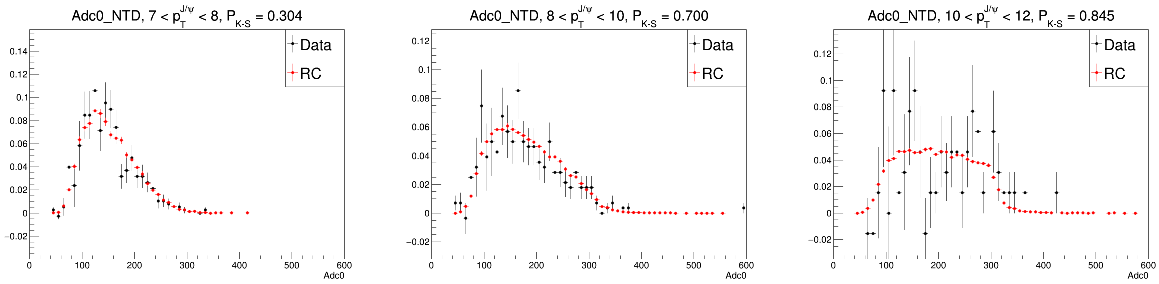

Dsmadc

Triggered, p+p:

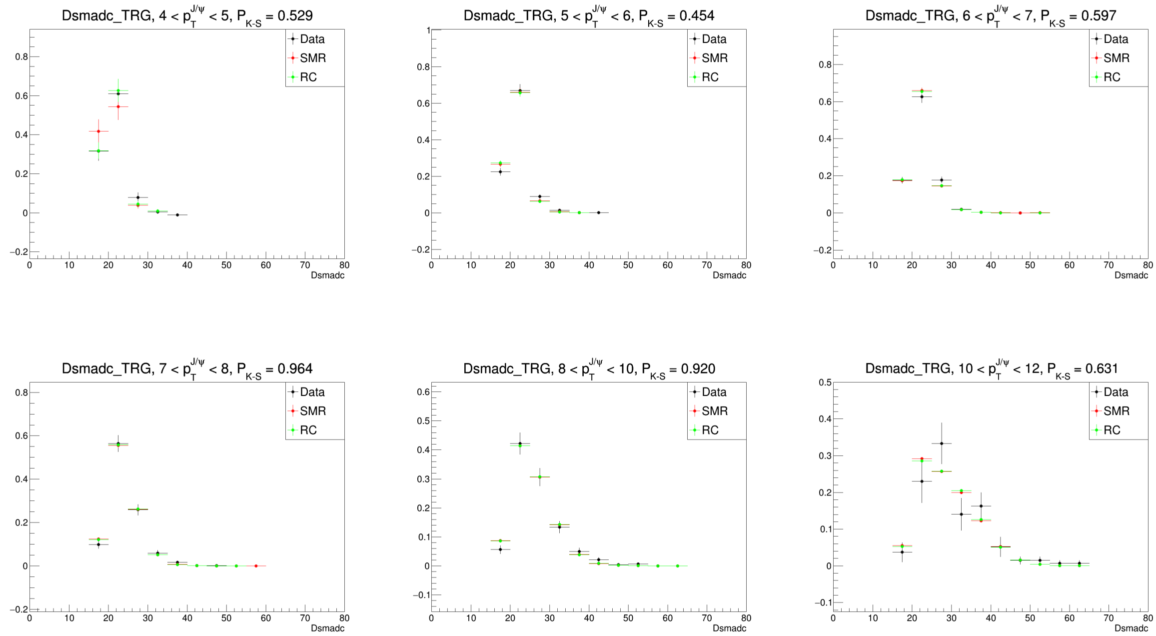

Non-triggered, p+p:

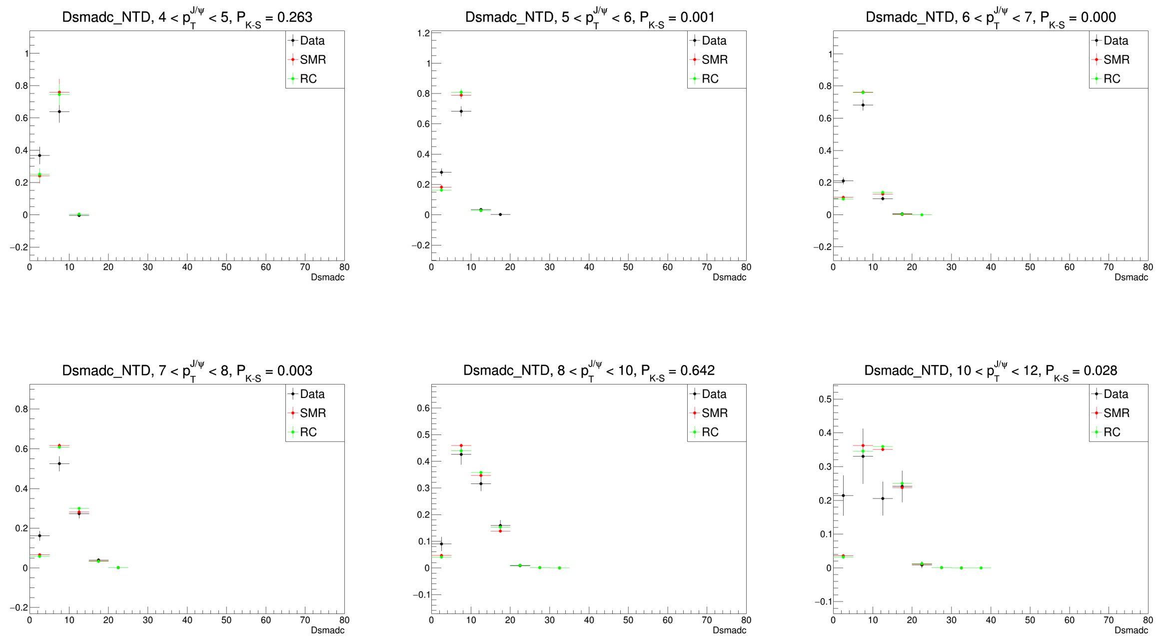

Triggered, p+Au:

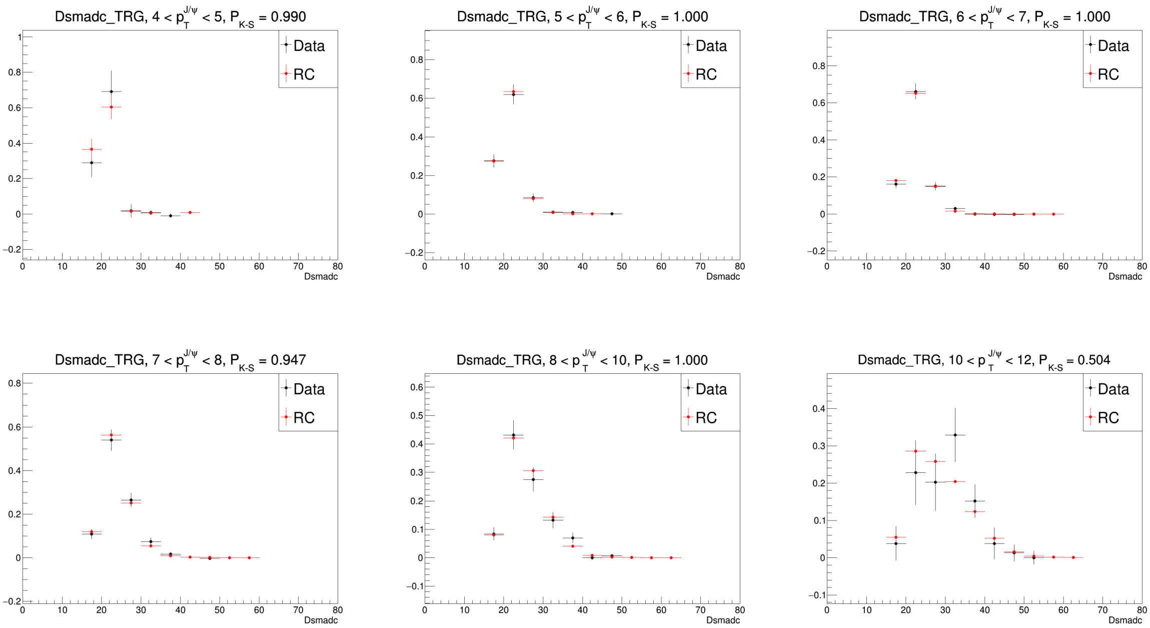

Non-triggered, p+Au:

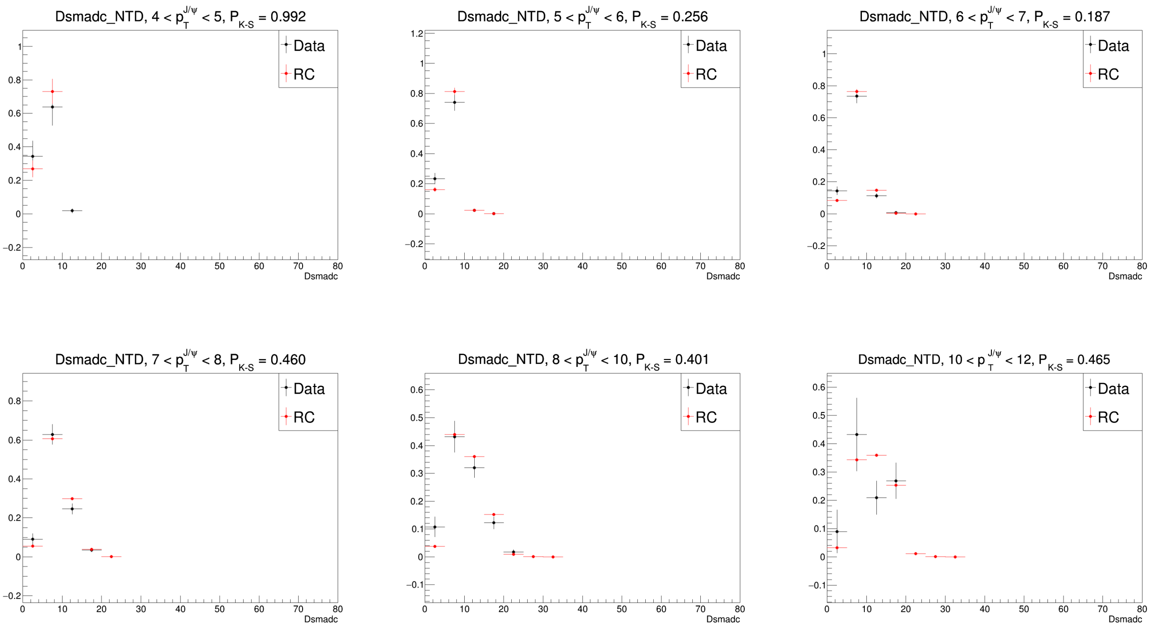

Dsmadc vs Adc0 (Integrated Over J/ψ $\mathbf{p}_T$)

Triggered, p+p:

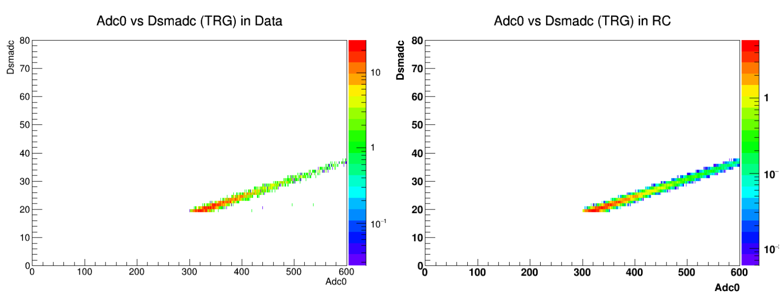

Non-triggered, p+p:

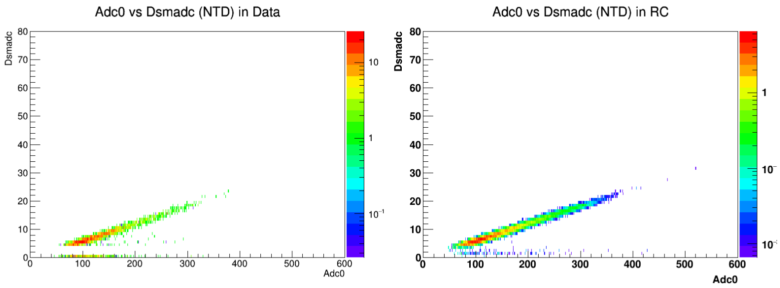

Triggered, p+Au:

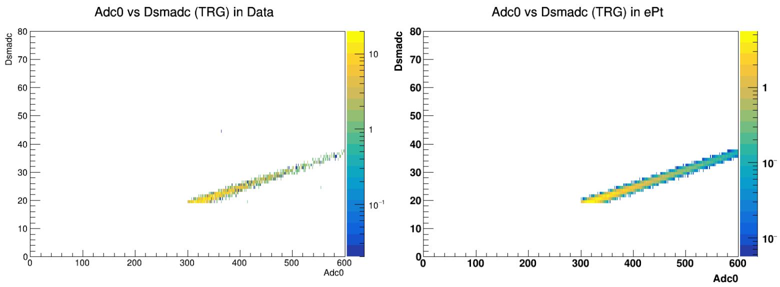

Non-triggered, p+Au:

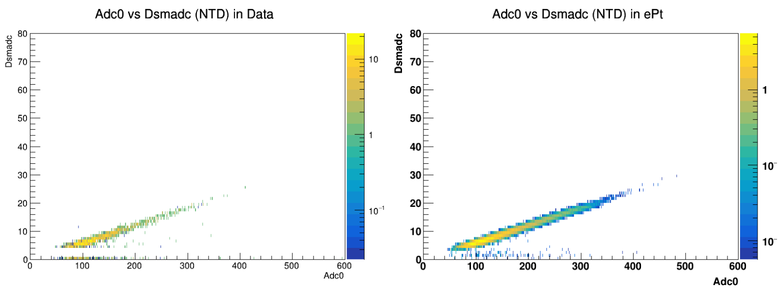

7.2 Smearing Templates

p+p

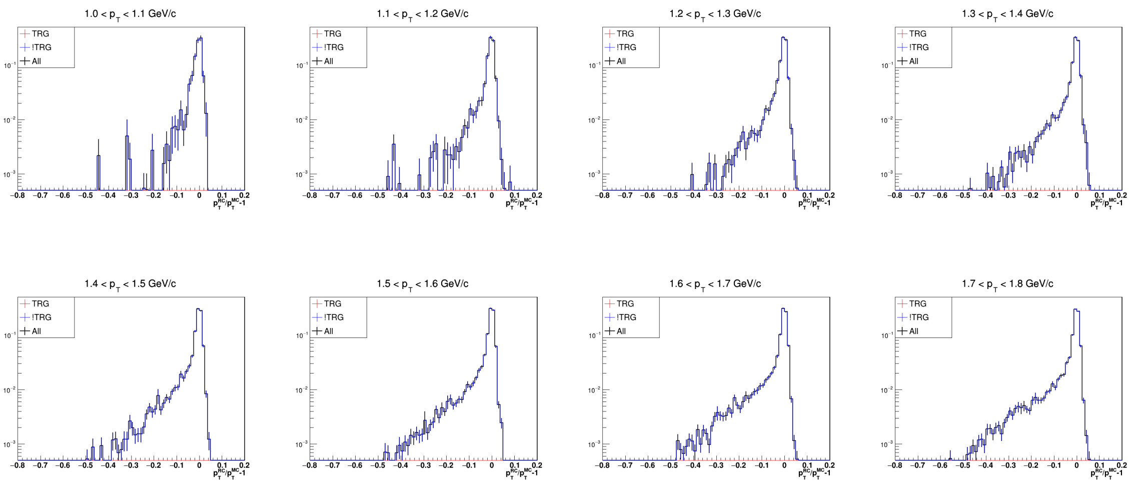

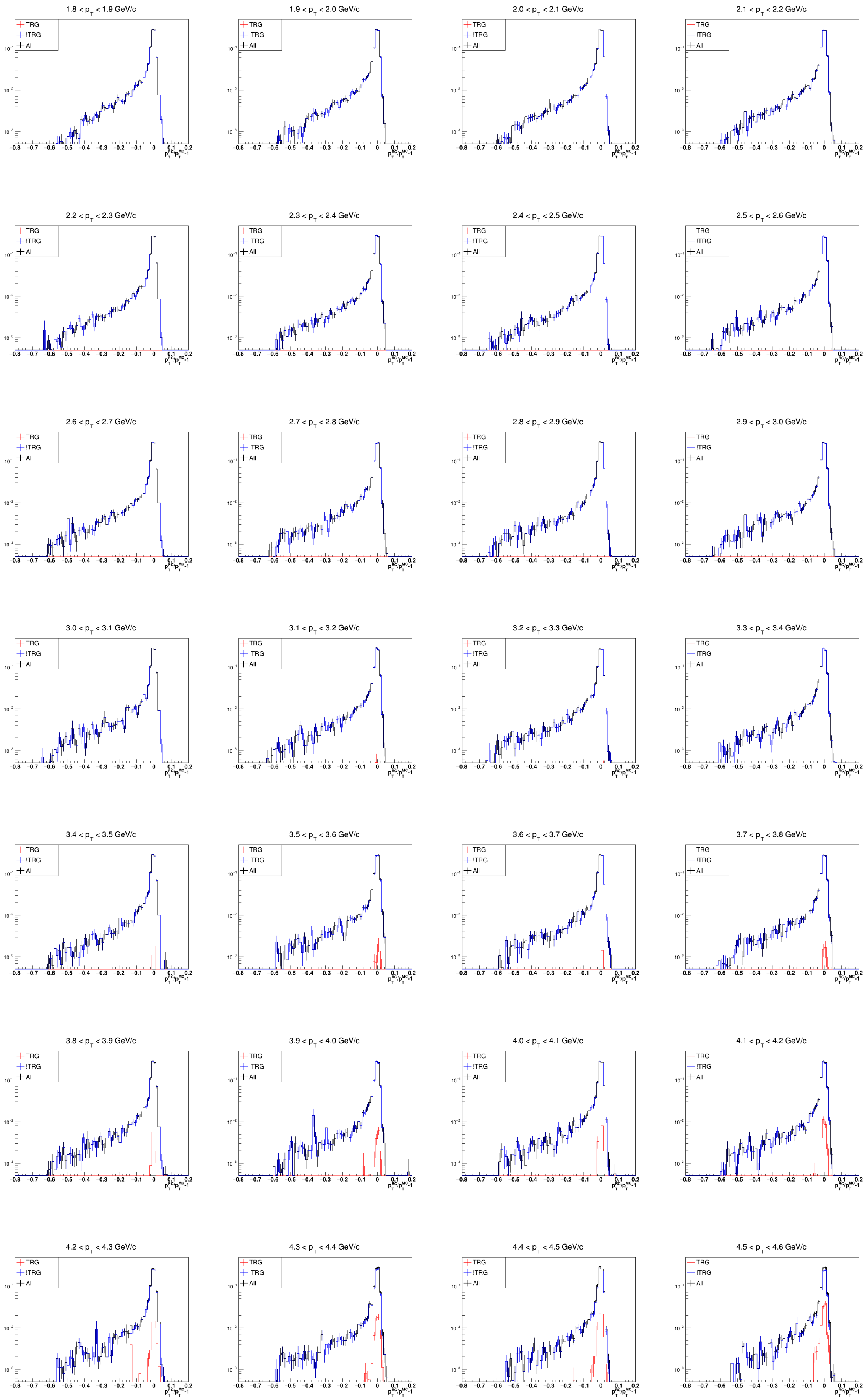

$1.8 < p_T < 1.9$ GeV/c
$1.9 < p_T < 2.0$ GeV/c
$2.0 < p_T < 2.1$ GeV/c
$2.1 < p_T < 2.2$ GeV/c
$2.2 < p_T < 2.3$ GeV/c
$2.3 < p_T < 2.4$ GeV/c
$2.4 < p_T < 2.5$ GeV/c
$2.5 < p_T < 2.6$ GeV/c
$2.6 < p_T < 2.7$ GeV/c
$2.7 < p_T < 2.8$ GeV/c
$2.8 < p_T < 2.9$ GeV/c
$2.9 < p_T < 3.0$ GeV/c
$3.0 < p_T < 3.1$ GeV/c
$3.1 < p_T < 3.2$ GeV/c
$3.2 < p_T < 3.3$ GeV/c
$3.3 < p_T < 3.4$ GeV/c
$3.4 < p_T < 3.5$ GeV/c
$3.5 < p_T < 3.6$ GeV/c
$3.6 < p_T < 3.7$ GeV/c
$3.7 < p_T < 3.8$ GeV/c
$3.8 < p_T < 3.9$ GeV/c
$3.9 < p_T < 4.0$ GeV/c
$4.0 < p_T < 4.1$ GeV/c
$4.1 < p_T < 4.2$ GeV/c
$4.2 < p_T < 4.3$ GeV/c
$4.3 < p_T < 4.4$ GeV/c
$4.4 < p_T < 4.5$ GeV/c
$4.5 < p_T < 4.6$ GeV/c
TRG
ITRG
All
$p_T^{RC}/p_T^{MC}-1$

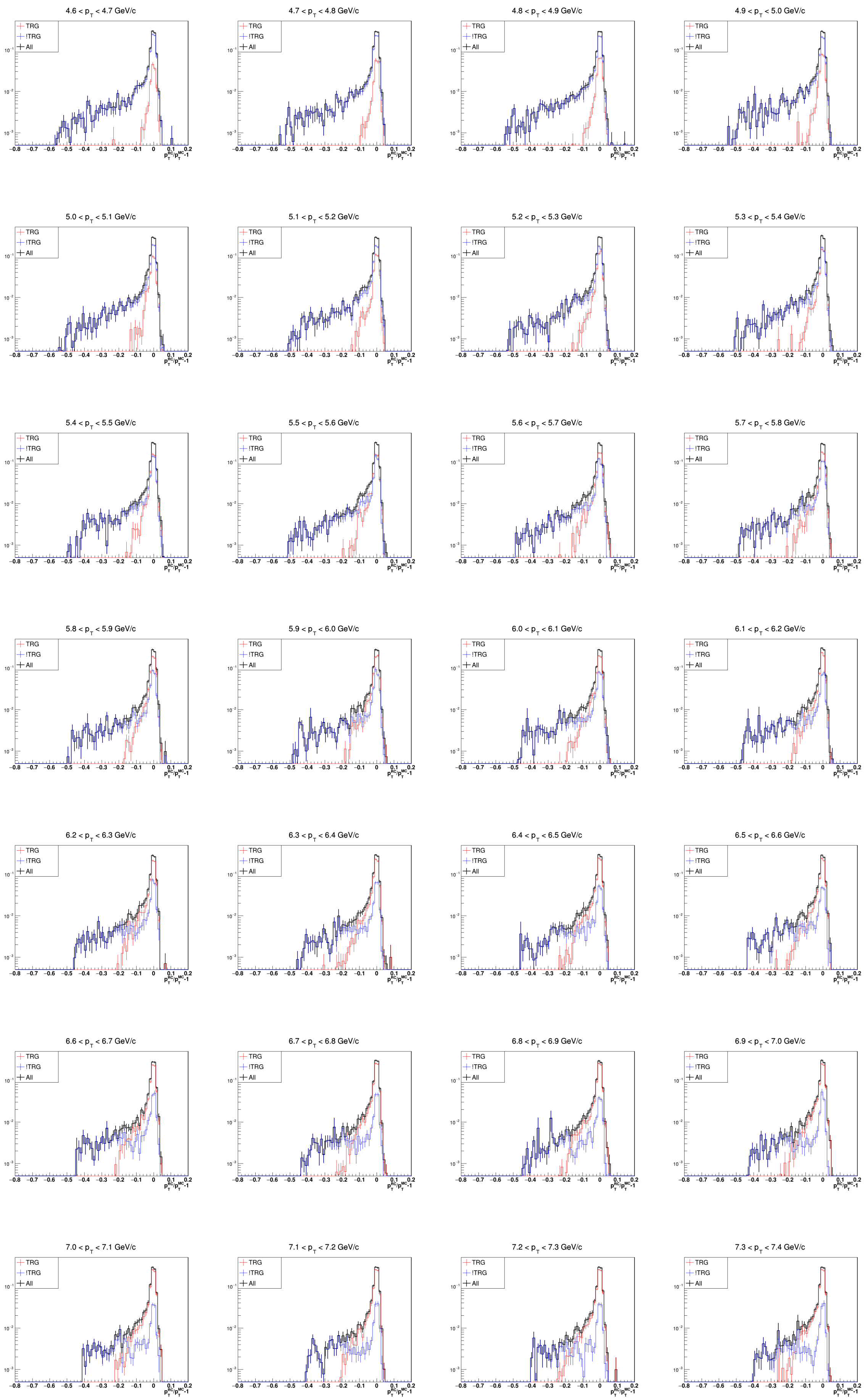
4.6 < p_T < 4.7 GeV/c
4.7 < p_T < 4.8 GeV/c
4.8 < p_T < 4.9 GeV/c
4.9 < p_T < 5.0 GeV/c
5.0 < p_T < 5.1 GeV/c
5.1 < p_T < 5.2 GeV/c
5.2 < p_T < 5.3 GeV/c
5.3 < p_T < 5.4 GeV/c
5.4 < p_T < 5.5 GeV/c
5.5 < p_T < 5.6 GeV/c
5.6 < p_T < 5.7 GeV/c
5.7 < p_T < 5.8 GeV/c
5.8 < p_T < 5.9 GeV/c
5.9 < p_T < 6.0 GeV/c
6.0 < p_T < 6.1 GeV/c
6.1 < p_T < 6.2 GeV/c
6.2 < p_T < 6.3 GeV/c
6.3 < p_T < 6.4 GeV/c
6.4 < p_T < 6.5 GeV/c
6.5 < p_T < 6.6 GeV/c
6.6 < p_T < 6.7 GeV/c
6.7 < p_T < 6.8 GeV/c
6.8 < p_T < 6.9 GeV/c
6.9 < p_T < 7.0 GeV/c
7.0 < p_T < 7.1 GeV/c
7.1 < p_T < 7.2 GeV/c
7.2 < p_T < 7.3 GeV/c
7.3 < p_T < 7.4 GeV/c
TRG
ITRG
All
p_T^RC/p_T^MC-1

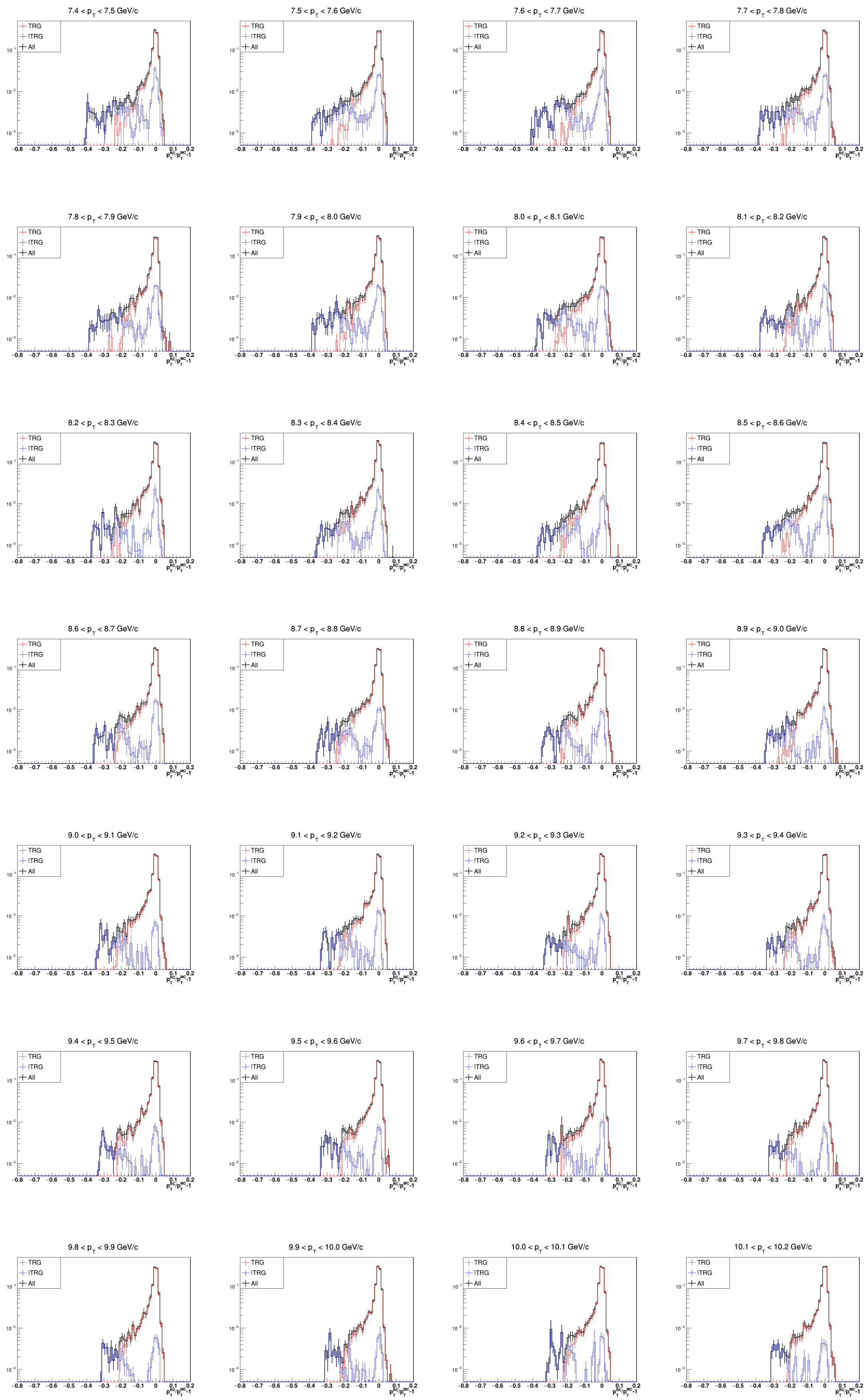
7.4 < pT < 7.5 GeV/c
7.5 < pT < 7.6 GeV/c
7.6 < pT < 7.7 GeV/c
7.7 < pT < 7.8 GeV/c
7.8 < pT < 7.9 GeV/c
7.9 < pT < 8.0 GeV/c
8.0 < pT < 8.1 GeV/c
8.1 < pT < 8.2 GeV/c
8.2 < pT < 8.3 GeV/c
8.3 < pT < 8.4 GeV/c
8.4 < pT < 8.5 GeV/c
8.5 < pT < 8.6 GeV/c
8.6 < pT < 8.7 GeV/c
8.7 < pT < 8.8 GeV/c
8.8 < pT < 8.9 GeV/c
8.9 < pT < 9.0 GeV/c
9.0 < pT < 9.1 GeV/c
9.1 < pT < 9.2 GeV/c
9.2 < pT < 9.3 GeV/c
9.3 < pT < 9.4 GeV/c
9.4 < pT < 9.5 GeV/c
9.5 < pT < 9.6 GeV/c
9.6 < pT < 9.7 GeV/c
9.7 < pT < 9.8 GeV/c
9.8 < pT < 9.9 GeV/c
9.9 < pT < 10.0 GeV/c
10.0 < pT < 10.1 GeV/c
10.1 < pT < 10.2 GeV/c
TRG
!TRG
All

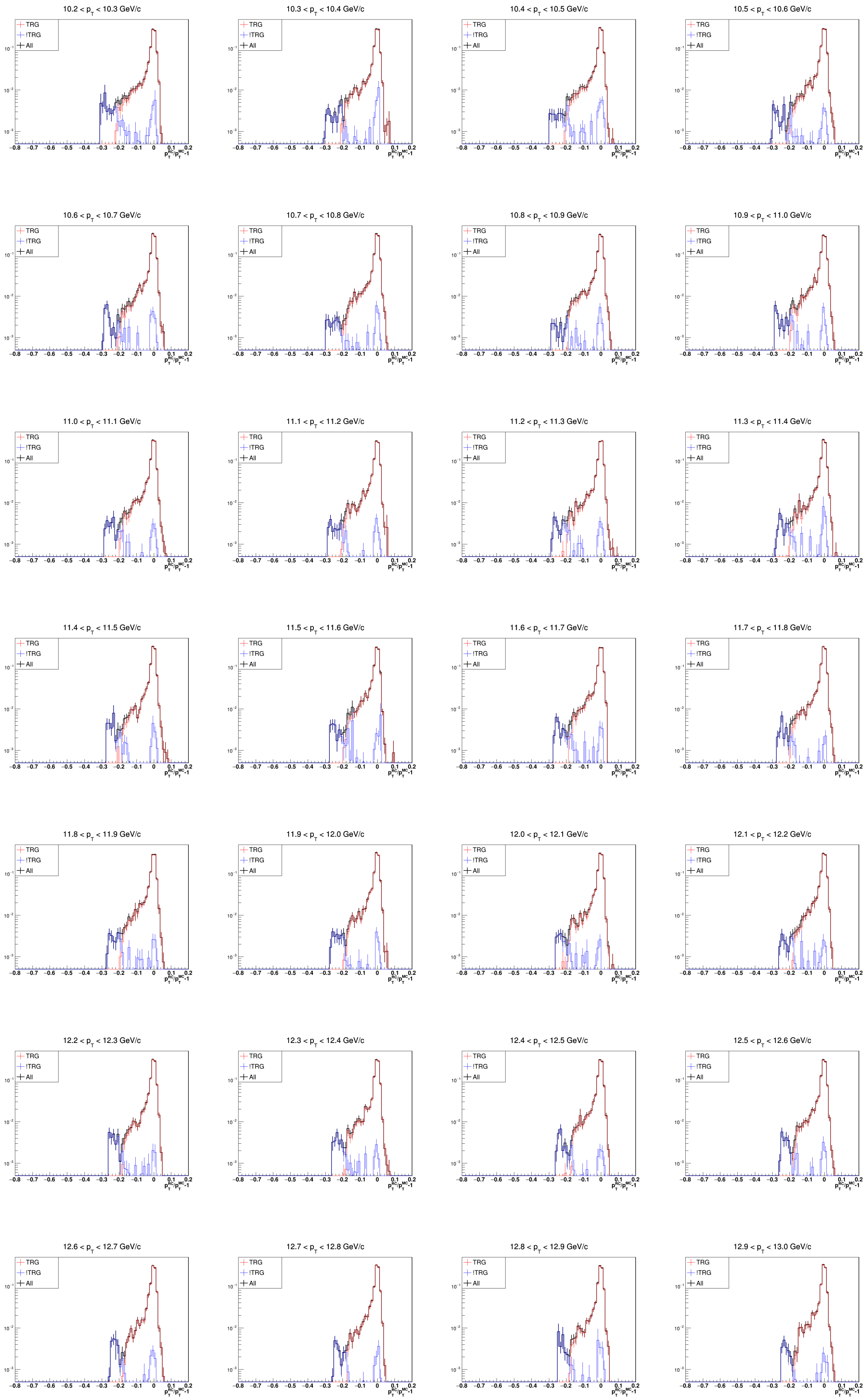
10.2 < p_T < 10.3 GeV/c
10.3 < p_T < 10.4 GeV/c
10.4 < p_T < 10.5 GeV/c
10.5 < p_T < 10.6 GeV/c
10.6 < p_T < 10.7 GeV/c
10.7 < p_T < 10.8 GeV/c
10.8 < p_T < 10.9 GeV/c
10.9 < p_T < 11.0 GeV/c
11.0 < p_T < 11.1 GeV/c
11.1 < p_T < 11.2 GeV/c
11.2 < p_T < 11.3 GeV/c
11.3 < p_T < 11.4 GeV/c
11.4 < p_T < 11.5 GeV/c
11.5 < p_T < 11.6 GeV/c
11.6 < p_T < 11.7 GeV/c
11.7 < p_T < 11.8 GeV/c
11.8 < p_T < 11.9 GeV/c
11.9 < p_T < 12.0 GeV/c
12.0 < p_T < 12.1 GeV/c
12.1 < p_T < 12.2 GeV/c
12.2 < p_T < 12.3 GeV/c
12.3 < p_T < 12.4 GeV/c
12.4 < p_T < 12.5 GeV/c
12.5 < p_T < 12.6 GeV/c
12.6 < p_T < 12.7 GeV/c
12.7 < p_T < 12.8 GeV/c
12.8 < p_T < 12.9 GeV/c
12.9 < p_T < 13.0 GeV/c
TRG
!TRG
All
p_T^RC/p_T^MC-1

p+Au

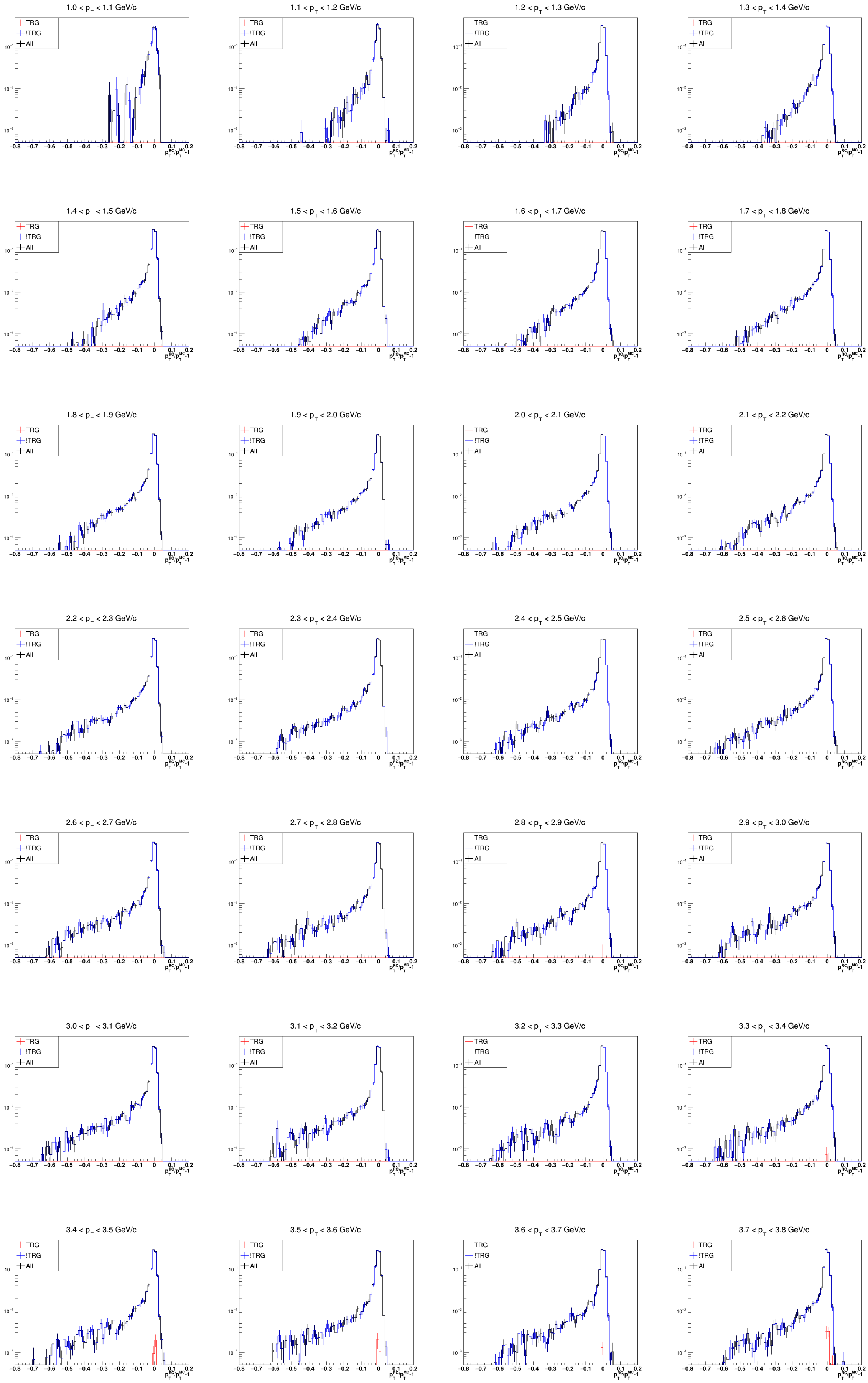
1.0 < p_T < 1.1 GeV/c
1.1 < p_T < 1.2 GeV/c
1.2 < p_T < 1.3 GeV/c
1.3 < p_T < 1.4 GeV/c
1.4 < p_T < 1.5 GeV/c
1.5 < p_T < 1.6 GeV/c
1.6 < p_T < 1.7 GeV/c
1.7 < p_T < 1.8 GeV/c
1.8 < p_T < 1.9 GeV/c
1.9 < p_T < 2.0 GeV/c
2.0 < p_T < 2.1 GeV/c
2.1 < p_T < 2.2 GeV/c
2.2 < p_T < 2.3 GeV/c
2.3 < p_T < 2.4 GeV/c
2.4 < p_T < 2.5 GeV/c
2.5 < p_T < 2.6 GeV/c
2.6 < p_T < 2.7 GeV/c
2.7 < p_T < 2.8 GeV/c
2.8 < p_T < 2.9 GeV/c
2.9 < p_T < 3.0 GeV/c
3.0 < p_T < 3.1 GeV/c
3.1 < p_T < 3.2 GeV/c
3.2 < p_T < 3.3 GeV/c
3.3 < p_T < 3.4 GeV/c
3.4 < p_T < 3.5 GeV/c
3.5 < p_T < 3.6 GeV/c
3.6 < p_T < 3.7 GeV/c
3.7 < p_T < 3.8 GeV/c
TRG
!TRG
All
p_T^RC/p_T^MC-1

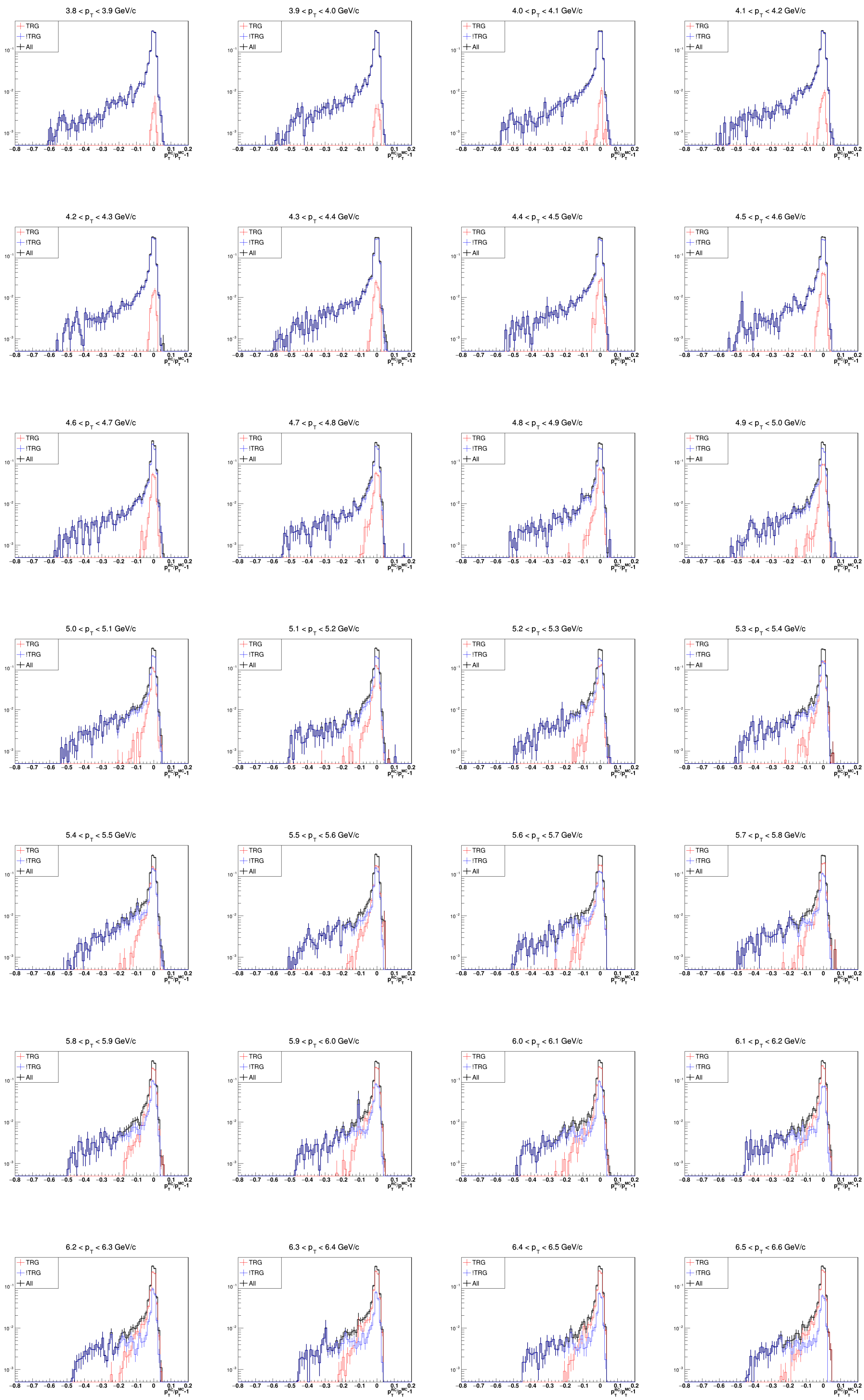

3.8 < p_T < 3.9 GeV/c
3.9 < p_T < 4.0 GeV/c
4.0 < p_T < 4.1 GeV/c
4.1 < p_T < 4.2 GeV/c
4.2 < p_T < 4.3 GeV/c
4.3 < p_T < 4.4 GeV/c
4.4 < p_T < 4.5 GeV/c
4.5 < p_T < 4.6 GeV/c
4.6 < p_T < 4.7 GeV/c
4.7 < p_T < 4.8 GeV/c
4.8 < p_T < 4.9 GeV/c
4.9 < p_T < 5.0 GeV/c
5.0 < p_T < 5.1 GeV/c
5.1 < p_T < 5.2 GeV/c
5.2 < p_T < 5.3 GeV/c
5.3 < p_T < 5.4 GeV/c
5.4 < p_T < 5.5 GeV/c
5.5 < p_T < 5.6 GeV/c
5.6 < p_T < 5.7 GeV/c
5.7 < p_T < 5.8 GeV/c
5.8 < p_T < 5.9 GeV/c
5.9 < p_T < 6.0 GeV/c
6.0 < p_T < 6.1 GeV/c
6.1 < p_T < 6.2 GeV/c
6.2 < p_T < 6.3 GeV/c
6.3 < p_T < 6.4 GeV/c
6.4 < p_T < 6.5 GeV/c
6.5 < p_T < 6.6 GeV/c
TRG
!TRG
All

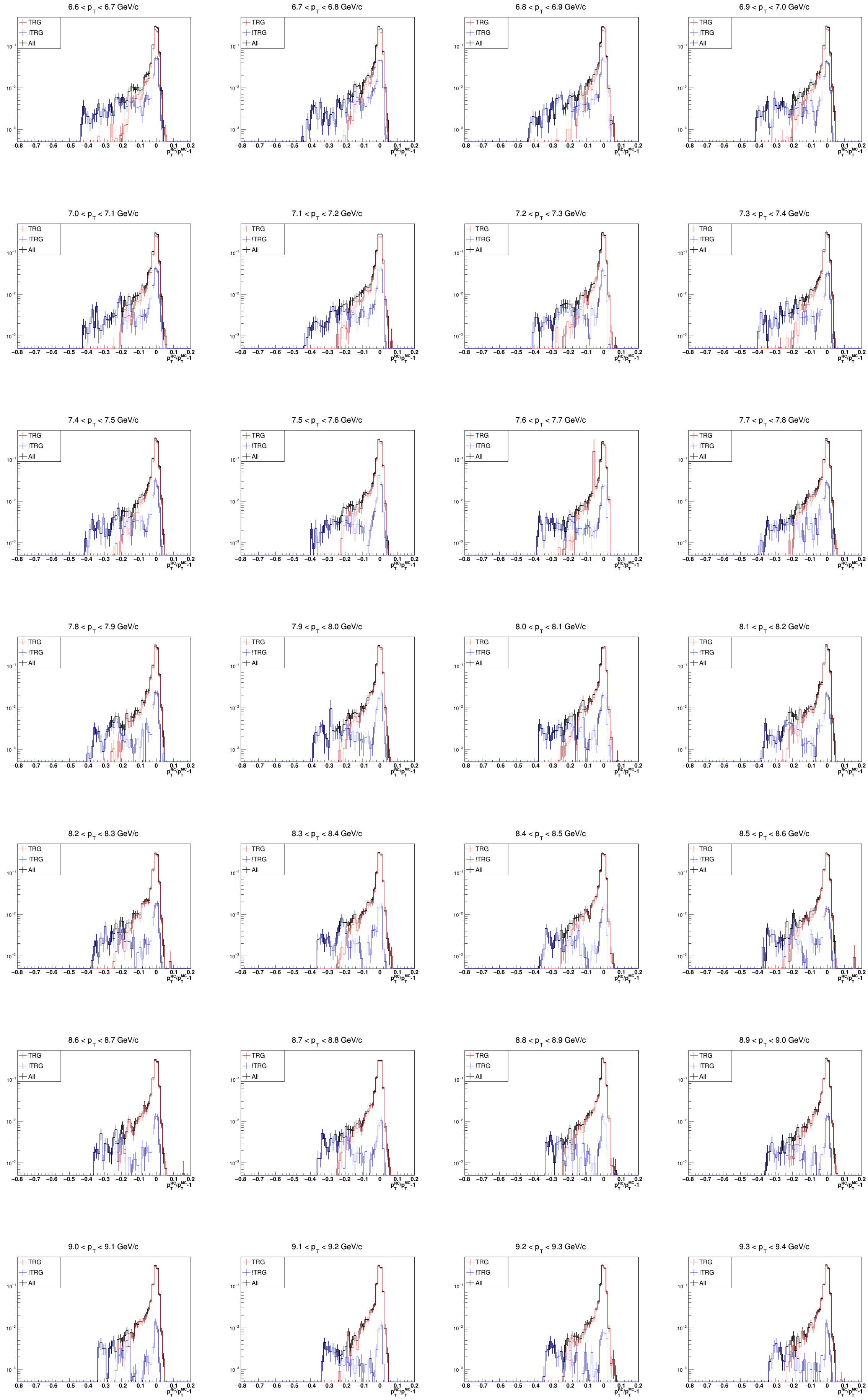
$6.6 < p_T < 6.7$ GeV/c
$6.7 < p_T < 6.8$ GeV/c
$6.8 < p_T < 6.9$ GeV/c
$6.9 < p_T < 7.0$ GeV/c
$7.0 < p_T < 7.1$ GeV/c
$7.1 < p_T < 7.2$ GeV/c
$7.2 < p_T < 7.3$ GeV/c
$7.3 < p_T < 7.4$ GeV/c
$7.4 < p_T < 7.5$ GeV/c
$7.5 < p_T < 7.6$ GeV/c
$7.6 < p_T < 7.7$ GeV/c
$7.7 < p_T < 7.8$ GeV/c
$7.8 < p_T < 7.9$ GeV/c
$7.9 < p_T < 8.0$ GeV/c
$8.0 < p_T < 8.1$ GeV/c
$8.1 < p_T < 8.2$ GeV/c
$8.2 < p_T < 8.3$ GeV/c
$8.3 < p_T < 8.4$ GeV/c
$8.4 < p_T < 8.5$ GeV/c
$8.5 < p_T < 8.6$ GeV/c
$8.6 < p_T < 8.7$ GeV/c
$8.7 < p_T < 8.8$ GeV/c
$8.8 < p_T < 8.9$ GeV/c
$8.9 < p_T < 9.0$ GeV/c
$9.0 < p_T < 9.1$ GeV/c
$9.1 < p_T < 9.2$ GeV/c
$9.2 < p_T < 9.3$ GeV/c
$9.3 < p_T < 9.4$ GeV/c
TRG
ITRG
All
$p_T^{RC}/p_T^{MC}-1$

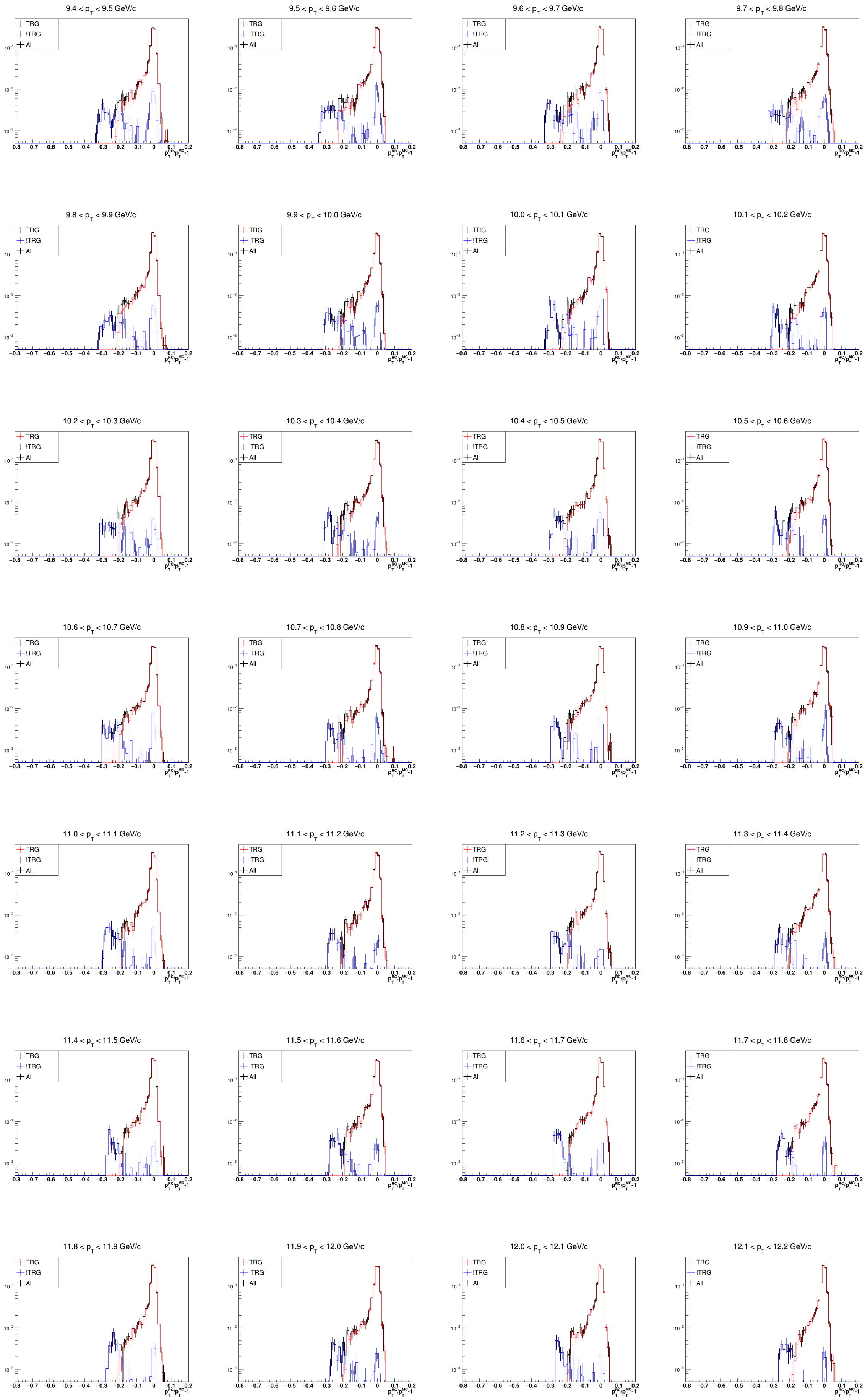
9.4 < p_T < 9.5 GeV/c
9.5 < p_T < 9.6 GeV/c
9.6 < p_T < 9.7 GeV/c
9.7 < p_T < 9.8 GeV/c
9.8 < p_T < 9.9 GeV/c
9.9 < p_T < 10.0 GeV/c
10.0 < p_T < 10.1 GeV/c
10.1 < p_T < 10.2 GeV/c
10.2 < p_T < 10.3 GeV/c
10.3 < p_T < 10.4 GeV/c
10.4 < p_T < 10.5 GeV/c
10.5 < p_T < 10.6 GeV/c
10.6 < p_T < 10.7 GeV/c
10.7 < p_T < 10.8 GeV/c
10.8 < p_T < 10.9 GeV/c
10.9 < p_T < 11.0 GeV/c
11.0 < p_T < 11.1 GeV/c
11.1 < p_T < 11.2 GeV/c
11.2 < p_T < 11.3 GeV/c
11.3 < p_T < 11.4 GeV/c
11.4 < p_T < 11.5 GeV/c
11.5 < p_T < 11.6 GeV/c
11.6 < p_T < 11.7 GeV/c
11.7 < p_T < 11.8 GeV/c
11.8 < p_T < 11.9 GeV/c
11.9 < p_T < 12.0 GeV/c
12.0 < p_T < 12.1 GeV/c
12.1 < p_T < 12.2 GeV/c
TRG
ITRG
All
p_T^{RC}/p_T^{MC}-1

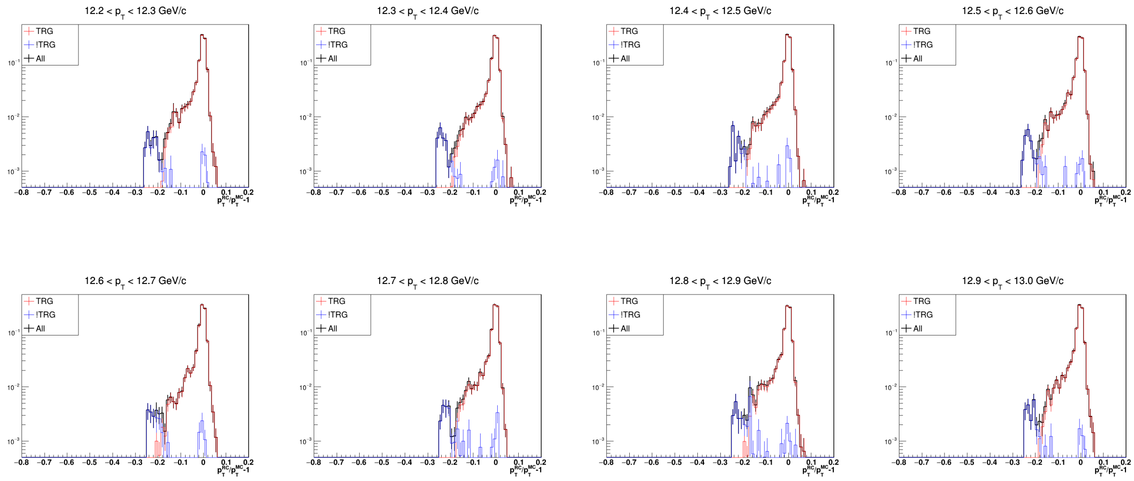

7.3 Electron RC Momentum Distribution Fit

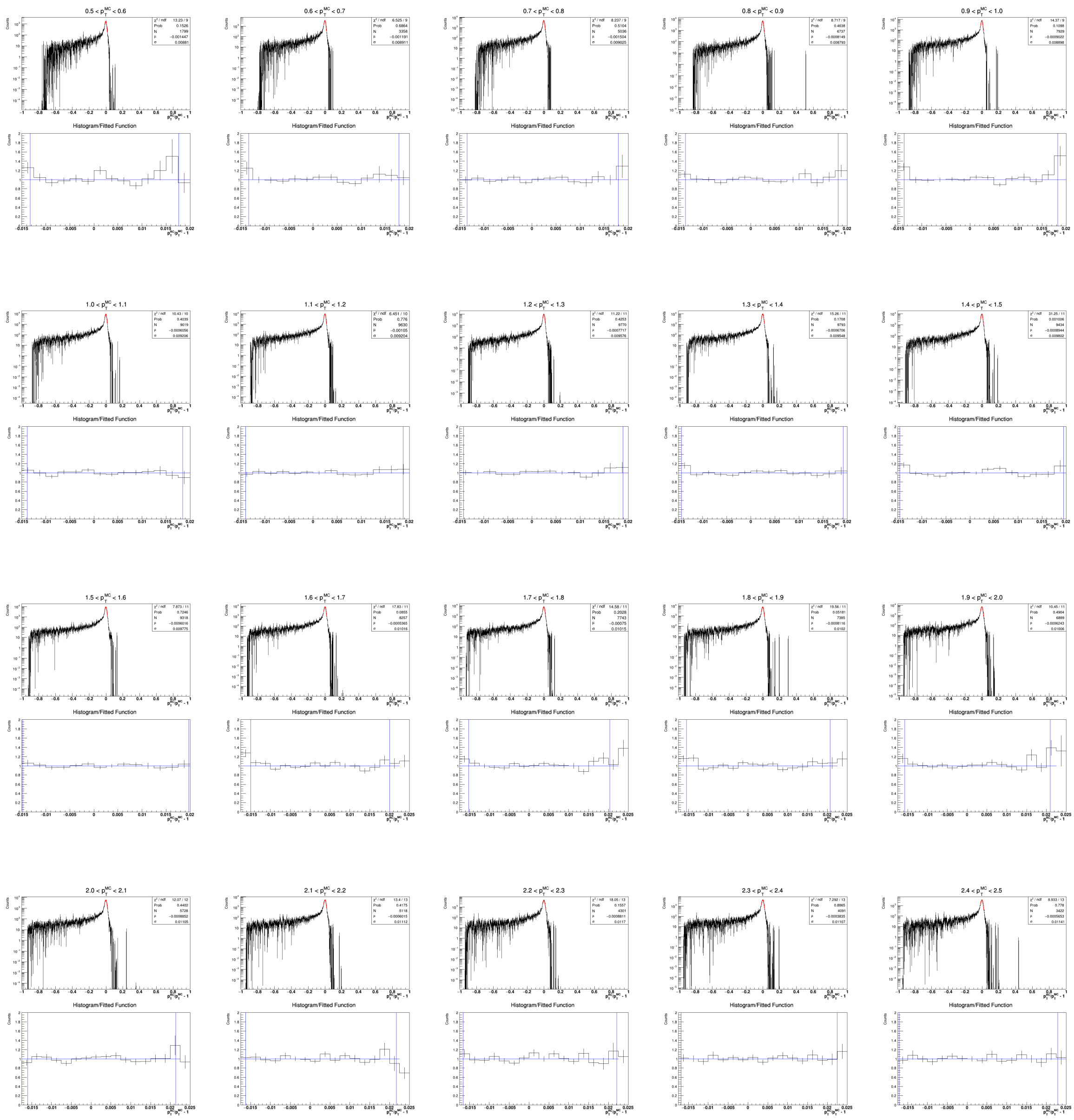

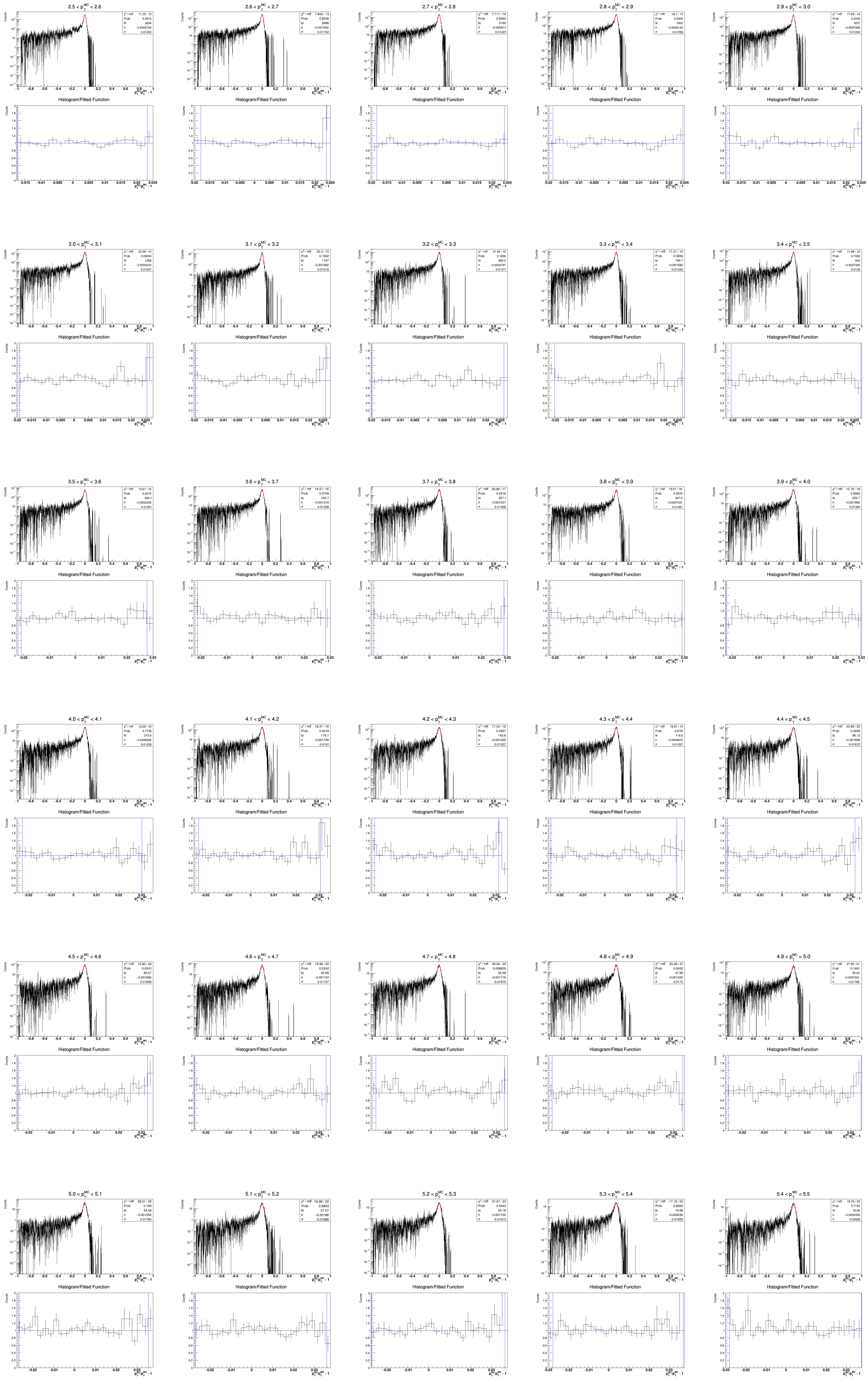
2.5 < p_T^MC < 2.6
2.6 < p_T^MC < 2.7
2.7 < p_T^MC < 2.8
2.8 < p_T^MC < 2.9
2.9 < p_T^MC < 3.0
3.0 < p_T^MC < 3.1
3.1 < p_T^MC < 3.2
3.2 < p_T^MC < 3.3
3.3 < p_T^MC < 3.4
3.4 < p_T^MC < 3.5
3.5 < p_T^MC < 3.6
3.6 < p_T^MC < 3.7
3.7 < p_T^MC < 3.8
3.8 < p_T^MC < 3.9
3.9 < p_T^MC < 4.0
4.0 < p_T^MC < 4.1
4.1 < p_T^MC < 4.2
4.2 < p_T^MC < 4.3
4.3 < p_T^MC < 4.4
4.4 < p_T^MC < 4.5
4.5 < p_T^MC < 4.6
4.6 < p_T^MC < 4.7
4.7 < p_T^MC < 4.8
4.8 < p_T^MC < 4.9
4.9 < p_T^MC < 5.0
5.0 < p_T^MC < 5.1
5.1 < p_T^MC < 5.2
5.2 < p_T^MC < 5.3
5.3 < p_T^MC < 5.4
5.4 < p_T^MC < 5.5
Histogram/Fitted Function


5.5 < p_T^MC < 5.6
5.6 < p_T^MC < 5.7
5.7 < p_T^MC < 5.8
5.8 < p_T^MC < 5.9
5.9 < p_T^MC < 6.0
6.0 < p_T^MC < 6.1
6.1 < p_T^MC < 6.2
6.2 < p_T^MC < 6.3
6.3 < p_T^MC < 6.4
6.4 < p_T^MC < 6.5
6.5 < p_T^MC < 6.6
6.6 < p_T^MC < 6.7
6.7 < p_T^MC < 6.8
6.8 < p_T^MC < 6.9
6.9 < p_T^MC < 7.0
7.0 < p_T^MC < 7.1
7.1 < p_T^MC < 7.2
7.2 < p_T^MC < 7.3
7.3 < p_T^MC < 7.4
7.4 < p_T^MC < 7.5
7.5 < p_T^MC < 7.6
7.6 < p_T^MC < 7.7
7.7 < p_T^MC < 7.8
7.8 < p_T^MC < 7.9
7.9 < p_T^MC < 8.0
8.0 < p_T^MC < 8.1
8.1 < p_T^MC < 8.2
8.2 < p_T^MC < 8.3
8.3 < p_T^MC < 8.4
8.4 < p_T^MC < 8.5
Histogram/Fitted Function

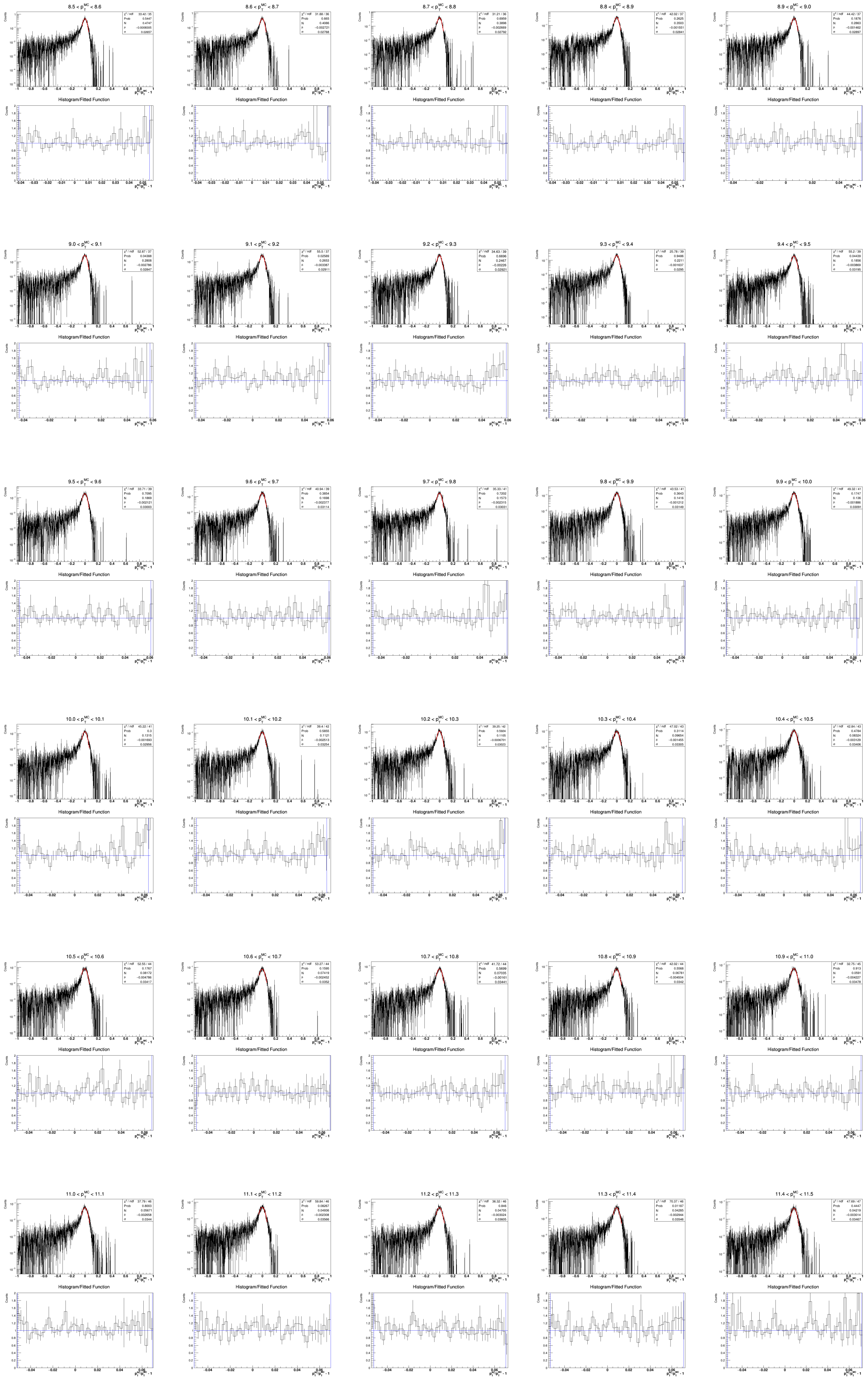
8.5 < p_T^MC < 8.6
8.6 < p_T^MC < 8.7
8.7 < p_T^MC < 8.8
8.8 < p_T^MC < 8.9
8.9 < p_T^MC < 9.0
9.0 < p_T^MC < 9.1
9.1 < p_T^MC < 9.2
9.2 < p_T^MC < 9.3
9.3 < p_T^MC < 9.4
9.4 < p_T^MC < 9.5
9.5 < p_T^MC < 9.6
9.6 < p_T^MC < 9.7
9.7 < p_T^MC < 9.8
9.8 < p_T^MC < 9.9
9.9 < p_T^MC < 10.0
10.0 < p_T^MC < 10.1
10.1 < p_T^MC < 10.2
10.2 < p_T^MC < 10.3
10.3 < p_T^MC < 10.4
10.4 < p_T^MC < 10.5
10.5 < p_T^MC < 10.6
10.6 < p_T^MC < 10.7
10.7 < p_T^MC < 10.8
10.8 < p_T^MC < 10.9
10.9 < p_T^MC < 11.0
11.0 < p_T^MC < 11.1
11.1 < p_T^MC < 11.2
11.2 < p_T^MC < 11.3
11.3 < p_T^MC < 11.4
11.4 < p_T^MC < 11.5
Histogram/Fitted Function

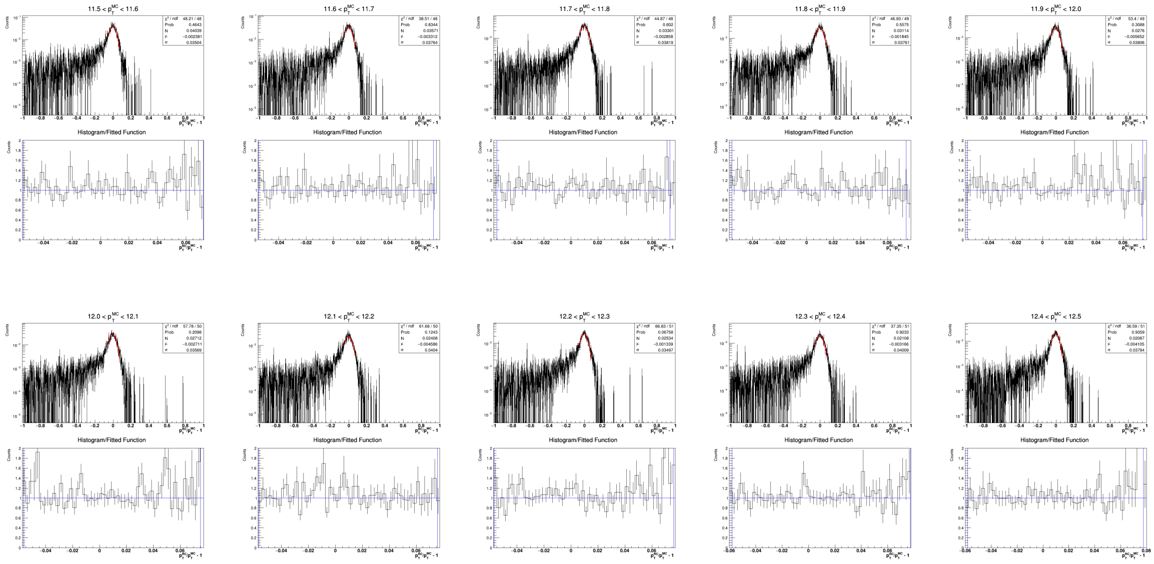
11.5 < p_T^MC < 11.6
11.6 < p_T^MC < 11.7
11.7 < p_T^MC < 11.8
11.8 < p_T^MC < 11.9
11.9 < p_T^MC < 12.0
12.0 < p_T^MC < 12.1
12.1 < p_T^MC < 12.2
12.2 < p_T^MC < 12.3
12.3 < p_T^MC < 12.4
12.4 < p_T^MC < 12.5
Histogram/Fitted Function

p+p

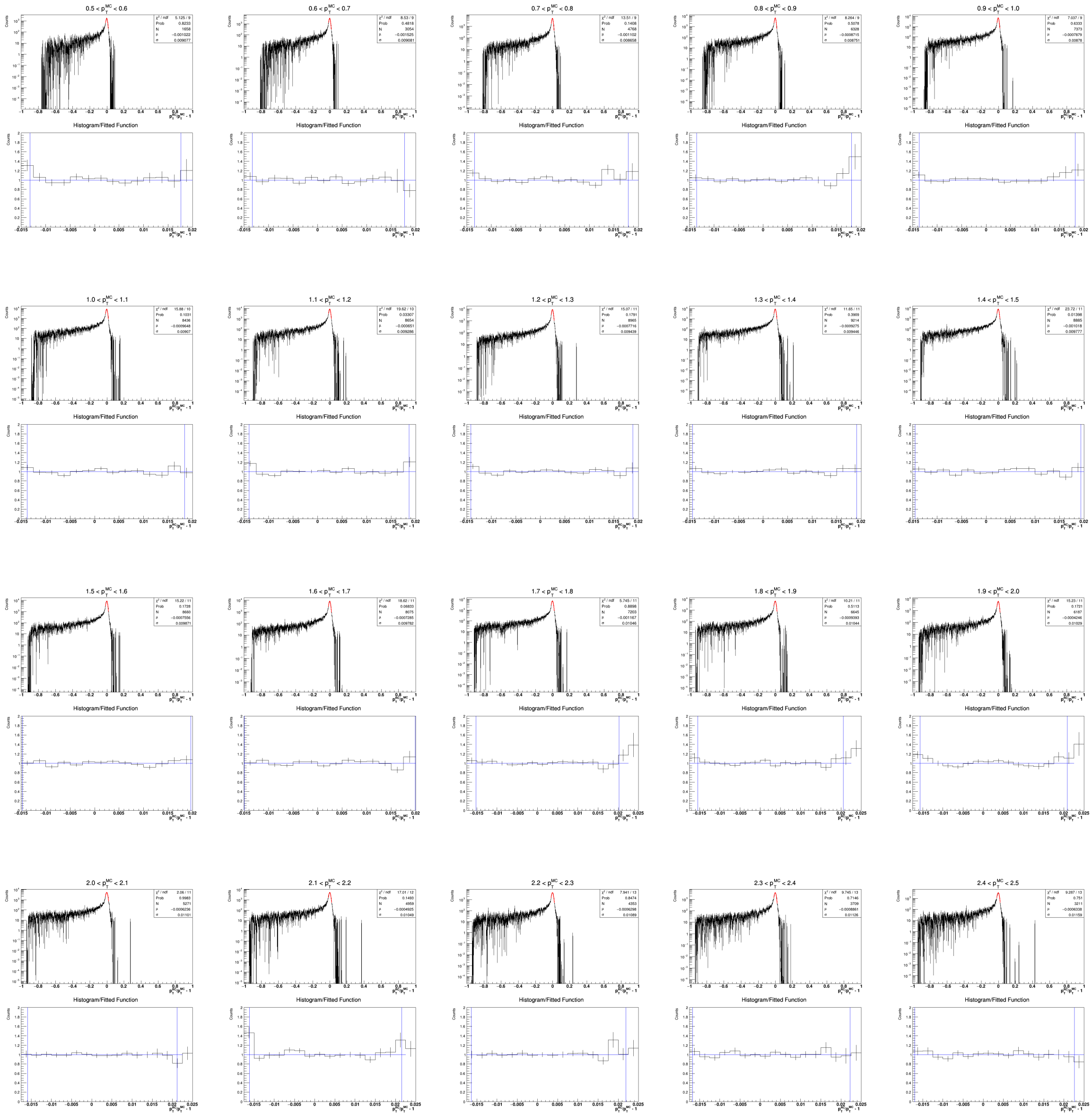
0.5 < p_T^MC < 0.6
0.6 < p_T^MC < 0.7
0.7 < p_T^MC < 0.8
0.8 < p_T^MC < 0.9
0.9 < p_T^MC < 1.0
1.0 < p_T^MC < 1.1
1.1 < p_T^MC < 1.2
1.2 < p_T^MC < 1.3
1.3 < p_T^MC < 1.4
1.4 < p_T^MC < 1.5
1.5 < p_T^MC < 1.6
1.6 < p_T^MC < 1.7
1.7 < p_T^MC < 1.8
1.8 < p_T^MC < 1.9
1.9 < p_T^MC < 2.0
2.0 < p_T^MC < 2.1
2.1 < p_T^MC < 2.2
2.2 < p_T^MC < 2.3
2.3 < p_T^MC < 2.4
2.4 < p_T^MC < 2.5
Histogram/Fitted Function

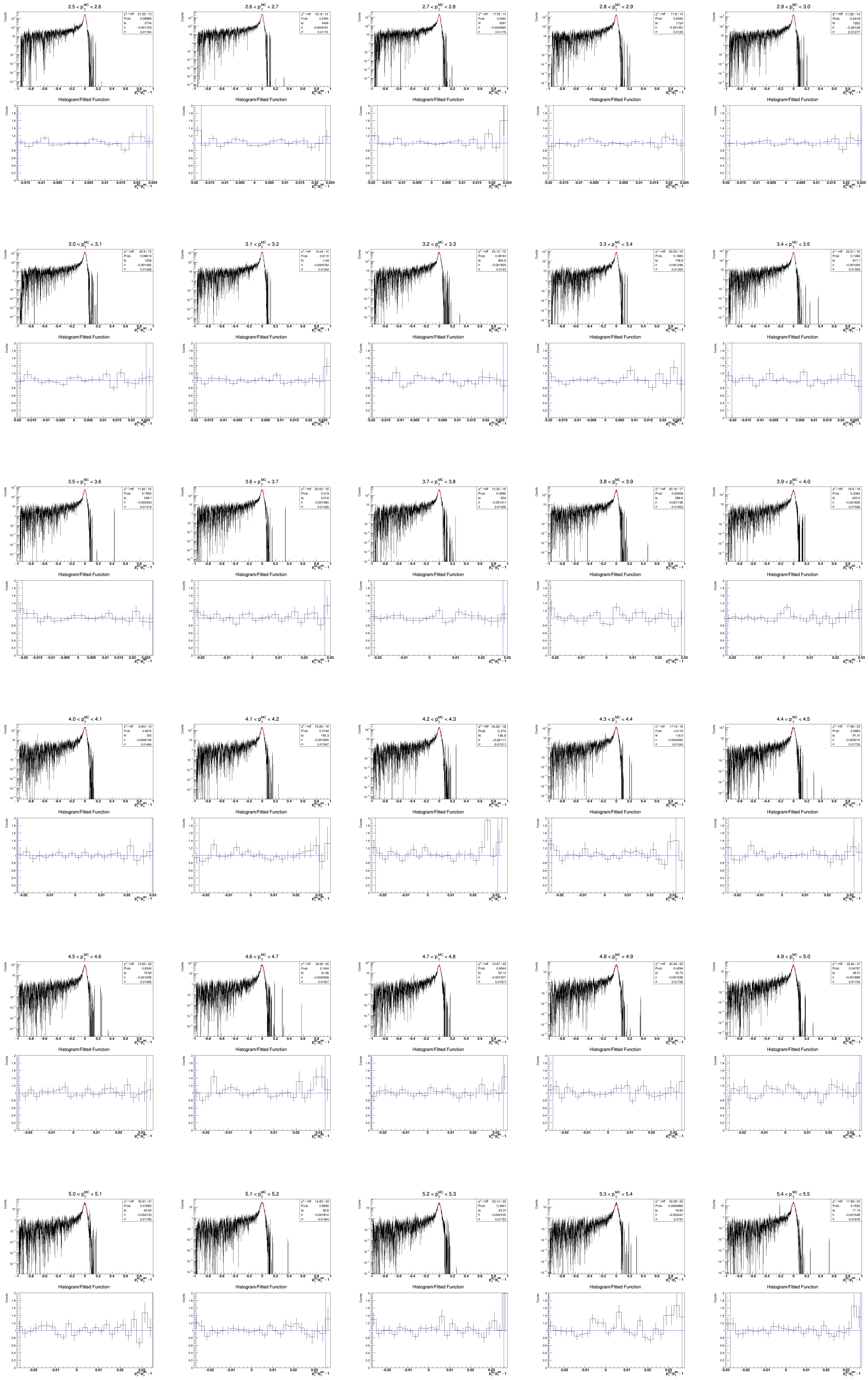
$2.5 < p_{T}^{MC} < 2.6$
$2.6 < p_{T}^{MC} < 2.7$
$2.7 < p_{T}^{MC} < 2.8$
$2.8 < p_{T}^{MC} < 2.9$
$2.9 < p_{T}^{MC} < 3.0$
$3.0 < p_{T}^{MC} < 3.1$
$3.1 < p_{T}^{MC} < 3.2$
$3.2 < p_{T}^{MC} < 3.3$
$3.3 < p_{T}^{MC} < 3.4$
$3.4 < p_{T}^{MC} < 3.5$
$3.5 < p_{T}^{MC} < 3.6$
$3.6 < p_{T}^{MC} < 3.7$
$3.7 < p_{T}^{MC} < 3.8$
$3.8 < p_{T}^{MC} < 3.9$
$3.9 < p_{T}^{MC} < 4.0$
$4.0 < p_{T}^{MC} < 4.1$
$4.1 < p_{T}^{MC} < 4.2$
$4.2 < p_{T}^{MC} < 4.3$
$4.3 < p_{T}^{MC} < 4.4$
$4.4 < p_{T}^{MC} < 4.5$
$4.5 < p_{T}^{MC} < 4.6$
$4.6 < p_{T}^{MC} < 4.7$
$4.7 < p_{T}^{MC} < 4.8$
$4.8 < p_{T}^{MC} < 4.9$
$4.9 < p_{T}^{MC} < 5.0$
$5.0 < p_{T}^{MC} < 5.1$
$5.1 < p_{T}^{MC} < 5.2$
$5.2 < p_{T}^{MC} < 5.3$
$5.3 < p_{T}^{MC} < 5.4$
$5.4 < p_{T}^{MC} < 5.5$
Histogram/Fitted Function

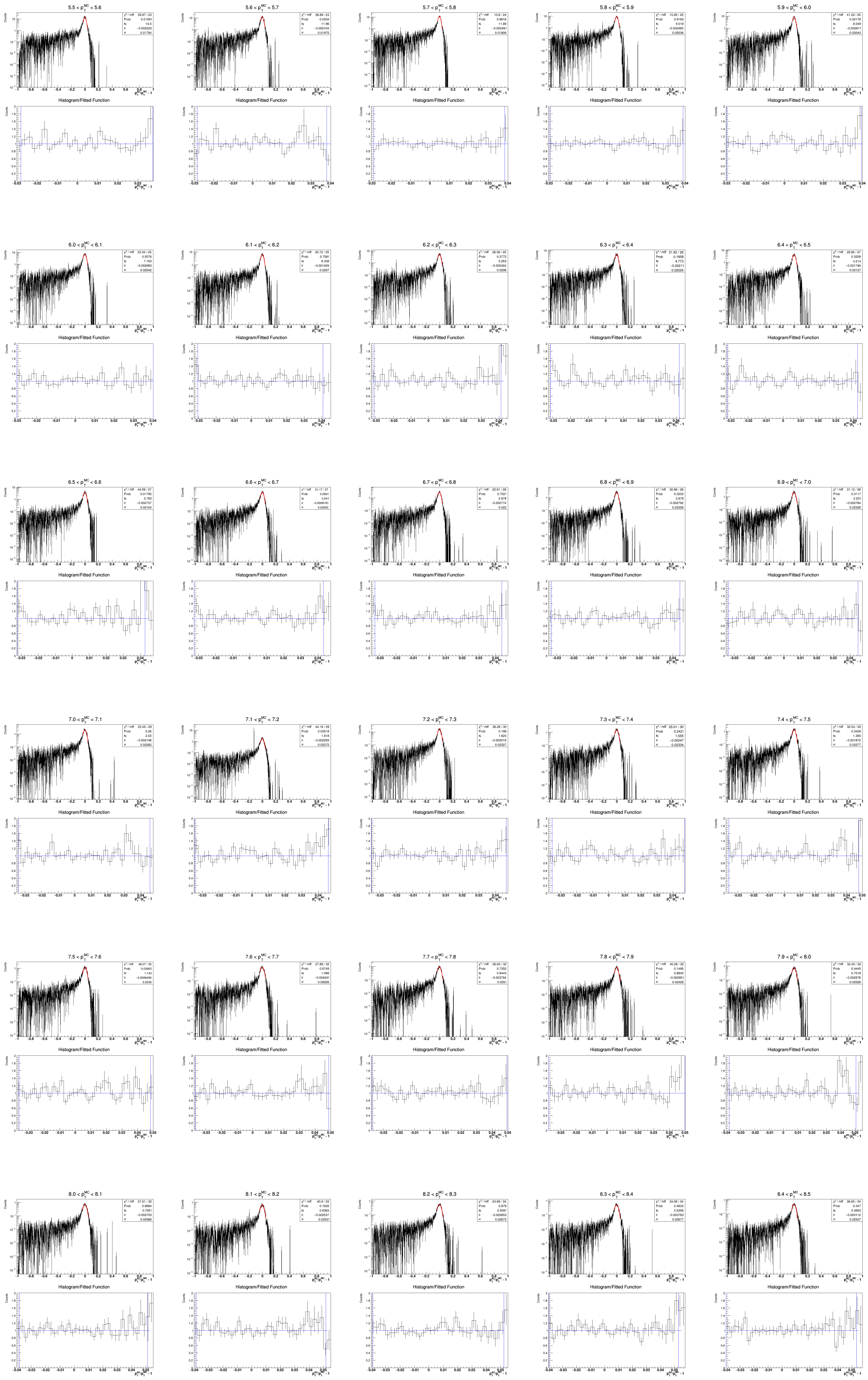
$5.5 < p_T^{MC} < 5.6$
$5.6 < p_T^{MC} < 5.7$
$5.7 < p_T^{MC} < 5.8$
$5.8 < p_T^{MC} < 5.9$
$5.9 < p_T^{MC} < 6.0$
$6.0 < p_T^{MC} < 6.1$
$6.1 < p_T^{MC} < 6.2$
$6.2 < p_T^{MC} < 6.3$
$6.3 < p_T^{MC} < 6.4$
$6.4 < p_T^{MC} < 6.5$
$6.5 < p_T^{MC} < 6.6$
$6.6 < p_T^{MC} < 6.7$
$6.7 < p_T^{MC} < 6.8$
$6.8 < p_T^{MC} < 6.9$
$6.9 < p_T^{MC} < 7.0$
$7.0 < p_T^{MC} < 7.1$
$7.1 < p_T^{MC} < 7.2$
$7.2 < p_T^{MC} < 7.3$
$7.3 < p_T^{MC} < 7.4$
$7.4 < p_T^{MC} < 7.5$
$7.5 < p_T^{MC} < 7.6$
$7.6 < p_T^{MC} < 7.7$
$7.7 < p_T^{MC} < 7.8$
$7.8 < p_T^{MC} < 7.9$
$7.9 < p_T^{MC} < 8.0$
$8.0 < p_T^{MC} < 8.1$
$8.1 < p_T^{MC} < 8.2$
$8.2 < p_T^{MC} < 8.3$
$8.3 < p_T^{MC} < 8.4$
$8.4 < p_T^{MC} < 8.5$
Histogram/Fitted Function

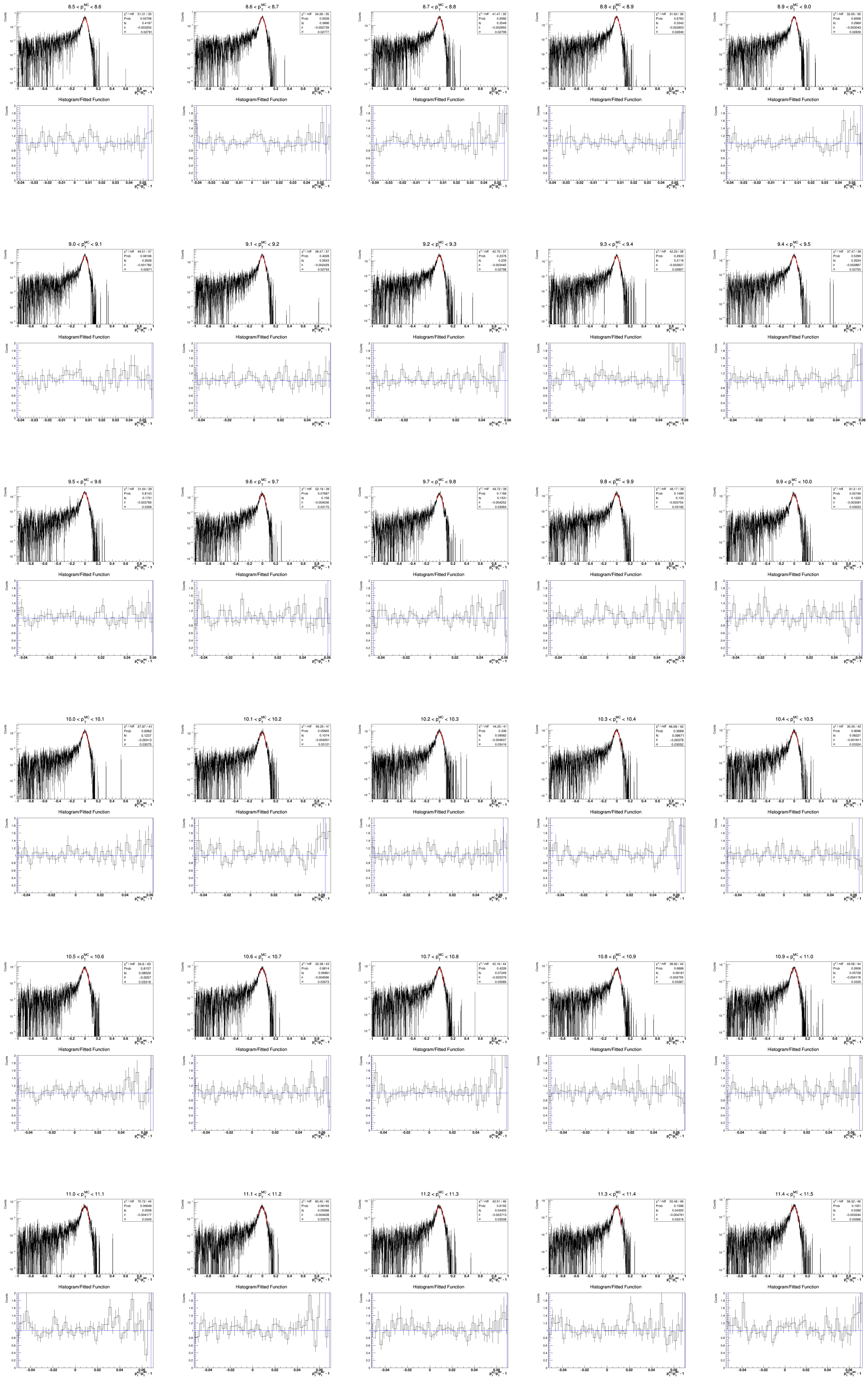
8.5 < p_T^MC < 8.6
8.6 < p_T^MC < 8.7
8.7 < p_T^MC < 8.8
8.8 < p_T^MC < 8.9
8.9 < p_T^MC < 9.0
9.0 < p_T^MC < 9.1
9.1 < p_T^MC < 9.2
9.2 < p_T^MC < 9.3
9.3 < p_T^MC < 9.4
9.4 < p_T^MC < 9.5
9.5 < p_T^MC < 9.6
9.6 < p_T^MC < 9.7
9.7 < p_T^MC < 9.8
9.8 < p_T^MC < 9.9
9.9 < p_T^MC < 10.0
10.0 < p_T^MC < 10.1
10.1 < p_T^MC < 10.2
10.2 < p_T^MC < 10.3
10.3 < p_T^MC < 10.4
10.4 < p_T^MC < 10.5
10.5 < p_T^MC < 10.6
10.6 < p_T^MC < 10.7
10.7 < p_T^MC < 10.8
10.8 < p_T^MC < 10.9
10.9 < p_T^MC < 11.0
11.0 < p_T^MC < 11.1
11.1 < p_T^MC < 11.2
11.2 < p_T^MC < 11.3
11.3 < p_T^MC < 11.4
11.4 < p_T^MC < 11.5
Histogram/Fitted Function
Counts

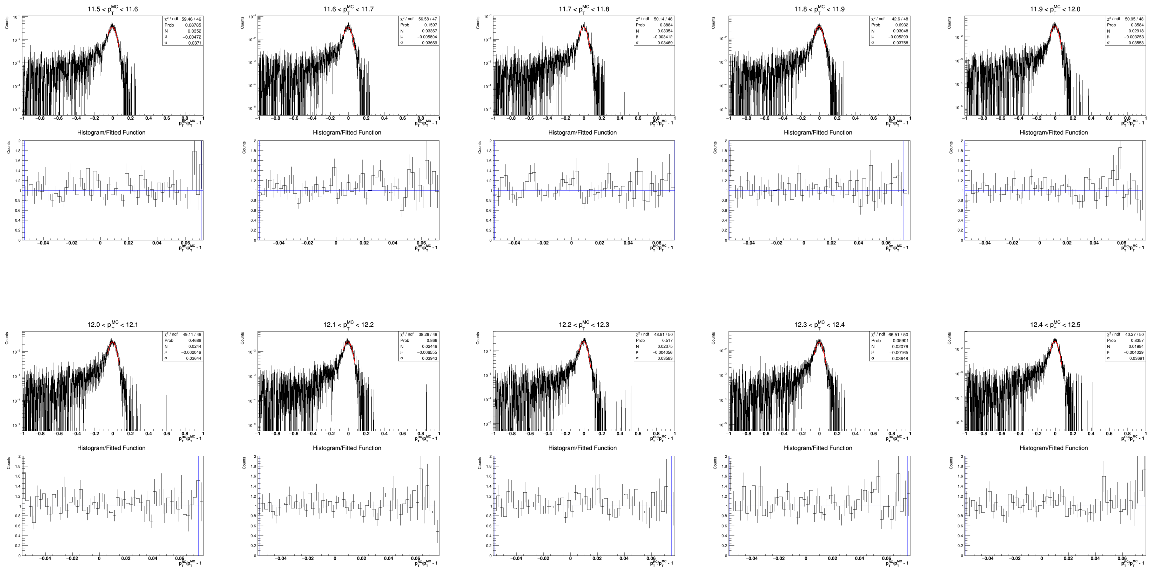

p+Au

7.4 p+p Cross Section - Results Combination

The inclusive J/ψ cross section in p+p collision result from this analysis is combined with measurements using data taken in year 2009 (Run09) and 2012 (Run12). The combined result is reported in the paper. The Run09 results utilize the BHT0 and BHT3 triggers, while the Run12 utilize MB, BHT0 and BHT2 triggers.

The method used is called “Best Linear Unbiased Estimate” (BLUE). It minimize the total variance (best), under the condition that the combined result is a weighted sum of each measurement (linear), while also keeping the sum of the weights is 1 (unbiased). The physics quantity undergoes the BLUE method is the yield. The yield in each p_T bin is combined independently. After getting the combined yield as a function of p_T, the combined invariant yield (equivalently the cross section) is calculated and the p_T position is decided in the same way as in this analysis.

The total variance is the sum of different variance entries. Each of the variance entries is calculated with an uncertainty entry, e.g. the statistical, various systematic or normalization uncertainties. Different uncertainty entries are assumed to be mutually independent between each other by design. Correlation between measurement from 3 dataset is considered when calculating each uncertainty entry. In general, statistical, data driven systematic uncertainties are assumed to be uncorrelated, while the rest is conservatively assumed to have correlation coeeficient of 1.

In each p_T bin, the total variance Δ^2 is given by:

$$\Delta^2 = \Sigma_i \left(\sigma_i^T P_i \sigma_i\right) \tag{1}$$

where i identifies different uncertainty entries, column vector σ_i is defined to simplify the right hand side of the above equation by:

$$\sigma_i = \begin{pmatrix} w_{09}\delta_{09,i} \\ w_{12}\delta_{12,i} \\ w_{15}\delta_{15,i} \end{pmatrix} \tag{2}$$

and P_i is the correlation matrix:

$$P_i = \begin{pmatrix} 1 & \rho_{09-12,i} & \rho_{09-15,i} \\ \rho_{12-09,i} & 1 & \rho_{12-15,i} \\ \rho_{15-09,i} & \rho_{15-12,i} & 1 \end{pmatrix} \tag{3}$$

w_{year} is the weight assigned to the year, $\delta_{year,i}$ is the uncertainty value corresponds to i and year, and $\rho_{yearX-yearY,i} = \rho_{yearY-yearX,i}$ is the correlation coefficients between year X and year Y. As discussed, $\rho_{X,Y,i} = 0$ when i corresponds to statistical and data driven systematic uncertainties, while $\rho_{X,Y,i} = 1$ for the rest uncertainties. The weights satisfy: $w_{09} + w_{12} + w_{15} = 1$. By substitute $w_{15} = 1 - w_{09} - w_{12}$, Δ^2 becomes a binary function of w_{09} and w_{12}. Since all the uncertainty entries are in the publication, and all the correlation coefficients has got an educated guess, the problem is simply finding the local minimum of $\Delta^2(w_{09}, w_{12})$ within $w_{09} \geq 0, w_{12} \geq 0, w_{09} + w_{12} \leq 1$.

The difference in analysis procedure and aspects taken into account when calculating the systematic uncertainties between the 3 measurement complex the combination. The following lists all the special treatment in this combination practice.

Absent of Estimation Some of systematic uncertainties are not estimated in all three analyses. In the case where the entry is not of concern, e.g. TOF related systematic uncertainties for Run09 and Run15 where TOF is not used, those absent uncertainties are naturally assigned to be 0. For the rest, an dedicated way to guess is established based on uncertainties from the "estimated year(s)" and combination weights, so that it will not bias the relative combined uncertainty. Specifically, for single-year absent case, the assigned value is essentially the relative uncertainty of the combined result of other 2 years with the given weights, while for dual-year absent case, i.e. the estimation is only given in one analysis, this estimation on relative uncertainty is simply copied to the other runs.

Assymetric Uncertainty The only case is the raw yield (RY) estimation uncertainty in Run09. One needs to construct the contribution related to Run09 reasonably. The solution is to replace the Run09 data (with assymetric uncertainty) with 2 "pseudo-data" (with symetric uncertainty, corresponding to the lower and higher limit respectively), each carrying a weight of $\frac{w_{09}}{2}$. The 2 "pseudo-data" is assumed to have correlation coefficients of 1 between each other. This happens to convey the "unbiased" assumption in the BLUE. The contribution in total variance that is solely related to Run09 is given by:

$$\begin{aligned}&\left(\frac{w_{09}}{2}\cdot\delta_{RY,low}\right)^2+\left(\frac{w_{09}}{2}\cdot\delta_{RY,high}\right)^2+2\cdot\left(\frac{w_{09}}{2}\cdot\delta_{RY,low}\right)\cdot\left(\frac{w_{09}}{2}\cdot\delta_{RY,high}\right)\\&=w_{09}^2\left(\frac{\delta_{RY,low}+\delta_{RY,high}}{2}\right)^2\end{aligned}\tag{4}$$

which happens to equal to the result if one takes the average of the 2 uncertainties that correspond to the lower and higher limit. Similarly, the contribution that reflects the correlation between Run09 and the other runs also takes the form of taking the average of the uncertainty correspond to the lower and higher limits. This replacement allow us to obtain the weights with the BLUE method, then the combined RY uncertainty entry for the lower and higher limit is calculated using w_{09} of $\delta_{RY,low}$ and w_{09} of $\delta_{RY,high}$ to calculate , respectively.

7.5 Paper Plots

These plots are simply overlaying the results from this analysis with published data.

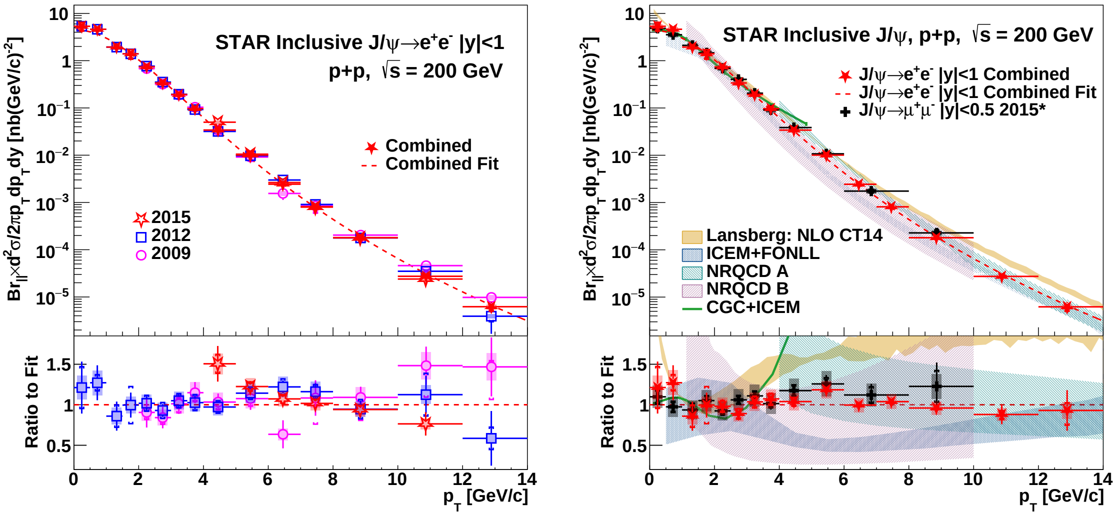

Figure 14: : Inclusive J/ψ cross section as a function of p_{T} in p+p collisions at $\sqrt{s} = 200$ GeV and comparison to STAR $J/\psi \rightarrow \mu^{+}\mu^{-}$ measurement for $|y| < 0.5$ at the same $\sqrt{s}$ and to various model calculations for $|y| < 0.5$. Notice the "*" marker indicates that the dimuon measurement is corrected for the rapidity coverage from $|y| < 0.5$ to $|y| < 1$. This analysis (2015) is combined with 2 other published STAR $J/\psi \rightarrow e^{+}e^{-}$ results with data taken in 2009 and 2012. The vertical bars represent the statistical uncertainties, while the brackets and transparent boxes represent the systematic uncertainty that is uncorrelated and correlated between p_{T} bins, respectively. The horizontal bars represent the bin width. The dashed line is a fit to the combined.

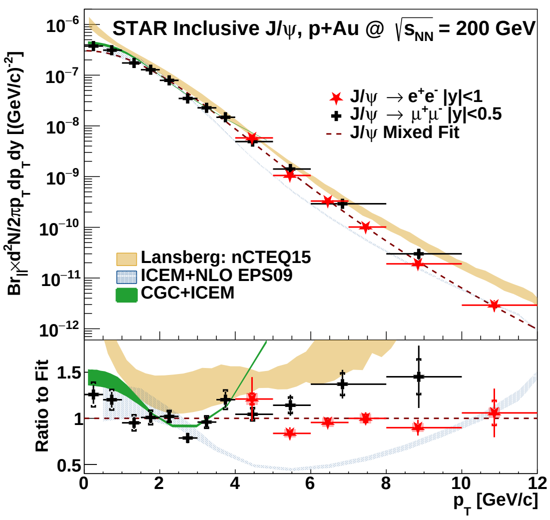

Figure 15: Inclusive $J/\psi \rightarrow e^{+}e^{-}$ invariant yield as a function of p_{T} in p+Au collisions at $\sqrt{s_{\mathrm{NN}}} = 200$ GeV and comparison to STAR $J/\psi \rightarrow \mu^{+}\mu^{-}$ measurement for $|y| < 0.5$ at the same $\sqrt{s_{\mathrm{NN}}}$, and to various model calculations. The dashed line is a mixed fit to dielectron and dimuon channel results, covering p_{T} range of 4–12 GeV/c and 0–4 GeV/c respectively. The representation of uncertainties and bin width is identical to Fig. 14.

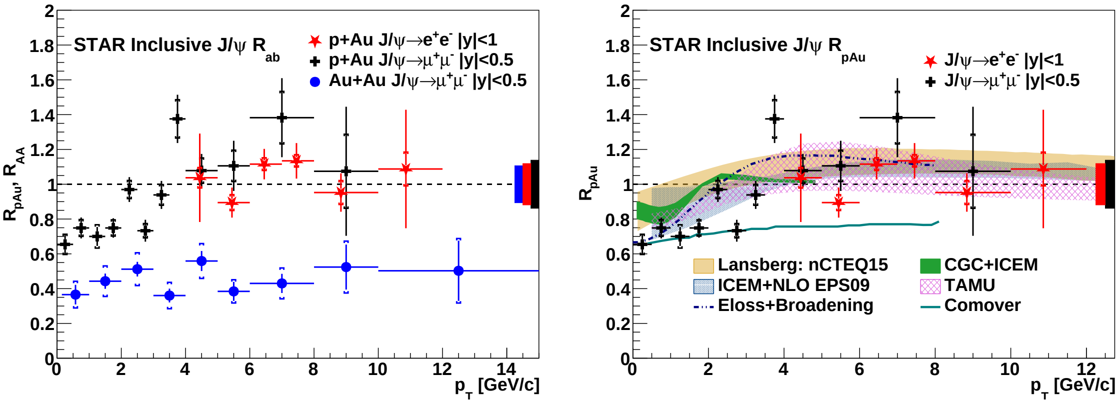

Figure 16: Inclusive $J/\psi \to e^+e^-$ R_{pAu} compared to the $J/\psi \to \mu^+\mu^-$ R_{pAu} as well as the R_{AA} in 0-20% central Au+Au collisions at the same $\sqrt{s_{\mathrm{NN}}}$, and comparison on R_{pAu} between STAR J/ψ R_{pAu} measurements dielectron and dimuon channel with various model calculations. The representation of uncertainties and bin width is identical to Fig. 14, with the exception of correlated uncertainties between p_{T} bins are represented by the boxes of the corresponding color around unity.